2020

Role of trib3 in progression and pathogenesis of diabetic retinopathy

Priyamvada Milind Pitale
University of Alabama at Birmingham

ROLE OF TRIB3 IN PROGRESSION AND PATHOGENESIS OF DIABETIC RETINOPATHY

by

PRIYAMVADA MILIND PITALE

MARINA GORBATYUK, CHAIR (Advisor)
ALECIA K. GROSS
TIMOTHY GARVEY
MACHELLE PARDUE
MARIA GRANT

A DISSERTATION

Submitted to the graduate faculty of The University of Alabama at Birmingham,
in partial fulfillment of the requirements for the degree of
Doctor of Philosophy

BIRMINGHAM, ALABAMA

2020

ROLE OF TRIB3 IN PROGRESSION AND PATHOGENESIS OF DIABETIC RETINOPATHY

PRIYAMVADA MILIND PITALE

VISION SCIENCE GRADUATE PROGRAM

ABSTRACT

Diabetic retinopathy (DR) is reported to be one of the leading causes of blindness in the United States by Center for Disease Prevention and Control. As the estimated prevalence of the disease will likely triple by 2020, the research in this area should focus on identifying novel targets and therapeutic approaches. One of the therapeutic approaches for DR is the reprograming of retinal metabolism to delay the progression of the disease. The unfolded protein response (UPR) is recognized as a cellular pathway activated in diabetic retina which interacts with key transcription factors to physiologically regulate glucose, lipid homeostasis, and angiogenic signaling. During development and progression of DR, persistent activation of UPR occurs. Tribbles homologous 3 (TRIB3) is one of the UPR mediators activated in response to stress. My current project is focused on exploring TRIB3 protein as a novel therapeutic target for DR treatment. We hypothesize that TRIB3 is elevated in diabetic retina leading to aberrant insulin signaling and neovascularization. We tested this hypothesis in animal models of STZ-induced diabetes and hypoxia-induced proliferative retinopathy. Moreover, we identified the mechanism of TRIB3-mediated progression of DR in primary cultured retinal Muller cells. Our data demonstrated that TRIB3 controls major molecular events in early diabetic retinas. It specifically, regulates a retinal glucose flux, and alters expression of inflammatory and metabolic markers. In addition, we found that

TRIB3 ablation leads to significant retinal ganglion cell (RGC) survival and functional restoration accompanied by a dramatic reduction in pericyte loss and acellular capillary formation in hyperglycemic retinas. In hypoxic conditions, TRIB3 KO retinas significantly diminished GFAP and VEGF expression, thus regulating gliosis and aberrant vascularization, and preserving retinal integrity. In conclusion, overexpression of TRIB3 in hyperglycemic and hypoxic retinas may accelerate the onset and progression of DR to proliferative stages indicating TRIB3 as a potential therapeutic target.

Keywords: Diabetic retinopathy, Glucose metabolism in the retina, Neovascularization, Retinal ganglion cells, and Muller gliosis

DEDICATION

I dedicate my thesis first, in the loving memory of my beloved grandmother, Mrs. *Malini Madhukar Pitale (1925-2010), (Bachelors in English literature*) who was one of the first females in our family to get college education. She had a long career in teaching for almost 35 years. When I was growing up, she was my teacher and best friend. It was her encouragement that I chose medicine and research as my career. Second, I want to dedicate my work to my amazing husband *Dr. Ninad Chaudhary* and our handsome son, *Avneesh*. They have been truly patient and supportive throughout my dissertation.

ACKNOWLEDGMENTS

This journey towards my PhD would not be possible without the support of family, mentor and friends. First and foremost, I am truly grateful to my family. My parents, *Milind* and *Radhika* and my aunts, *Mrudula (1955- 2020)* and *Mrunalini* have been a strong pillar of support throughout my academic career. My husband, *Ninad* and my sister *Madhura* have always believed in me and encouraged me to work hard and with honesty. I am thankful to my sister-in-law *Nayana*, brother-in-law *Tushar* and my parents-in-law for their love and support. I have heartful gratitude and appreciation towards my advisor, *Dr. Marina Gorbatyuk*. I am thankful for the vision science expertise she offered in my dissertation work. She mentored me in molecular biology, retinopathy research and laboratory protocols. I am sincerely thankful to my entire dissertation committee for the guidance, expertise and support. Last but not the least, I am in deep gratitude to all my friends, lab mates and entire vision science- optometry school colleagues. Sincere appreciations to *Pravallika* who has been a great friend.

TABLE OF CONTENTS

LIST OF TABLES

LIST OF FIGURES

CHAPTER 1

INTRODUCTION

Glucose Metabolism and Transport in the Retina

Retina is a multi-layered structure lining the posterior segment of the eye. These layers are composed of several functionally different neuronal and glial cells (Figure-1). From the outermost to innermost neural layer, these cells are photoreceptor cells, bipolar cells (BP), horizontal cells (HC), amacrine cells (AC), muller cells, retinal ganglion cells (RGC) and the astrocytes.

The retinal cell functions and glucose metabolism have a co-dependent relationship.[1] The preferred energy substrate for any mammalian cell is glucose. Glucose is catabolized to lactate and pyruvate with generation of the energy molecule adenosine triphosphate (ATP). Pyruvate then moves to the mitochondria where it is converted to Acetyl-coenzyme A. Acetyl-coenzyme A is further utilized in the citric acid cycle to produce energy precursor nicotinamide adenine dinucleotide/hydrogen (NAD^+/NADH) which is required for oxidative phosphorylation (OXPHOS).[1,2] Glycolysis and OXPHOS co-exist in the mammalian cells and fulfills the cellular energy demands but their relationship can be competitive. For example, most cancer cells utilize glycolysis as a major pathway to produce energy independent of normoxia or hypoxia. This phenomenon is called as aerobic glycolysis, also known as a Warburg effect.[3] One of the tissues with the greatest metabolic

rate and the energy demand in the human body using aerobic glycosylation is the retina.[1] Among the retinal cells, photoreceptors are the cells with highest metabolic rate and the light dependent energy utilization. The energy demand is prioritized for utilization in the outer segments (OS) of photoreceptors in the light and in the inner segments (IS), and synapses in the dark.[2] Additionally, glucose metabolism is compartmentalized depending on the presence of glycolytic enzymes like Hexokinase (HK) II and PK-M2.[1] For example, pyruvate kinase -isoenzyme M2 (PK-M2) is present only in the outer retina, implicating photoreceptors as a primary site of glycolysis in the retina.[2] In addition to photoreceptors, RPE cells in the outer retina also catabolize glucose obtained from choroidal blood circulation by glycolysis.[4] Further, glial Muller cells metabolize glucose to lactate even in presence of oxygen.[5] Recent studies have reported that glucose oxidation in Muller cells is limited to its external limiting membrane (ELM), the cell compartment with a high number of mitochondria.[1] However, the activity of OXPHOS enzymes is reported to be weak in the Muller cells.[1] Researchers have proposed that Muller cells spare oxygen for the retinal neurons,[6] and produce lactate for utilization by surrounding neurons to meet their high energy requirements.[5]

Glucose influx into the retina is mediated by a facilitated transport via glucose transporters (GLUT) particularly, GLUT-1. GLUT-1 transporter is expressed in the IS of photoreceptors where it transports glucose from the RPE.[2,4] The apical and basolateral membranes of the RPE, Muller, and the retinal endothelial cells also express GLUT1 transporters.[2,4,7] GLUT-1 has a high affinity for glucose which explains why the retinal cells are more prone to hyperglycemic damage.[8,9] Further the monocarboxylate transporters (MCT) 1 and 3 are important for lactate efflux from the retinal cells. For

example, lactate generated from glycolysis is carried out from IS of the photoreceptors and secreted by monocarboxylate transporter-1 (MCT-1) into the subretinal space.[4] The excess of lactate produced by photoreceptors is taken by the RPE cells via MCT-1 transporter. Lactate efflux from the RPE cells to transepithelial choroidal circulation is carried out by MCT-3 transporter.[4] A balance between GLUTs and MCTs in the retina is required to achieve homeostasis of glucose and lactate shuttle (Figure-2).

Pathophysiology of Diabetic Retinopathy

The American Academy of Ophthalmology defines that diabetic retinopathy (DR) is a neurovascular eye complication associated with damage of retinal vasculature and growth of abnormal new vessels in the retina in response to high glucose levels. The number of cases with diabetes-associated visual impairments has increased by 64 percent over the past twenty years.[10] DR is classified into two stages based on the pathological changes in affected retinas observed over the period of the disease progression. An early stage of DR is known as a non-proliferative diabetic retinopathy (NPDR) and the later advanced stage is known as a proliferative diabetic retinopathy (PDR). NPDR is characterized by presence of microaneurysms, retinal hemorrhages, intraretinal microvascular abnormalities (IRMA), and venous beading. In the advanced proliferative stage, there occurs aberrant vascular signaling, ischemia, neovascularization and finally diabetic macular edema (DME).[11] DME is clinically significant manifestation of DR which results from the disruption of the blood retinal barrier (BRB) leading to leakage of blood and cellular fluids in the neural retina.[12,13] Chronic hyperglycemia is one of the severe

crucial risk factors for DR and glycemic control has shown to delay the progression of DR.[14,15]

Both hyperglycemia and hyperglycemia-induced hypoxia are the hallmarks of retinal pathobiology in diabetes that trigger development and progression of DR.[16] In the streptozotocin(STZ) -induced diabetic rats as early as 2 weeks post induction of diabetes, the GLUT-1 expression is reduced by 50 % in the neural retinal cells and retinal microvasculature. However, isolated RPE cells did not show a sign of reduction in GLUT-1 expression at 8 weeks post hyperglycemia induction.[9] This fact is particular interesting since RPE is the major cell that supplies glucose from the choroidal blood vessels to the photoreceptors.

In normal conditions, the utilization of glucose in the retina occurs primarily via glycolysis. In the diabetic retina, excessive glucose is subsequently diverted to activation of polyol, hexosamine monophosphate (HMP), advanced end glycosylation products (AGE), and protein kinase--c (PKC) pathways.[16] In presence of excess glucose flux, the retinal response is a complex interplay between these signaling pathways. Thereby, the enzyme aldose reductase utilizes nicotinamide adenine dinucleotide phosphate (NADPH) cofactor for activating the polyol (sorbitol) pathway. The NADPH cofactor levels subsequently drops resulting in its deficiency to perform other physiological cellular functions such as maintenance of the antioxidants. Thus, the polyol pathway makes cells vulnerable to oxidative damage.[17] Secondly, in the PKC pathway, increased activation of diacylglycerol (DAG) leads to upregulation of protein kinase C. Activation of PKC signaling in turn affects gene expression of cytokines, enzymes, and growth factors that modulate vascular health.[18,19] In addition to mentioned above signaling, upregulation of

AGEs in the cells modifies the extracellular matrix components and disrupts the regulation of gene transcription.[20]

Hyperglycemia reduces the levels of glucose-6-phosphate dehydrogenase (G-6PD) enzyme which is crucial for pentose pathway shunt, HMP, and N-acetyl glucosamine. Cappai et al. reported that patients with deficiency of G-6PD are vulnerable to proliferative retinal damage.[21] [22] Activation of HMP signaling in turn affects gene transcription profile and post-translational modification. In particular, the expression of the proteins that play a critical role in the maintenance of vascular health were reduced in these studies.[23,24] In addition to mentioned above cellular pathways, the unfolded protein response is activated in diabetic retina which is an important contributing factor in diabetic retinal pathobiology and is therefore, an aspect of my dissertation.

Unfolded Protein Response and PERK/ATF4 Pathway in DR

"The unfolded protein response (UPR) or the endoplasmic reticulum (ER) stress response is a series of evolutionarily conserved signaling pathways aimed at restoring homeostasis under conditions of ER stress.[25] Cellular stress, particularly excess of glucose and hypoxia, can trigger UPR activation in diabetic retina.[26] The protein kinase RNA-like endoplasmic reticulum kinase (PERK) signaling is the one of the UPR pathways. One of the downstream targets of this pathway is activating transcription factor 4 (ATF4). During the stress conditions, auto-phosphorylation of PERK leads to phosphorylation of the eukaryotic initiation factor 2α (eIF2α) causing the selective translation of ATF4 even though peIF2α causes global attenuation of protein translation. Upregulation of

PERK/ATF4 pathway results in activation of inflammation in response to hyperglycemia as well as hypoxic stress.[25] Li et al. reported that both the vascular endothelial growth factor (VEGF) and the tumor necrosis factor (TNF)-alpha cytokines were upregulated in Akita mouse retinas as early as 12- weeks of age. The authors also demonstrated that the elevation of TNF-alpha along with activation of ATF4 and p-eIF2a in oxygen induced retinopathy (OIR) mouse retinas occurs at postnatal day (p) 15-16.[27] Experiments with retinal endothelial cells cultured in high glucose medium also revealed the activation of ATF4. Moreover, the inhibition of ATF4 in these cells resulted in downregulation of VEGF and intercellular adhesion molecule (ICAM-1), and the inflammatory cytokine promoting leukostasis and leucocyte adhesion.[28] In contrast, Zhong et al. considered consistent hyperglycemia as not a powerful stress trigger of the UPR activation in the retinal pericytes even though the intermittent high glucose incubation of human retinal pericyte cells results in upregulation of ATF/CHOP pathway and downregulation of VEGF cytokine expression.[29] However, other researcher emphasized that these intermittent hyperglycemic surges compared to other types of the stress cause even more damage to the cells in patients with DM who often have blood glucose fluctuations.[30]

PERK pathway plays a critical role in triggering angiogenesis. In cancer cells, the activation of PERK pathway in response to hypoxia has been associated with angiogenic stimulation , upregulation of VEGF, and cell adhesion cytokines.[31] Similarly, in proliferative retinopathies, PERK signaling activates the nuclear factor kappa-light-chain-enhancer of activated B cells (NF-kB) transcription factor, an endogenous controller of angiogenesis and inflammatory signaling.[32,33] In addition, ATF4 , a PERK pathway mediator, plays a key role in promoting proliferative retinopathy. Our lab's prior work

demonstrated that heterozygous knockdown of ATF4 in OIR mice results in significant reduction of neovascularization at p17. Moreover, expression of VEGF and UPR were significantly reduced in ATF4 (+/-) OIR retinas as early as p12.[34]

In summary, upon the ER stress activation, the PERK/ATF4 pathway regulates the cytokine activation, modulates angiogenesis, and controls vascular health. However, the question of how ATF4 governs these downstream signaling is still not answered. It is also unknown whether the downstream signaling of ATF4 regulates glucose metabolism in diabetic retinas. Therefore, we hypothesis that the ATF4 promotes angiogenesis and cytokine activation through its downstream targets, one of which is tribbles homologous 3 (TRIB3) also known as Tribbles Pseudokinase 3.

Tribbles Pseudokinase 3 (TRIB3)

TRIB3 is a pseudokinase originally found in Drosophila and was first designated as the gene associated with programmed cell death.[35,36] There are three mammalian homologs of Drosophila tribbles TRIB1,2 & 3. The human *TRIB* 1 and 2 share homology 71%, 1 and 3 shares 53%, and 2 and 3 share 54%. Past research has described *TRIB3* as apoptotic and hypoxia responsive gene,[37] and gene associated with autophagy.[38] TRIB3 protein is a pseudo-kinase protein with a kinase like domain that is functionally inactive due to the numerous amino acid substitutions at catalytically important positions.[38] *TRIB3* gene overexpression leading to the UPR activation has been investigated in response to different stress triggers. Some of the known cellular stressors are hypoxia, excess glucose, upregulation of fatty acids and certain chemicals causing cell toxicity.[38] For example, AFT4/ CHOP (C/EBP Homologous Protein) upregulation induces TRIB3 expression in

response to metabolic stress. Interestingly, increased TRIB3 in turn can subsequently downregulate ATF4/CHOP signaling via negative feedback loop mechanism maintaining homeostasis.[35]

TRIB3 is most exclusively investigated protein amongst tribbles family members in glucose metabolism. The foremost work on TRIB3 in liver cells reported that TRIB3 binds to protein kinase- B (AKT) at the threonine (THR^{308}) and serine (Ser^{473}) residues and inhibits the AKT phosphorylation. Inhibition of AKT phosphorylation causes disruption in downstream signaling.[39] One such AKT downstream signaling is the production of Nitric Oxide (NO). Studies on human umbilical vein endothelial cell culture (HUVEC) have reported that phosphorylation of AKT leads to activation of endothelial NO synthetase enzyme (eNOS) which releases the NO and regulates vascular health.[40] NO in turn functions as a vasodilator and an antithrombotic preventing ischemia. Additionally, NO also regulates the inflammation and cell proliferation. In human endothelial cells, TRIB3 overexpression has been shown to attenuate the insulin-mediated eNOS Ser1177 activation.[41]

Role of TRIB3 has been also investigated in insulin resistance signaling in muscular cells. Using skeletal muscles of the STZ injected rodents, Dr. Garvey's group demonstrated that TRIB3 overexpression impairs the insulin mediated glucose transport via inhibition of GLUT-4 transporter. They also highlighted the role of TRIB3 in glucose toxicity by characterizing the glucose dependent TRIB3 upregulation in L6 cells.[42] Glucose induced overexpression of TRIB3 was also reported to be reliant on the activation of hexosamine biosynthetic pathway (HBP).[43] In the mice with muscle cell specific TRIB3 ablation, the STZ injection resulted in attenuation of glucose induced insulin resistance. Alternatively,

the overexpression of TRIB3 in these cells augmented the inflammatory and oxidative damage via downregulation of the AKT phosphorylation upon the treatment with STZ.[44]

TRIB3 gene is also described as a controller of the NOTCH-EGFR (epidermal growth factor receptor) pathway in the cancer studies. TRIB3 upregulation promotes cell proliferation, decreases survival of healthy cells, and activates JAG-1 ligand of NOTCH signaling.[45] Given the JAG-1 ligand possess pro-angiogenic properties similar to ones reported in tumor cells with aberrant neovascularization,[46,47] it is no wonder that overexpression of TRIB3 serves as a marker of a poor prognosis for patients with breast cancer. Moreover, TRIB3 overexpression is strongly associated with abnormal angiogenesis and pathological neovascularization through TRIB3-NOTCH-VEGF signaling in the human endothelial cells.[48] These data provide rationale to further explore role of TRIB3 in PDR pathology.

Overall, our attention towards TRIB3 stems from the published studies on the role of TRIB3 in glucose-induced insulin resistance and the association of TRIB3 with ischemic damage causing endothelial cell apoptosis. Although the role of TRIB3 in cell survival or death has been previously highlighted in diabetes and cancer research, the role of TRIB3 in retinal pathology has not been studied yet.[38] To address this gap in the literature, we proposed to understand whether TRIB3 overexpression plays pathological role in diabetic retinas.

Our central hypothesis is that TRIB3 is involved in aberrant insulin signaling and neovascularization. Thus, we aimed to characterize the role of TRIB3 in DR pathology.

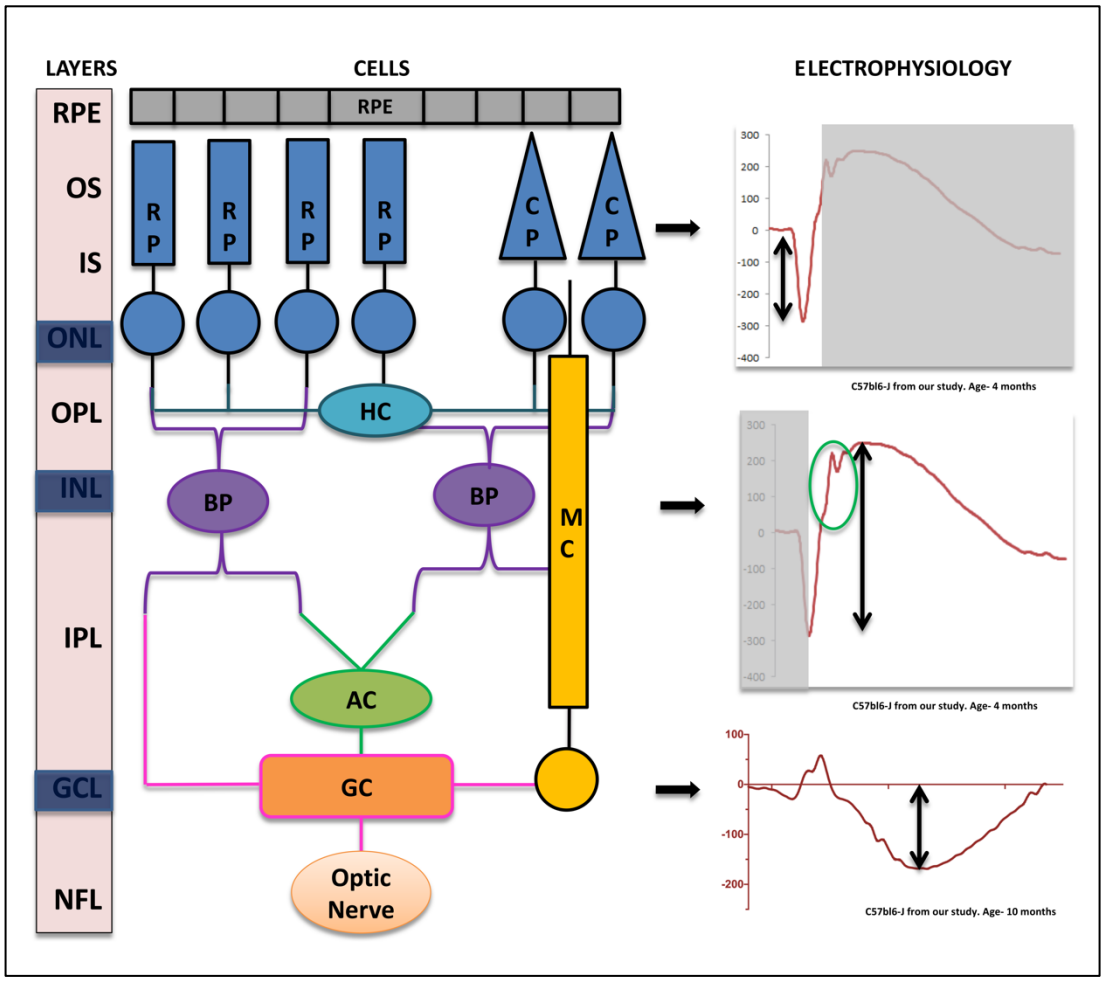

Figure 1. Distribution of retinal cells throughout ten layers of the retina. From outer to inner retina, the retinal layers are RPE layer, ONL composed of photoreceptors' nuclei, INL composed of bipolar cells' nuclei, OPL and IPL composed of horizontal cells and amacrine cells respectively, RGC layer, and finally NFL comprised of the RGC axons as shown in the left panel. The retinal cells' electrophysiological function is measured by ERG. Waveforms representative for different retinal cells in the C57BL6 retina are shown in the right panel. Top- a wave and middle- b wave represent scotopic responses of photoreceptor and BP cells respectively. The bottom right panel depicts amplitudes measured with photopic ERG known as PhNR. These amplitudes reflect the

function of RGCs. (RPE: retinal pigment epithelial cell, OS: outer segment, IS: inner segment, ONL: outer nuclear layer, INL: inner nuclear layer, OPL: outer plexiform layer, IPL: inner plexiform layer, RGC: retinal ganglion cell, NFL: nerve fibre layer, RP: rod photoreceptor, CP: cone photoreceptor, BP: bipolar cell, AC: amacrine cell, HC: horizontal cell, MC: muller cell, ERG: electroretinogram, PhNR: photopic negative response)

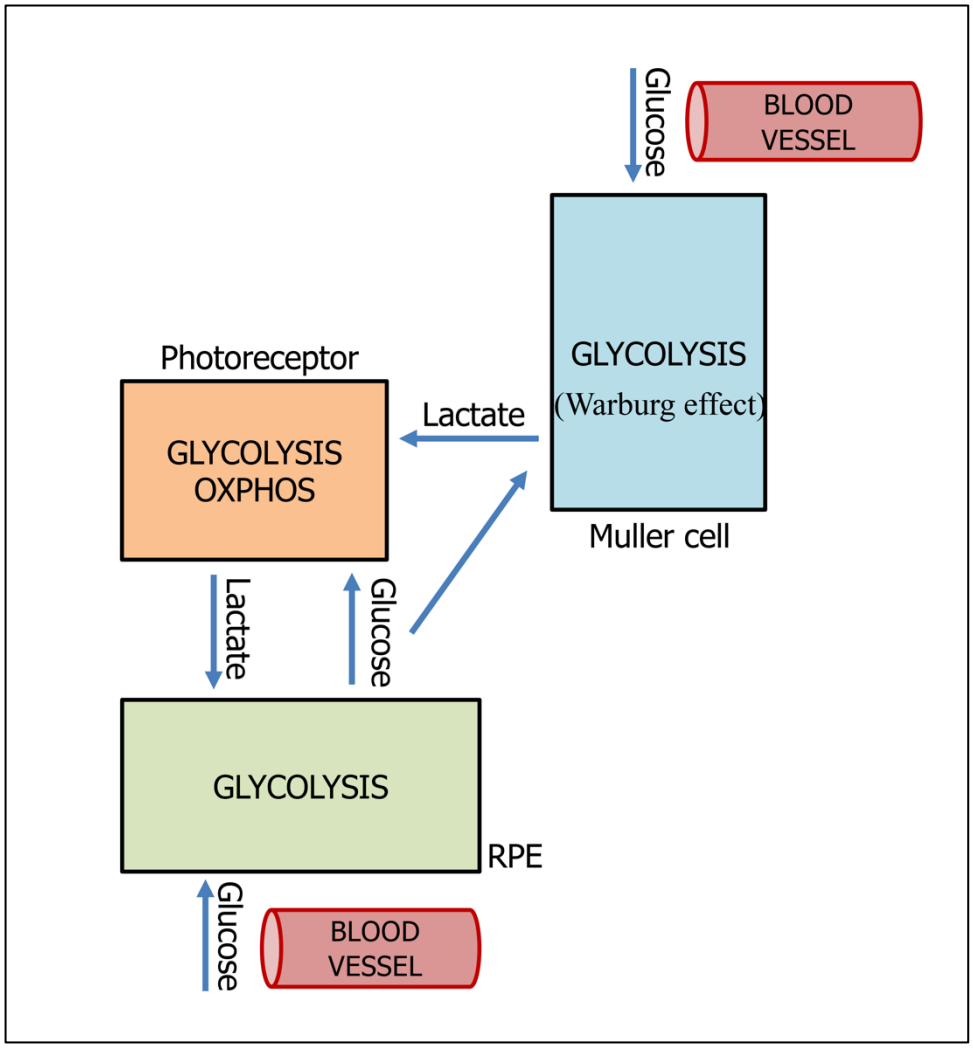

Figure 2. Schematic representation of glucose transport and metabolism in retinal cells. Photoreceptors have high energy demand and have competitive glycolysis and oxidative phosphorylation pathways. Muller cells primarily produce lactate from glycolysis and aerobic glycolysis and release this lactate in subretinal space for photoreceptors. RPE cells not only provide glucose and lactate to photoreceptors but also clear out excess of lactate via transepithelial transport to choroidal blood vessels from subretinal space. Overall, a balance between glucose and lactate transporters is required for the health of the cell.

CHAPTER 2

CHOOSING APPROPRIATE ANIMAL MODEL EXHIBITING HUMAN PATHOLOGICAL CHANGES IN DIABETIC RETINA

Pathobiology of Diabetic Retina

Current clinical trials using *in vivo* imaging techniques have demonstrated retinal morphological changes associated with diabetes. A study with 124 human subjects using spectral domain optical coherence tomography (SD-OCT) demonstrated decreased thickness of the retinal nerve fiber layer (NFL) with no changes in the outer neural retina in patients with early stages DR. In addition to changes detected in NFL, the thickening of the inner nuclear layer (INL) in the diabetic retina has been also reported as a sign of Müller cell hypertrophy and activation.[49] Furthermore, retinal microangiopathy associated with diabetes is suggested to be a result of increased retinal blood circulation.[50] A prospective clinical study of 35 subjects showed that multifocal electroretinogram (ERG) analysis employed in patients with severe ocular diabetic complications can be used to successfully evaluate the progression of DME.[51] In another study conducted with 29 individuals with NDPR, the multifocal ERG procedure was used to register the N1 amplitude measured as a peak from a baseline, P1 amplitude measured as a peak from N1 trough, and an N2 amplitude measured as a peak from P1 peak to N2 trough. The amplitudes of these ERG modules were significantly decreased along with delayed implicit time as compared to normal subjects, demonstrating the dysfunction of

the outer neural retina. These functional changes are also associated with the changes in the visual acuity and central macular thickness in the individuals with DME.[52] In addition, Pardue and colleagues reported results from a cross sectional clinical study involving 16 patients with type II diabetes (T2D) that the follow up ERG examination accompanied with low intensity stimuli may provide earlier detection of neuronal pathology in the diabetic retina.[53]

While clinical trials concentrate on risk factors and early detection and evaluations of the progression of DR in vivo, access to human donor eye tissue provides a great opportunity to study early molecular changes in the diabetic retina to further understand pathological markers. Multiple studies with postmortem donor eye reported glial cell dysfunction as a primarily manifestation of diabetic retinopathy. A recent study on four postmortem diabetic eyeballs, applied immunolabelling technique for detection of carbonic anhydrase (II) and glial fibrillary acidic protein (GFAP).[54] The authors revealed the Müller cell nuclei migration and the presence of glial cells in the pre-retinal membranes.[54] The reported data are in agreement with another study involving 14 donor eyes which demonstrated that the GFAP levels are increased in diabetic eyes as compared to non-diabetic eyes.[55]

In addition to structural and morphological changes occurring in diabetic retinas, there are molecular changes of equal prominence. Studies on post-mortem diabetic eyes have shown presence of inflammation as well as increase in the immunolabelled signal for caspase 3, Fas, and Bax in RGCs and GFAP in the inner retina. [56].[57,58] Studies on vitreous from PDR patients have demonstrated that levels of interleukin-8, monocyte chemotactic protein-1, and macrophage-colony stimulating factor, platelet-derived

growth factor (PDGF) and vascular endothelial growth factor (VEGF) are elevated as compared to non-diabetic individuals.[59-62] Microarray analysis of gene expression of fibrovascular membranes extracted from PDR patients during vitrectomy have identified extracellular matrix proteins and elevated expression of genes associated with angiogenesis and apoptosis.[63] These analyses have also helped to identify potential therapeutic targets.

Molecular and structural changes observed in the studies using human tissue or postmortem eyeballs have indicated neuronal cell loss in diabetic retinas.[64] For example, it has been reported that VEGF plays an important role in the development of aberrant neovascularization in diabetic retinas and it's increase can serve as a biomarker of microangiopathy in PDR.[65] They also found that, in addition to VEGF, increases in the number of apoptotic cells – as measured by a terminal deoxynucleotidyl transferase-mediated dUTP nick end labeling (TUNEL) assay - and pericyte and endothelial cell loss are associated with diabetic microvascular complications.[66] Overall, the studies with postmortem human retinal tissues have informed us on major structural, morphological and molecular changes occurring human diabetic retinas.

Though studies with human donor tissues are an excellent asset for improving our understanding of molecular signaling in diabetic retinas, they cannot provide a complete picture of the mechanism of retinopathy related to diabetic complications. Moreover, the tissues may not be readily available. The use of genetic animal model addresses these limitations as well as, it is an excellent approach for comprehensive understanding of the cellular pathways associated with DR. While choice of the

appropriate animal model mimicking all aspects of human DR pathology is a challenging, several models can capture key cellular and physiological events of diabetic retinopathy in humans. Here in this literature review, we attempted to summarize current status on the developed animal models used in the research focusing on diabetic retinopathy.

Experimental models of DR

One of the key regulators for homeostatic balance of the glucose metabolism in the body is insulin produced by the beta cells of the pancreas. The insulin receptor-signaling pathway facilitates the glucose entry into the cell through the protein kinase B (AKT)-mediated glucose transporter (GLUT1) activation. In humans, fasting blood glucose level is maintained in the range of 92-126 mg/dl while the postprandial blood glucose level is in the range of 97-140 mg/dl. It is well-accepted that under fasting and postprandial conditions, the blood glucose level (BGL) above 126 mg/dl and 180 mg/dl, respectively are considered sustained hyperglycemia.[67]

NPDR is primarily driven by hyperglycemia while PDR is primarily caused by hypoxia. Thus, animal models mimicking events of DR are developed using these two prime inducers. There are several species which have been used for development of DR, including rat, mouse, rabbit, monkey, zebrafish, dog, pig, cat and tree shrew. Accordingly, the experimental diabetes is achieved by induction of a) hyperglycemia using pharmaceutical agents, pancreatectomy, or genetically modified animals.[68-72]; b) hypoxia leading to neovascularization (Table.1).

Induction of hyperglycemia

Pharmacological induction of Hyperglycemia. STZ is most frequently used approach to develop T1D model. STZ is an antibiotic produced by the bacterium Streptomyces achromogens and possesses a broad spectrum of antibacterial properties. It has highly reactive methylnitrosourea moiety that exerts the cytotoxic effects resulting in pancreatic β cell necrosis, and the glucose moiety that transports the chemical to the pancreatic β cells. STZ acts via GLUT2 receptor that is abundant on β cell plasma membranes. Therefore, pancreatic β cells are a specific target of STZ.[68] STZ can be administered either for five consecutive days or as a single dose.[73] For example, the range of STZ dosage for multiple doses format is 40-80 mg/kg body weight (bw) injected intraperitoneally (IP) in mouse. The single dose is administered within the range of 150- 200mg/kg bw in mice or 30-100 mg/kg bw in rats by IP injections.[74-77] In rabbits, a single dose of 110 mg/kg bw STZ by intravenous administration has been used. In contrast, recently developed tree shrew model of DR requires a single dose of 300mg/kg bw of STZ administrated by IP injections.[78,79] The maintenance of fasting or non-fasting conditions before STZ injection does not change the post-induction hyperglycemic effect of STZ.[80] The hyperglycemia after STZ injection is usually seen within 1-4 weeks in most of the species. In some cases, the insulin injections are given to mice and rats to control the extreme fluctuations in the blood glucose levels, although this is not mandatory for STZ models.[73]

An alternative to STZ, Alloxan, can also induce hyperglycemia and is commonly used in mice, rat, rabbits and pigs. Alloxan is a pyrimidine derivative that directly targets beta cells of the pancreas causing apoptosis by inhibition of glucokinase enzyme and subsequent increase in blood sugar levels due to lack of insulin production.[70,81] In rodent models, Alloxan-induced hyperglycemia can be developed within 1 week of administration, while it takes less than a day in dogs.[82]

Surgical and Diet induced Hyperglycemia. Another method to experimentally induce hyperglycemia is surgical removal of pancreas (pancreatectomy) resulting in T1D. Pancreatectomies can be used together with pharmacological agents to get faster induction. For example, in canine models, hyperglycemia develops in 3-4 weeks after the surgery.[81,83]

In addition to the above methods, dietary modifications can cause changes in the blood glucose levels. The high glucose/galactose diet method is one such approach. Engerman et al. proposed the high galactose diet to induce T2D in dogs.[71] Diet-induced diabetes leading to development of DR has been investigated in several species.[81] However, in dogs and monkeys, this approach can take years to develop changes in the retina secondary to increased blood glucose levels compared to.[71,84] Rajagopal et. al proposed a high fat diet – induced T2D mouse model. In this model, hyperglycemia was reported to develop at 6 months of age.[85]

Spontaneous (Genetic) model of hyperglycemia

Rodents and zebrafish are the most well-studied genetic models that carry an endogenous mutation leading to spontaneous hyperglycemia. It is relatively easy and economical to develop these models, inbreed them with control backgrounds, and generate a statistically required number of animals for the experiments.

Rat models. There are several spontaneous hyperglycemic rat models: biobreeding (BB) T1D rats, Wistar Bonn/Kobori (WBN/Kob) T2D rats, Zucker diabetic fatty (ZDF) T2D rats, Otsuka Long- Evan Tokushima fatty (OLETF) T2D rats and spontaneous diabetic Torii (SDT) T2D rats. The BB rats are autoimmune DM model which develops hyperglycemia at 3 months of age and shows retinal vascular changes by the 8-11 months.[86,87] In WBN/Kob rats, the onset of hyperglycemia occurs at 9 months of age, and the male rats are gender preference is.[88] In contrast, the ZDF rats develop hyperglycemia earlier, between 5-10 weeks of age. These animals are considered a non-insulin-dependent DM model. They are obese and carry missense mutation known as fatty/fa in the leptin receptor gene (Lepr). Originally, these rats are derived from the Zucker rats which are obesity disease model.[89,90] OLETF male rats develop high blood sugar levels starting from 5 months.[91] In SDT rat model, detection of glucose in urine was reported at 20 weeks of age in males and at 45 weeks of age in females.[92]

Mouse models. $Ins2^{Akita}$ (T1D) mice, non-obese (NOD) (T1D), db/db mice (T2D), Kimba and Akimba mice are the most popular genetic DM models. The $Ins2^{Akita}$ mice have a point mutation in *insulin2* (earlier reported locus *Mody4*) which causes abnormal insulin production by pancreatic cells leading to pancreatic cell death. The heterozygous

$Ins2^{Akita}$ males are progressively hyperglycemic starting at 4 weeks of age while females exhibit mild symptoms of DM. They have an average life span of 305 days and are primarily a model of early retinal complications.[93,94] Another T1D model with DR is the NOD mice which mimic the human autoimmune insulin-dependent DM. These mice exhibit CD4 and CD8 cell mediated autoimmune process which destroys the pancreatic cells.[95,96] Interestingly, there is a gender-based variability in the timeline for the development of hyperglycemia in these mice. Eighty percent of the NOD females develop hyperglycemia at the age of 12 weeks, while males develop hyperglycemia later around 20 weeks of age.[96] Db/db mice developing T2D model are homozygous for the mutation ($Lepr^{db}$) leading to spontaneous diabetes and exhibit hyperglycemia at the age of 8-10 weeks (300mg/dl). The db/db ($Lepr^{db}$) females become hyperglycemic as early as 3-4 weeks of age. In addition to hyperglycemia, these mice are also widely used as a model of obesity and metabolic diseases.[97] Recently developed Kimba mice are a transgenic line (tr029VEGF) that mimics NPDR and mild PDR.[98] Another genetically modified Akimba mice are the newly generated model for comprehensive study of the mechanism of DR. These mice are generated by crossing the $Ins2^{Akita}$ and the Kimba mice resulting in the $Ins2^{Akita}/VEGF^{+/-}$ genotype.[99] They mimic early molecular and advanced microvascular changes in the pathology of DR.

In addition to rodent genetic DR models, *vhl* mutant zebrafish and transgenic zebrafish (Fli-EGFP-Tg) exposed to hypoxic conditions are also the novel genetic models of DM.[100,101]

Neovascularization model

The most critical pathologic findings of PDR are neovascularization, hemorrhage, and fibro-vascular proliferation observed in the vitreous and the retina, leading to traction retinal detachment and vitreous hemorrhage.[102] The oxygen-induced retinopathy (OIR) in rodents is an accurate and reproducible model of vascular proliferative changes in the retina.[103] In this model, hypoxia-driven vascular proliferative changes are similar to those seen in retinopathy of prematurity, age-related macular degeneration, and diabetic retinopathy. The OIR in canine and rat models were the first described in early 1950s. In canine models, Arnall Patz and colleagues investigated the effects of hyperoxia on the retinal vessel development to study proliferative retinopathy.[104,105] To develop a canine model, one-day-old pups were exposed to hyperoxia for 4 consecutive days. In early 1990s, this approach was reintroduced in rodents by Dr. Smith and her colleagues and has gained more popularity. In addition to OIR canine and rodents, the aberrant angiogenesis has also been reported in zebrafish, rabbit, and monkey models (Table1.).

The rodent OIR model is the most common approach to investigate the effect of hypoxia on the retina because it resembles the characteristics of human retinal proliferative changes.[103,106,107] As the rodent retinal vasculature develops in the first two weeks of birth, researchers can leverage this opportunity to analyze the aberrant vascular development triggered by hypoxia. In this model, hypoxia is induced at p7 after the regression of hyaloid vessels to avoid the development of mixed hyaloidopathy. The rodent pups were then exposed to to hyperoxia (75% oxygen) for five consecutive days from p7 to p12, and then observed at room air from p13 to p17.[103] The peak changes of neovascularization were seen at p17 which were resolved by p25. The C57BL/6 mice or

the Sprague Dawley (SD) rats are the common strains employed in this model due to their neovascular susceptibility to hypoxia.[106-108]

Cellular signaling changes in the pathobiology of DR

Insulin signaling in diabetic retina

Rat models. The basal insulin receptor (IR) signaling has been extensively studied in the STZ-induced diabetic SD rat retina. It was observed that phosphorylation of insulin receptor (IR) in the hyperglycemic retinas remained unchanged up to 8 weeks post-injection, but its kinase activity was reduced by 25% as compared to controls. At 12 weeks post-STZ injection, both kinase activity and auto-phosphorylation of the IR were significantly decreased suggesting that the basal IR activity is diminished in diabetic retina. It was also demonstrated that IRS-2, PI3Kinase expression were significantly reduced at 12 weeks after the STZ injection.[109]

Mouse models. Kondo and colleagues observed important differences in insulin signaling between STZ-induced hyperglycemic models and db/db mouse models of DR. Specifically, the IR expression and the tyrosine phosphorylation were upregulated in the first week post STZ treatment in mouse retinas, but no changes were observed in 8 to10-week-old db/db mice. The IRS-1 expression was unaltered while the IRS-2 expression was increased in both db/db and STZ treated mouse retinas. In contrast, few studies reported reduction in IR phosphorylation and increase in the protein tyrosine phosphatase-1B activity (PTP1B) activity in the rod's inner segments 1 week post STZ

injection.[110] Analysis of phosphorylated PTP1B in these mouse retinas pointed out PTP1B as a promising therapeutic target to delay the neurodegeneration in diabetic retinas.[111] Reduced IR kinase activity as early as 12 weeks of hyperglycemia was also reported in study with $Ins2^{Akita}$ mice.[94]

Endoplasmic Reticulum Stress Signaling and Inflammation in the Diabetic Retina

Endoplasmic reticulum (ER) stress is one of the important components of the pathophysiology of the DR. All three branches of the unfolded protein response (UPR), specifically PKR-like ER kinase (PERK)–eukaryotic translation initiation factor 2α (eIF2α), inositol-requiring protein 1α (IRE1α)–X-box binding protein 1 (XBP1) and activating transcription factor 6 (ATF6) are activated in the diabetic retina.[26] Cellular stresses such as hypoxia and the glucose imbalance can trigger the UPR in diabetic retina.

Rat models. The ER stress markers are upregulated as early as 8 weeks after the onset of diabetes in the SD rats. For example, increase of apoptotic protein caspase 12, C/ERB homologous protein (CHOP), and phosphorylated c-Jun N-terminal kinase 1 (MAPK) was seen at 8 weeks post STZ-induced diabetes in rat retinas. Further, the expression of caspase 12 and MAPK were observed in ganglion cells, while the CHOP levels together with increased GFAP activity were detected in these STZ-treated retinas.[112] In another study with SD rats, there was increased expression of *chop* and *vegf* at 3 months after STZ injection. However, the differences in expression of *atf4* and *grp78* genes and their related proteins were not detected. These findings suggest that AFT4 might not be the only a signaling molecule responsible for the increased VEGF level in

diabetic retinas.[113] In contrast, immune-histochemical detection of HIF-1α, ATF6, XBP1 and CHOP in STZ -induced diabetic rat retinas showed elevated protein levels at 2 and 4 months. This elevation was accompanied by a decrease in autophagy marker LC3B-II levels indicating potential reduction in autophagy in diabetic retina of mice with 4 months of hyperglycemia.[114] The ZFD rat retinas demonstrated apoptotic protein BAX at 6 weeks of age.[115]

There were also important inflammatory changes across rodent models for DR. For example, the 6 week-old ZFD rat retinas showed increase in the levels of TNF-α and NF-kB.[115] Inflammatory proteins like clusterin, tissue inhibitor of metalloproteinase (TIMP)-1, β-2 microglobulin and von Willebrand factor were increased at 4 weeks and significantly overexpressed at 3 months post-STZ injection in the SD rat retinas. In addition, the fibroblast growth factor-2 overexpression was detected in ONL of the diabetic rat retinas at 3 months post-STZ. This group also showed that inflammatory changes were strain dependent in the rats. Thus, as compared to Long Evan and Brown Norway rats, the SD rats have inflammatory changes similar to ones found in human diabetic retinopathy.[116] In the OIR SD rat retinas, the activation of inflammatory markers was reported as early as p16.[106,107]

Mouse models. Using STZ-induced DR mouse retinas, Chung et al. and Zhong et al. have also reported interesting findings on ER stress activation and inflammation. The diabetic mouse retinas had increased expression of GRP78, pPERK, CHOP, VEGF and peIF2α 4 weeks after STZ-induced hyperglycemia.[117,118] The inflammatory gene expression is altered in the diabetic retinas deficient in ATF4.[118] In addition, the MCP-1

and TNF-α were simultaneously increased in these retinas during the 4-week period.[117] The study also highlighted that the ER stress markers, though peaked at 4-weeks, were lower at 6 weeks post-STZ. The Akita mice had increased levels of p-elF2α and GRP78 proteins in addition to elevated IRE-1 and PERK pathways and the increase in TNFα at 12 weeks of age .[27,119] Elevated levels of GRP78, ATF4 and peIF2α were also found in the OIR model at p15.[27,34] Fifteen-month-old db/db (Lepr ^{db}) mice had increased expression of GRP78, p-IRE-1α, CHOP, Caspase-3 & ATF4 in the retina along with microglial activation and elevated HIF-1α/ VEGF levels.[120] The retinal autophagy was also reported to be increased at 40 weeks in the other diabetic models of hypercholesterolemic mice.[121] Overall, these studies emphasized that alterations in the cellular molecular signaling often preceding the retinal pathophysiological events. These findings suggest that dysfunctional insulin signaling, ER stress response, and inflammation are involved in the pathological progression of DR and can be targeted to develop novel cellular therapies for DR.

Retinal cell death and gliosis

Rat models. GFAP activation is often demonstrated in the rodent diabetic retinas. An increase in GFAP immunoreactivity was observed in STZ induced hyperglycemic rat retinas early at 6-7 weeks,[122] and later at 8-16 weeks post injection.[114,122] The retinal cell loss and functional changes have also been reported in the STZ induced diabetic rat retinas as early as 2 weeks and later after 24 weeks post STZ injection. In the OIR rats, thinning of the outer segments (OS) of photoreceptors ,and reduction in the INL and IPL thickness have been reported at p18.[123,124] Moreover, the diabetic rat retinas showed

increased apoptotic cells in the ONL, INL, and RGC layer between 12-16 weeks post STZ injections resulted in decrease in a total retinal thickness.[114,125] At 4 weeks post STZ treatment , ribbon synapses and post synaptic terminals of photoreceptors showed degenerated mitochondria while RGCs developed necrosis.[125] The WBN/ Kob rat retinas have shown photoreceptor degeneration at 4 weeks [88] while STZ-induced diabetic rats manifest severe loss of photoreceptors at 12 and 24 weeks.[125] Interestingly, the RPE degeneration was also detected in diabetic retinas. For example, 4-month old diabetic BB rat demonstrated the hyperglycemia-induced RPE degeneration with focal necrosis.[126]

The SD rat retinas showed increase in the thickness of the retinal inner limiting membrane (ILM), and degenerating photoreceptors and the OPL at 28 months after hyperglycemia induction.[126] Extensive glial activation, photoreceptor outer segment (OS) degeneration and decreased RPE-65 were also reported in 32 week-old ZFD retinas.[127] Further, 9 months after hyperglycemia, decrease in the thickness of the INL, ONL , and the RPE layer have been reported in the retinas of OLETF rats.[91] The hyperglycemic spontaneously diabetic Torii (SDT) rats showed retinal detachment and fibrous proliferation after 50 weeks post hyperglycemia induction.[92] Recently, in a pre-diabetic rat model, the reversible changes in retinal pathology such as thinning of the inner retina without vascular changes was reported.[128] Finally, in the OIR SD rat retinas, multiple studies have demonstrated Müller cell reactivity and the thinning of the INL and IPL at p18.[123,124,129]

Mouse models. STZ-induced diabetic mice have shown the RGCs loss as early as 6 to 12 12 weeks.[130] Another study conducted with C57BL6/J mice showed the apoptotic

RG cell death at 14 weeks post STZ induced diabetes while decrease in the thickness of total retina was observed earlier at 10 weeks post STZ treatment. They also observed that the number of RGC apoptotic positive cells measured by TUNEL were 25% higher as compared to control retinas.[131] However, the RGC density across the retina varied at 20 weeks post STZ treatment.[132] Few studies on $Ins2^{Akita}$ mice detected early cone photoreceptor cell loss at 3 months along with reduction in IPL, INL, and RGCs at 22 weeks and reduction in photoreception pre-synaptic and post-synaptic ribbons at 36 weeks of hyperglycemia.[94,133] Similarly, the OCT analysis of 16-week or 28-week old diabetic db/db mice retinas showed the thinning in NFL and RGC layer at the rate of 0.104 μm per week resulted in reduction of the total retinal thickness by 28-week.[132,134] The 28-week old diabetic db/db mice also showed TUNEL positive photoreceptor cells and reduction in the ONL. STZ-induced hyperglycemic mouse retinas manifested GFAP overexpression in retinal astrocytes as early as 5 weeks post STZ treatment while Muller cell gliosis was not seen even after 15 months of DM.[135,136] In the OIR mouse model, there is a reduction in the total retinal, INL and IPL thicknesses as well as distorted photoreceptor OS, neuronal loss, hyperactivity of Müller cells, microglial activation at p18 .[137]

Functional changes in the neural retina

Rat models. Several studies have reported ERG findings in diabetic SD rats. First, there is a delay in the implicit time detected at 4-7 weeks post STZ. Second, a decrease in the a- wave of the scotopic ERG amplitude was detected at 10 weeks while the b- wave amplitude was found to be reduced only at 25 weeks after induction of

hyperglycemia.[53,122,138,139] Similar ERG findings were observed in SDT rats at 44 weeks post STZ treatment.[140,141] The OIR rats also demonstrated decreases in the a and b wave amplitudes at p18.[123,124,129]

Mouse models. The ERG experiments in STZ injected mice have shown decrease in the implicit time for OP at 6 weeks and reduction in b-wave amplitude at 6 months after induction of hyperglycemia.[115,142,143] Moreover, development of T2D models like db/db (Lepr ^{db}), Ins2^{Akita}, and high fat diet induced DM mice have also reported a chronic timeline of 6, 9 and 12 months, respectively to observe similar ERG changes.[85,133,144,145] On the other hand, the OIR mice showed reduced a and b wave to OIR rats at p18 similar.[137]

Microvascular changes and neovascularization

Rat models. In albino rats (Wistar–Kyoto), the BRB disruption occurs as early as 2 weeks post STZ injection. Several studies have reported early neovascular changes such as adherent leukocytosis and thickened basement membrane that occur at 8 and 12 weeks, respectively.[57,146,147] Gong et. al reported that neovascularization occurring in the STZ injected SD can be observed at 3-4 months after induction of hyperglycemia. The neovascularization in these animals correlated with the increase in VEGFR1 and VEGFR2 expression levels.[148] These findings were also observed in the Alloxan induced diabetic rat retinas where leukocytosis and neovascularization were reported at 2 and 9 months after induction of hyperglycemia, respectively. Later at 2 months of sustained hyperglycemia the authors observed pericyte loss, formation of acellular capillaries and the basement membrane thickening.[149,150] In contrast to previous data, several studies

reported that the BB rat retinas manifested these changes as early as 4 months, while BB, ZDF and OLETF rat retinas demonstrated BRB breakdown and the pericyte loss at 6- 8 months.[86,87,91,151,152] Downie and colleagues reported increase in extraretinal neovascularization and impaired pericyte distribution in the OIR SD rat retinas as early as p18.[124]

Mouse models. The STZ mice developed microvascular changes early in the course of diabetes than the STZ-induced hyperglycemic rats. For example, vascular permeability measured by imaging of the distribution of fluorescein-conjugated dextran, was compromised as early as 8 days post STZ injection.[153] However, decrease in arteriolar diameter and velocity were reported at 4 weeks and 8 weeks post STZ injection respectively.[75] The pericyte loss and acellular capillaries were observed in STZ injected mice from 6 to 9 months later in the course of DR.[135] The $Ins2^{Akita}$ mice demonstrated increased leukocytosis at 8 weeks, compromised vascular permeability at 12 weeks , microaneurysms at 6 months and neovascularization at 9 months of hyperglycemia[94,144] In Kimba mice, abnormal blood vessel development was seen early at p28 while increase in vascular permeability and adherent leukocytes was observed at 6 weeks of age. Additionally, loss of retinal capillaries, neovascularization, increased avascular area and alteration in the vessel length and pericyte loss were reported from 9 weeks to advanced age of 24 weeks.[98,154] Akimba mice were specifically developed to study the microvascular changes of DR and showed these changes at the early age of 8 weeks old.[99]

The db/db mice resembling T2D showed increase in vascular permeability and basement thickness at 13-14 weeks of hyperglycemia.[155-157] Further, high fat diet-

induced T2D mouse model demonstrated pericyte loss, blood retinal barrier disruption and vascular leakage at 12 months of age.[85] Finally, the OIR mice developed irregular blood vessel and reduction in the retinal inner and deep plexuses at p18, mimicking retinal proliferative events triggered by hypoxia in patients with diabetic complications.[158]

Pathological changes in the non-rodent animal models of DR

Apart from rodents, several other species have been used to develop DR models. Characteristics of some of the non-rodent DR models reported over the past two decades have been discussed in this section.

Rabbit

Forty percent of diabetic rabbits with average blood glucose levels of 200mg/dl develop retinopathies after 135 days of initial STZ injections. These retinopathies were classified as degree "3" of retinal pathology representing serious vasculopathy with retinal hemorrhages, vascular lesions and venous thrombosis while 50% were classified as degree "4" corresponding to proliferative retinopathy.[78] In another rabbit angiogenesis model created by the implantation of human recombinant VEGF at dose of 30 μg, the vitreous showed abnormal tortuous blood vessels followed by vascular leakage at 14 days, and the neovascularization at 21 days of transplantation.[159]

Zebrafish

After 12 days of exposure to hypoxia, the zebrafish retina demonstrated new sprouts in the optic capillary plexus and formation of capillary tips.[100] In the *vhl* mutant zebrafish, the increase in aberrant blood vessel formation and the VEGF mRNA expression were observed at 2 days post-fertilization.[101] Alternatively, immersions of zebrafish in a high-glucose solution over a period of 30 days caused irreversible reduction in the IPL and INL of zebrafish retina.[160] It has been emphasized that the genetic manipulation and easily achievable hypoxic conditions with this model favors the use of zebrafish as a model for DR.

Monkey

Primate retina is the closest animal model for mimicking the normal morphology and DR pathology of the human retina. The implantation of 100 μg of human recombinant VEGF in the rhesus monkey resulted in increase in vascular permeability, breakdown of BRB and the tortuosity of the blood vessels in the vitreous at 2-3 weeks post-treatment.[159] The STZ induced diabetic monkey model demonstrated retinal pathology after 6-years of hyperglycemia duration. The primary retinal findings in these diabetic animals were cotton-wool spots, macular atrophy, arteriolar occlusion, focal intraretinal capillary leakage and capillary dilatation.[161] In addition to STZ induced hyperglycemia, the markers similar to diabetic retinal pathology were also observed in mild hypertensive rhesus monkey and were categorized into three stage of retinopathy: 1) Stage I- microvascular abnormality with capillary dropout; 2) Stage II- vascular leakage, intraretinal exudates and cystoid degeneration with cotton wool spots; and 3) Stage III- vascular occlusion and retinal atrophy.[162]The above stated retinal findings slowly

developed in the T2D obese monkey over the period of 1.25 to 15 years.[163] The functional changes in the retina such as decline in the mERG recording, reduced a-wave and oscillatory potential were observed in the aged diabetic rhesus monkey with T2D over 5 years.[164]

A recent diet-induced primate model of marmoset monkey developed DR within 2.5 years as compared to other models developing retinal phenotype over the period of 15 years. The marmoset monkeys are smaller than the rhesus macaques, and easier to be maintained. In addition to manifesting a retinal pathological phenotype make these animals as an excellent model of DR.[84]

Tree shrew

Tree shrews are closely related to the primates and have cone-dominant retinas. Tree shrew model generated with either 300mg/kg bw single dose,[79] or two doses of 80 mg/ kg bw,[165] have resulted in hyperglycemia within a week post STZ injection thus mimicking T1D. Unfortunately, the validation of tree shrews as a model of DR is still under investigation. The only reported findings with the T1D tree shrew retina is the presence of corneal autofluorescence within 7 days as a results of a single STZ dose injection of 300mg/kg bw.[79]

Dog

Induction of hyperglycemia with high-galactose diet is the most common method for development of DR in dogs. Dogs fed with high-galactose diet develop DR changes similar to ones found in human DR pathology and were reported as the first animal model

to develop both NPDR and PDR.[166] For example, the pericyte loss, an NPDR marker, is developed in these animals at 9 months post STZ injections. The PDR complications such as hemorrhages, microaneurysms, basement membrane (BM) thickening, vitreous detachment, and neovascularization can be developed in this model within 28 to 68 months post STZ treatment.[166,167]

Swine

Diabetic pigs are another model of DR. Their retinas have many similarities with human retinal tissues. Alloxan-induced T1D and diet-induced T2D pig model are frequently used models of DR. Alloxan treated pig retinas developed pericyte loss and BRB breakdown at 20 weeks after hyperglycemia.[168] In contrast, another study found that Alloxan induced DM resulted in the Müller cell contraction-promoting activities in the vitreous at 30 days after induction of hyperglycemia. [169] These findings suggested that swine Müller cell contraction-promoting activity and resultant retinal detachment at advanced stages of diabetes are similar to the changes seen in human retinopathy. In the combination model of DM and hypercholesteremia (DMHC), at there was increased BRB permeability, gliosis, microglial activation, and decreased retinal thickness at 24 weeks.[170] Kleinwort et al. reported that intraretinal microvascular abnormalities and central retinal edema were observed in swine DR model 2 years after the onset of hyperglycemia.[171] Lim et al. recently reported an innovative approach where the 4-month-old Ossabaw pigs developed chronic DM by feeding the with the western (high-fat/high-fructose corn syrup/high-calories) diet for 10 weeks. These animals developed

retinal INL disruption, thickened BM, pericyte ghosts, acellular capillaries and increased fibronectin expression at the age of 6 months.[172]

Cat

The major drawback of DR studies in large animals is the delay in development of histological features, making large animals less attractive species. Hatchell and colleagues were first who developed the feline diabetic model using pancreatectomy and monitored them for 9 years with regular checks for hyperglycemia every 6 months. They subsequently reported presence of thickened BM at 3 months, microaneurysms at 5 years, and neovascularization around 6.5- 8 years post-surgery in the diabetic cat retina.[173]

Limitation of DR models

In this review, we identified the discrepancies in the rodent models of DR induced by STZ injections. The cellular pathology upon long-term development of diabetes was not uniform across different research groups. For example, Martin and colleagues reported retinal cell loss while Feit-Leichman and co-authors observed no changes in the number of retinal cells in STZ treated mouse retinas.[131,135] These findings could be attributed to different strains used for the development of STZ-induced hyperglycemia. For example, some rodents have consistent high blood glucose level across the studies, while others require additional dosages of STZ over time. Interestingly, STZ induced hyperglycemia is gender dependent. Male mice are more prone to STZ induced pancreatic damage as compared to females, in which the STZ effect is inhibited by the female hormone estrogen.[174] Saadane and colleagues recently reported that increasing

the STZ dose by almost 36 % yields hyperglycemia levels and subsequent retinal pathological changes in females similar to ones found in males.[175]

Moreover, in our experience, 20% of the STZ injected males developed normal blood glucose after 20 weeks post STZ, while 45% did not develop hyperglycemia even after 6 weeks with a single high dose of STZ injection. Despite these limitations, the chemical induction of hyperglycemia is still the fastest method to induce diabetes as compared to spontaneous T1D and T2D models. The OIR mouse model is particularly strain dependent model and the maintenance of genetic background in experimental mice is of utmost importance.[108] The rodent models, in comparison to large mammals, provide better accessibility for molecular changes, genetic manipulation, shorter duration to develop diabetes and easy handling. The only advantage of using primates and other large animals is their close resemblance to human retinal physiology. Thus, choosing appropriate animal model for DR research is a challenging process and requires a careful evaluation of all available models and related research resources.

Conclusion

In conclusion, the current review emphasizes the needs f for considering several factors before deciding on the use of DR model. We highlighted the variability in the duration of the study, methods of induction, molecular techniques, and the markers of diabetic retinopathy across different animal models. Because not all animal models accurately mimic the human retinal pathology, it is important to evaluate the strength and weakness of each animal model. (Figure 1).

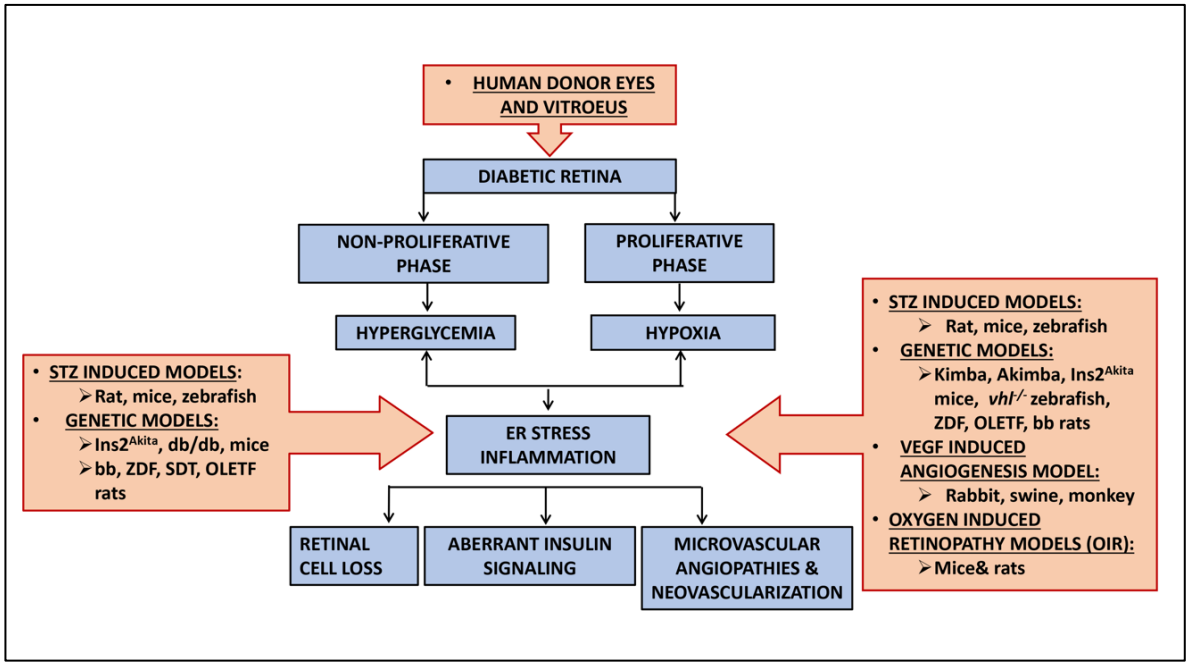

Figure 1. Summary of animal models of diabetic retinopathy. Diabetes – associated ocular complications are divided into non- proliferative and proliferative phases. These phases are governed by hyperglycemia and eventually hyperglycemia-driven hypoxia. The diabetic retinopathy models include pharmacological models, spontaneously diabetic models and finally hypoxia-induced models.

Table 1: Summary of the animal models of DR

A	**Hyperglycemia Induction**				
	Method	**Species**	**Dosage**	**Hyperglycemia**	**References**
1.	Streptozotocin (STZ)	mouse, rat, rabbit, tree shrew, monkey, cat	mouse and rat- IP 40-80mg/kg (5 days), mouse- IP 150-200mg/kg (single dose), rat- IP 30-80mg/kg (single dose), rabbit- IV 110mg/kg (single dose), tree shrew- IP 80 mg twice a week apart and IP 300mg/kg (single dose).	mouse & rat approx. 1-week post STZ	[73-79, 160,164]
2.	Alloxan	mouse, rat, rabbit, swine, dog			[68,76,82,167-168]
3.	Pancreatectomy	cat, monkey, dog			[81,83,172]
4.	High galactose /fat type 2 diet	mouse, rat, dog, swine, zebrafish, monkey			[71,81,84-85,159,162]
B	**Spontaneous Hyperglycemia**				
	Mouse			Hyperglycemia	References
1.	Ins2Akita mouse: Type I DM, mutation in insulin			4 weeks	[93-94]
2.	Non-obese mouse (NOD): Type I DM, autoimmune model			12 weeks	[95-96]
3.	db/db (Leprdb) mouse: Type II DM			8-10 weeks	[97]
4.	Kimba mouse: Transgenic mouse (tr029VEGF)				[98]
5.	Akimba mouse: $Ins2^{Akita}$ / VEGF $^{(+/-)}$			4 weeks	[99]
	Rat			Hyperglycemia	References
1.	Biobreeding rats: Type I DM, autoimmune model			3 months	[86-87]
2.	Wistar Bonn/Kobori (WBN/Kob) rats: Type II DM			9 months	[88]
3.	Zuker diabetic fatty (ZDF) rats: Type II DM			5-10 weeks	[89-90]
4.	Otsuka Long- Evan Tokushima fatty (OLETF) rats: Type II DM			5 months	[91]
5.	Spontaneous diabetic torii (SDT) rats: Type II DM			5 months	[92]
C	**Neovascularization**				
	Mouse				References
1.	Oxygen induced retinopathy (OIR)				[103]
2.	Kimba mouse				[98]
3.	Akimba mouse				[99]
	Rat, Canine				References
1.	Oxygen induced retinopathy (OIR)				[104-105,107]
	Rabbit				References
1.	Implantation of human recombinant VEGF in the vitreous				[158]
	Zebrafish				References
1.	Angiogenesis				[100,101]
	Monkey				References
1.	Implantation of human recombinant VEGF in the vitreous				[158]

Table 2: Summary of the pathological changes in different models of DR

A. Molecular Signaling				
	Model	**Changes**	**Duration of hyperglycemia**	**References**
1.	STZ Rat	Elevated CHOP, Caspase 12, MAPK retinal cytokines	8 weeks	[112-114, 116,109]
		Reduced IR kinase activity	8 weeks	
		Elevated retinal cytokines	3 months	
		Reduced IR kinase activity & auto phosphorylation and downregulation of IRS-2 & PI3K	3 months	
		Upregulation of HIF-A, ATF-6, XBP1	4 months	
2.	ZFD Rat	Elevated Bax, TNF-α and NF-kappaB	6 weeks	[115]
3.	OIR Rat	Elevated VEGF, PDEG & TNF-α	P16	[106-107]
4.	STZ Mouse	Upregulation of GRP78, pPERK, CHOP, VEGF, pEIF2α, retinal cytokine & TNF-α	4 weeks	[27,110-111 , 117-119]
		Elevated IR expression and tyrosine phosphorylation; upregulated IRS-2 and reduced PDK1/ AKT protein levels & phosphorylation	1 week	
		Reduced IR phosphorylation	1 week	
5.	Ins2Akita Mouse	VEGF and TNF-α elevation, increased mRNA expression; protein expression of GRP78 and elevated peIF2α and ATF4 and reduced IR kinase activity	12 weeks	[27,94,119]
6.	Leprdb (db/db) Mouse	Increased IRS-2 expression and reduced PDK1/ AKT protein levels and phosphorylation	10 weeks	[120,121]
		GFAP activation, increased expression of HIF-A, VEGF, GRP78, p-IRE-1, CHOP, Casapase-3 and ATF4	15 months	
B. Microangiopathy				
	Model	**Changes**	**Duration of Hyperglycemia**	**References**
1.	STZ Rat	Blood retinal barrier disruption	2 weeks	[57,146-148]
		Adherent leukocytes	8 weeks	
		Thickened Basement Membrane (BM)	12 weeks	
		Neovascularization	3-4 months	
2.	Alloxan Rat	Leukocytosis	2 months	[149-150]
		Neovascularization	9 months	
		Pericyte loss, acellular capillaries and BM thickening	12 months	
3.	BB Rat	Basement membrane thickening	4 months	[86-87,151]
		Blood retinal barrier breakdown	6 months	

		Pericyte loss	8 months	
4.	ZDF Rat	BM thickening, pericyte loss and acellular capillaries	6 months	[91]
5.	OLETF Rat	BM thickening, pericyte loss and acellular capillaries	9 months	[152]
6.	OIR SD Rat	Increased extra retinal neovascularization and impaired pericyte distribution	P18	[124]
7.	STZ Mouse	Increased vascular permeability	8 days	[75,135,153]
		Decreased arteriolar diameter and velocity	8 weeks	
		BM thickening	4 to 15 months	
		Pericyte loss, acellular capillaries and pericyte ghost	6-9 months	
8.	Ins2Akita Mouse	Leukocytosis	8 weeks	[94,144
		Increased vascular permeability	12 weeks	
		Blood vessels in the outer plexiform layer (OPL) and microaneurysms	6 months	
		Acellular capillaries, BM thickening and neovascularization.	9 months	
9.	Kimba Mouse	Abnormal blood vessel development around photoreceptor	P28	[98,154]
		Increased vascular permeability and adherent leukocytes	6 weeks	
		Loss of retinal capillaries, neovascularization, increased avascular area and alteration in the vessel length	9 weeks	
		Pericyte loss	24 weeks	
10.	Akimba Mouse	Microaneurysms, neovascularization, blood vessel constriction, beading, vessel edema, capillary dropout and new vessel formation it the ONL	8 weeks	[99]
11.	OIR Mouse	Irregular blood vessel development and reduced inner retinal plexus and deep plexus	P18	[158]
12.	Db/db Mouse	Increased vascular permeability and BM thickening	13-14 weeks	[155-157]
		Pericyte loss	18 weeks	
		Acellular capillaries	26 weeks	
13.	High Fat diet Mouse	Pericyte loss, blood retinal barrier disruption and vascular leakage	12 months	[85]
C. Retinal Cell Biology				
	Model	**Changes**	**Duration of Hyperglycemia**	**References**

1.	STZ Rat	Decreased pre and post synaptic photoreceptor ribbon synapses	4 weeks	[114,122, 125]
		Increased GFAP reactivity	6-7 weeks	
		Loss of ONL, INL, GCL	12-16 weeks	
		Severe photoreceptor cell loss	24 weeks	
2.	WBN/Kob Rat	Photoreceptor degeneration	4 weeks	[88]
		Severe OS and ONL degeneration	5 months- 14 months	
3.	BB Rat	RPE degeneration	4 months	[126]
4.	ZDF Rat	Decreased OS, damage to amacrine cells and RPE with gliosis	32 weeks	[127]
5.	OLETF Rat	Decreased INL and photorecptor cells	9 months	[127]
6.	OIR Rat	Reduction in OS, INL, IPL, total retinal thickness, astrocytes and increased muller activity	P18	[123-124]
7.	High galactose fed Rat	Increased gliosis and reduced INL and OPL	28 months	[126]
8.	STZ Mouse	GFAP hyperactivity	5 weeks	[130,132, 135-136]
		Reduced ONL, INL thickness	6-14 weeks	
		Total retinal thickness reduced	20 weeks	
		No retinal cell loss and gliosis	8-12 months	
9.	Ins2Akita Mouse	GFAP hyperactivity	8 weeks	[94,133]
		Reduced IPL, INL and cone photoreceptors	3 months	
		Reduced RGCs	22 weeks	
		Decreased presynaptic and post synaptic photoreceptor ribbons	36 weeks	
10.	db/db Mouse	GFAP (8 weeks), (10-16 weeks) and	8 weeks	[132,134]
		Reduced NFL and RGCs	10-16 weeks	
		Reduced total retinal thickness	28 weeks	
11.	Akimba Mouse	Photoreceptor cell death	25 weeks	[99]
12.	OIR Mouse	Total retinal thickness reduction, distorted photoreceptor OS, neuronal loss, hyperactivity of Müller cells, microglial activation and disrupted INL and IPL	P18	[137]

D. Electrophysiology

	Model	Changes	Duration of Hyperglycemia	References
1.	STZ Rat	Decrease in OP amplitude	2-7 weeks	[122,153, 140-141]
		Decrease in OP implicit time	7 weeks	
		Decreased a- b wave amplitude	10-12 weeks & 44 weeks	
2.	OIR Rat	Decreased a and b wave amplitude	P18	[123-124 ,129]
3.	STZ Mouse	Reduced OP amplitude and implicit time	4-6 weeks	[115,142-143]
		a and b wave amplitude reduced	6 months	
4.	Ins2Akita Mouse	Decreased OP amplitude, delay in the OP and decreased b wave	9 months	[133-134]
5.	Db/db Mouse	Delay in the b wave, delay in the OP implicit time and decreased amplitude of both photopic and scotopic b wave	16-24 weeks	[145]
6.	OIR Mouse	Significant decrease in the amplitude of a and b wave	P18	[137]
7.	High fat diet Mouse	decreased OP amplitude	12 months	[85]

CHAPTER 3

ROLE OF TRIB3 IN PROGRESSION AND PATHOLOGY OF DR

Introduction

Treatments of severe NPDR with intraretinal hemorrhages and PDR are often focused on vascular abnormalities presented as micro aneurism, vascular leakage, capillary blockade and dropouts, acellular capillaries, and aberrant angiogenesis. The mild and moderate forms of NPDR in patients are controlled by BGL and blood pressure (BP). Although clinical evidence clearly demonstrates that the management of BGL implemented early in the course of diabetes may reduce the development and progression of NPDR,[11] a breakthrough treatment that interferes with early DR stages, thus preserving retinal integrity against subsequent damage and preventing progression of DR, remains an unmet critical need.

The tribbles homolog 3 (TRIB3) protein has been proposed as a regulator of insulin signaling (IS) in diabetes. TRIB3 is a metabolic stress indicator and is a critical "stress adjusting switcher," endorsing cell homeostasis shift to metabolic dysfunction. It functions by regulating AKT and AKT/mTOR phosphorylation through pseudokinase activity and controlling autophagy flux and protein degradation.[38] TRIB3 overexpression has been linked to aberrant angiogenesis. In a study that employed human umbilical vein endothelial cells (HUVECs) treated with oxidized phospholipids, the induction of VEGF strongly correlated with the highest level of TRIB3.[48] Mechanistically, TRIB3 reportedly

regulates the nuclear factor kappa B (NF-kB) pathway,[176] promotes activation of TGF-β1 signaling,[177] controls cytokine expression,[178] and governs macrophage health.[179]

Recent studies conducted in patients with T2D revealed that the expression of a single nucleotide polymorphism, Q84R in TRIB3 can increase the risk of diabetes and the likelihood of carotid atherosclerosis in part through the effects of abdominal obesity, hypertriglyceridemia, and insulin resistance in the body.[180] These studies have also emphasized that the variant with arginine at position 84 manifests a "gain-of-function" effect due to TRIB3's superior pseudokinase activity in binding AKT and inhibiting insulin-stimulated AKT phosphorylation (Thr308, Ser473).[41,181-183] TRIB3 mRNA and protein are significantly elevated in human T2D islets, and a substantial reduction of C-peptide has been observed in the plasma of Q84R allele carriers.[184] Q84R polymorphism frequently manifests not only as aberrant insulin signaling, but also with vascular dysfunction and metabolic abnormalities.[185] All of these events occur in the diabetic retina as well.

Furthermore, clinical research conducted with human fibrovascular membranes excised from patients with PDR showed elevated levels of TRIB3.[63] However, the exact mechanistic link between TRIB3 overexpression and disease development and progression in DR has not been established. In this study, we explored the effects of abrogated TRIB3 expression in the survival of retinal ganglion, endothelial cells, and pericytes in diabetic mice. Our data reveal distinct underlying mechanism that involves reduced hypoxia regulated GLUT1 and EGFR signaling, which contributes to diminishing neovascularization in DR. Using mouse models of pharmacologically induced diabetes and hypoxia-driven proliferative retinopathies, we demonstrated for the

first time that TRIB3 is a potentially novel therapeutic target that may accelerate the onset and progression of DR to proliferative stages in humans.

We planned to test out hypothesis in three independent specific aims.

1. To investigate role of TRIB3 in early metabolic and inflammatory changes in diabetic retina.

The objective of this aim was to identify whether hyperglycemia can induce the expression of TRIB3, the UPR mediator in diabetic retina. Though the link between the UPR activation and hyperglycemia is known for diabetic retinopathy, the question of whether TRIB3 is upregulated and what the consequences of its upregulation in diabetic retinas are still remained unanswered. Therefore, in aim#1, we hypothesized that TRIB3 expression is elevated in diabetic retinas and its ablation can attenuate early metabolic changes in diabetic retina. First, using TRIB3KO mice, we investigated whether TRIB3 affects glucose transport and metabolism in diabetic retina. Then we examined whether TRIB3 ablation changes the inflammatory profile of retinal cells in diabetic environment.

2. To investigate role of TRIB3 in the retinal neuronal and vascular health in mice with NPDR.

The objective for this aim was to understand the role of TRIB3 in the promoting a neurovascular deficit in diabetic retina. Prior literature has shown that neurodegeneration preceded the vascular damage in diabetic retinopathy.[132] Therefore, we decided to examine whether TRIB3 ablation can rescue the neural cell loss, in general and the RGC, in particular. We further examined whether rescued RGCs retained the physiological function. Given that one of the hallmarks of early vascular damage in diabetic retina is pericyte loss and increase in acellular capillaries, in the aim #2, we next

investigated whether TRIB3 plays role in pericyte apoptosis and whether its ablation can support pericyte and endothelial cell survival in diabetic retinas.

3. To investigate the role of TRIB3 in aberrant neovascularization and activation of gliosis in hypoxic retinas.

The proliferative phase of DR is driven by hypoxia. The oxidative stress and ischemic damage occur in response to hypoxia-mediated VEGF expression resulting in aberrant vascular growth and neovascular tufts formation. Muller cells in the retina are also sensitive to hypoxic changes. Hypoxic stress promotes gliosis and VEGF upregulation in these cells. Therefore, in aim #3, we hypothesized that TRIB3 ablation attenuates aberrant neovascularization and gliosis in hypoxic retinas. In addition, using the in-vitro model of human Muller cells, we revealed HIF1α as the downstream target of TRIB3 that mediates the TRIB3 –induced VEGF upregulation.

Development of mice hyperglycemic model using STZ: (Aim #1& 2)

Mice were housed at the University of Alabama (UAB) animal facility in a 12-hour light-dark cycle condition with unlimited access to food and water as per the UAB-IACUC protocol #09793 and the Association for Research in Vision and Ophthalmology guidelines on the use of animals in ophthalmic and vision research. TRIB3KO mice were generated as previously described,[186] and C57BL6J mice were purchased from the Jackson laboratory. We intraperitoneally injected 8-week-old male TRIB3KO and C57BL6J mice with STZ for both Aims 1& 2. We first developed an acute DM mouse model to observe early metabolic and pro-inflammation retinal changes at 4-weeks. For the proposed Aim-1, we injected mice with 150 mg/kg bw single dose of STZ or vehicle

(0.1 M citrate buffer, pH 4.5). We extracted retinas at 4-weeks after injection to conduct RNA analysis as previously described.[109,111,118] We next developed non-proliferative chronic DM mouse model to explore cellular and neural damage 8 months post STZ. Therefore, for aim #2, we injected mice with five consecutive doses of 50 mg/kg bw of STZ or vehicle over 5 days.[44] Electroretinogram and histological analysis were conducted in these mice 32 weeks after injection.

Blood was initially collected via a tail vein, and fasting glucose levels were measured at 1-week post STZ to confirm hyperglycemia in both the STZ models using glucometer. The final measurement of fasting BGL was later conducted at the end of 4th week for the mice used in aim #1. We also measured retinal glucose levels (RGLs) using a calorimetric assay kit in the fourth week. To this end, mice used in aim #2 were analyzed for the fasting BGL every 3 weeks until 32 weeks. Additionally, HbA1c measurements using HbA1c kit were conducted at 15-weeks and 30-weeks post STZ (Supplemental Table 2). Hyperglycemia was considered achieved when the fasting BGL was above 250 mg/dl and >6.5% HbA1c. The animals did not require insulin injections.

Limitation of the STZ mouse model. As previously mentioned, the effect of STZ to induce hyperglycemia is sustained in the male mice only. Estrogens in females inhibit STZ effect eventually giving no rise in BGL .[174] The hyperglycemia in mice also seems to fluctuate over time. The mice might develop acute toxicity initially resulting in transient hyperglycemia and further recovery of BGL. The recovery from hyperglycemia raises the question of whether we should re-inject the mice with STZ after initial

recovery. To overcome these limitations, we used a) male mice only and b) the mice with sustained hyperglycemia throughout the experimental timeline.

Development of OIR mouse model and MIO-M1cells in the hypoxic conditions: (Aim #3)

The OIR model is one of the most reproducible models of retinal vascular proliferative changes occurring in retinopathy of prematurity, age-related macular degeneration and diabetic retinopathy.[103] Therefore, we employed the OIR mouse model to generate oxygen-induced retinopathy in C57BL6 and TRIB3 KO pups to study neovascular changes in addition to activated gliosis. The murine OIR model is a well-accepted model to investigate the effect of hypoxia. Therefore, we hypothesized that neovascularization resulting from hypoxia is delayed and revascularization occurs in the OIR mice deficient in TRIB3 and that direct cytoprotective mechanism is associated with regulation of VEGF expression. A hyperoxia chamber for oxygen exposure was used in the study. Pups were exposed to hyperoxia (75% oxygen) at p7 as described.[103] At p12, the pups were placed at room air until p17. The choice of time points was determined by the peak of neovascularization and the appearance of revascularization at p17 and p25 respectively.[103] Thus, it was important to terminate our experiments at p17. Two sets of pups with nursing mothers were placed in the chamber while control mother and pups stayed at room air.

MIO-M1 cells (immortalized human Müller glia cell line)[187] were used to develop a cellular model mimicking hypoxic events in the retinas of mice used aim #3. The MIO-M1 cells were cultured at 37°C in an atmosphere of 5% CO_2 in DMEM optimal

containing 25mM glucose supplemented with 10% fetal bovine serum (FBS) and 1% antibiotic solution.[187] MIO-M1 cells were incubated in the ANAEROgen (W-Zip compact) bags for 48 hours to maintain hypoxic conditions as previously reported.[188]

Limitations of the OIR model. OIR animal model is a widely used model to study the impact of hypoxia on angiogenesis, endothelial proliferation, and the role of VEGF in proliferative retinal vasculopathy and inflammation.[108] Although popular, this model has certain limitations. There is a variability in the generation of OIR model depending on the mouse strain.[103,108] So it is very important to maintain same genetic background in control and experimental animal groups. Therefore, both the experimental and control mice had the same C57BL6 background. Another limitation is the lethal effect of hyperoxia that may occur sometimes in adult mice.[103] Therefore we used surrogate mothers if needed.

Materials and Methods

The reagents and their catalog numbers and the suppliers are indicated in the Supplemental Table 1.

Quantitative real-time polymerase chain reaction (qRT-PCR) and western blot analysis

Four weeks post STZ injection, mouse retinas were isolated, and RNA was extracted using Trizol. cDNA was synthesized using the Bio-Rad iScript™ Reverse Transcription Supermix kit. A Thermo Fisher Quantstudio-3 machine was used to perform quantitative real-time polymerase chain reaction (qRT-PCR) using Thermo

Fisher TaqMan primers (Supplemental Table 1). Results were normalized to housekeeping Gusb and Gapdh genes and expressed as ratios of mRNA fold changes obtained in diabetic retinas normalized to own nondiabetic controls. For protein analysis, retinal protein extracts were isolated from the OIR and control pups at P13 and separated by polyacrylamide gel electrophoresis, as previously described.[189] Detection of proteins was performed using anti-VEGF, anti-glia fibrillary acidic protein (GFAP), and anti-b-Actin antibodies detecting 21 kDa, 50 kDa, and 42 kDa bands, respectively. Horseradish peroxidase (HRP) goat anti-mouse and infrared (IR) goat anti-mouse antibodies were used as a secondary antibody (Supplemental Table 1). Immunoblots were imaged and analyzed using the LICOR imager system. Differences in VEGF and GFAP levels in diabetic retinas are presented as ratios of band intensities normalized to nondiabetic controls.

Histological and immunohistochemical (IHC) analyses

Human diabetic (84-year-old) and normal (82-year-old) retinal tissues were obtained from the National Disease Research Interchange (IDRI). The tissues were processed for IHC analysis using anti-TRIB3 and anti-CD31 antibodies. Before IHC procedure sections were deparaffinized and rehydrated by immersing the slides through xylene and alcohol of descending concentrations.

Diabetic and the OIR mice were subjected to enucleation at 32-weeks post STZ injection and at P17, respectively. The eyes were fixed for 3.5 hours in 4% paraformaldehyde (PFA) and stored in 30% sucrose before cryopreservation in optimal cutting temperature (OCT) compound. Twelve-micron retinal sections were stained with

hematoxylin and eosin (H&E). A blinded-to-results investigator counted the numbers of retinal ganglion cells (RGCs) and the thicknesses of the inner nuclear layer (INL) and the outer and inner plexiform layer (OPL and IPL). The number of the RGC in 32-week post STZ retinal sections was counted as described in previous studies.[94,135,190,191] To evaluate the pericyte loss and formation of acellular capillaries, fixed eyes were washed in 1x phosphate-buffered saline (PBS) and the retina cups were excised, as previously described.[192] After digestion, separated retinal vascular tissues were placed on a slide, dried out at room air temperature, and stained with periodic acid-Schiff (PAS) reagent. IHC analysis was performed on retinal sections using anti-TRIB3, anti-GFAP, BRN3A, CD-31/ PECAM-1 and Vimentin antibodies (Supplemental Table 1). Co-localization of individual TRIB3 and CD-31/PECAM-1, TRIB3 and BRN3A or GFAP and vimentin proteins in the retinal sections were detected using fluorescent confocal microscopy. To count IBA1 positive microglial cells at P30, mice were injected intraperitoneally (IP)-with 10 µl/g (stock solution of 1 mg/ml) of lipopolysaccharide (LPS). The eyes were enucleated 24 hours after the injection, cryosectioned, and subjected to immunostaining with anti-IBA1 antibody. Blinded-to-results investigators counted the numbers of IBA1 positive cells in the retinal sections.

To detect neovascularization, the eyes of the OIR pups were enucleated at P17, fixed for 1.5 hours and incubated with Isolectin1B-4 diluted in 1x phosphate buffered saline (PBS) overnight. After washing with PBST (PBS +0.02% Triton), the retinal cups were dissected to obtain flat mounts. The flat mount images were used to run a computer program developed by Xiao et al. to analyze areas of neovascularization (NV) and vaso-

obliteration (VO). [193] The retinal NV and VO were expressed as ratios of the area with NV or VO to the whole mouse retina.

Retinal physiology

At 32 weeks post STZ injection, the mice were anesthetized to perform electroretinography (ERG) using an UTAS BigShot LKC machine to measure RGC function. Mice were exposed to 15 sweeps (1 sec apart) of white flash of 2.5 cd·s/m2 with a white background of 25 cd·s/m2 intensity and bright fixation to measure the photopic negative response (PhNR) amplitude. The waveforms were measured using LKC EM software.

Seahorse measurement

In Seahorse analysis, the extracellular acidification rate (ECAR) and oxygen consumption rate (OCR) were measured at baseline, post-glucose, and post-oligomycin injections as described in the study.[194,195] The eyes were collected 4 weeks post STZ injection in the cold 1X PBS. The retinal cup without RPE was dissected in Seahorse XF DMEM medium containing 5 mM HEPES and 2 mM glutamine with no glucose. Retina was placed with RGC layer facing down (Supplemental Figure 1) and secured by the capture screen using an insert tool in each well of a Seahorse XF24 Islet Capture microplate containing 50 µL of Seahorse XF DMEM. After securing retina in the microplate, 400 µL of the same dissecting medium were added to each well for final volume of 450 µL. The microplate was placed in the incubator at 37 °C for one-hour non-CO2 incubation before starting the stress test assay to achieve an even CO2 distribution.

The ports of the Seahorse XF24 Sensor Cartridge were loaded for a final well concentration of 10 mM glucose and 3.0 μM Oligomycin for measuring pH and O_2. Seahorse Wave Desktop Software was used to analyze the data.

Cell culture experiments

MIO-M1 cells (immortalized human Müller glia cell line developed by Limb and colleagues in 2002[187]) were cultured at 37°C in an atmosphere of 5% CO_2 in DMEM optimal containing 25mM glucose supplemented with 10% fetal bovine serum (FBS) and 1% antibiotic solution. Cells were exposed to hypoxia or treated with advanced glycosylation end products (AGE-BSA) at dose of 500 mM for 48-72 hours. Protein was extracted using RIPA lysis buffer. Western blot analysis was performed using the anti-TRIB3 antibody and horseradish peroxidase conjugated (HRP) goat anti-mouse secondary antibody.

Experiments were also performed with MIO-M1 cells overexpressing mouse TRIB3-DDK for 72 hours. The cells were harvested, lysed in the IP buffer, and subjected to incubation with TRIB3 anti-body for immunoprecipitation (IP) using agarose G-Plus beads. After verifying expression of TRIB3 by western blot (Supplemental Figure 2), the pull-down samples were submitted to UAB & CCC Mass Spectrometry & Proteomics Shared Facility for protein mass spectrometry and to identify the binding proteins partners of TRIB3. To perform cell toxicity assay, the MIO-M1 TRIB3 overexpressing cells were incubated in MTT solution (0.5 mg/ml/well) for 4 hours at 5% CO2. Following MTT incubation; the cells were incubated with DMSO solution for 15 minutes. The cell survival was measured by estimating optical density at 570 nm using a microplate reader.

To generate hypoxic conditions, 24 hours after transfection, MIO-M1 TRIB3 overexpressing cells were transferred to ANAEROgen (W-Zip compact) bags for 48 hours to maintain hypoxic conditions as previously reported, which generated 1% oxygenation, thus inducing hypoxia.[188] Proteins were extracted using RIPA buffer and TRIB3 (45 kDa), HIF1α (120 kDa), EGFR1 (170 kDa), GLUT1 (60 kDa), GFAP (50 kDa) and VEGF (21 kDa) were detected, with bands normalized intensities to Actin (42 kDa). Secondary HRP goat anti-mouse and anti-rabbit antibodies and infrared (IR) goat anti-mouse and anti-rabbit antibodies were used for detection. Immunoblots were imaged and analyzed using the LICOR imager system. Experiments with downregulation of HIF1α and EGFR in MIO-M1 hypoxic cells were conducted using respective siRNAs at concentration of 100 nm.

Glucose uptake assay was performed in MIO-M1cells transfected with siRNA *Hif1α* and exposed to hypoxia 24 hours later. At 72 hours post transfection, the cells were incubated at 5% CO_2 in glucose-free medium with 0.5% FBS for 45 minutes. Cells were then treated with florescent 2-NBDG glucose for 30 minutes, as recommended by manufacturer, washed with 1x analysis buffer, and resuspended in 400 µl of 1x analysis buffer. The glucose uptake was measured by flow cytometry using Fortessa at UAB Comprehensive Flow Cytometry Core (CFCC). Confocal microscopy was used to obtain florescent images of cellular glucose uptake at 488 nm and florescent signal was quantified using the ImageJ program.

Statistics

Data were analyzed using either two-tailed unpaired Student's t test or one-way/two-way Analysis of variance (ANOVA). Statistical significance was set at $p < 0.05$. The results were plotted in graphs using GraphPad Prism 8 software and data were presented as mean ± SEM.

Results

In this study, we investigated the role of TRIB3 in the development and progression of human diabetic retinopathy and leveraged STZ-injected and hypoxia driven mouse models mimicking early molecular[109,111,118] and advanced neurovascular pathophysiological complications of DR, respectively. First, we assessed the TRIB3 level in human diabetic retinas.

Human diabetic retinas overexpress TRIB3 protein

Recent studies conducted with diabetic animal models have clearly demonstrated associations between TRIB3 and numerous diabetes-associated complications, such as hyper-homocysteinemia,[41,196] non-alcoholic fatty liver disease (NAFLD),[197,198] diabetic nephropathy (DN),[199,200] and visceral obesity.[201] Therefore, we tested the hypothesis that TRIB3 expression is also altered in hyperglycemic retinas. To this end, we analyzed TRIB3 immunoreactivity in the human control and diabetic retinas (Figure 1A). The diabetic retinas of 84-year-old man showed a strong signal for TRIB3 immunoreactivity as compared to the control, the retinas of an 82-year-old man control. Increased TRIB3 staining was observed in retinal endothelial, ganglion, and photoreceptor cells (ONL).

IHC analysis with antibody against CD31, a known endothelial cell marker[202], revealed the colocalization (in yellow) of TRIB3 (in red) and CD31 (in green) signals suggesting expression of TRIB3 in the human fibrovascular membrane of diabetic retina (Figure 1A).

STZ-induced mouse diabetic retina and hypoxic muller cells demonstrate overexpression of TRIB3 protein

To proceed further, we took advantage of the TRIB3 KO mice and employed both a pharmacological approach to induce hyperglycemia based on injection with STZ and a hypoxia-induced vascularization approach using an OIR model to mimic the NPDR and proliferative retinopathy, respectively. RNA analysis of four-week post-STZ injected retinas demonstrated about four-fold upregulation of TRIB3 mRNA in hyperglycemic retinas, suggesting that the TRIB3 overexpression occurs early (Figure 1B). TRIB3 expression level was also significantly upregulated in the hypoxic Muller MIO-M1 cells, compared to normoxia, based on western blot analysis (Figure 1C), suggesting that hypoxia in human diabetic retinopathy could upregulate TRIB3 expression level.

The results of the RNA and protein analyses were confirmed in mouse hyperglycemic and hypoxic retinas, which showed a strong immunoreactivity for TRIB3 in IHC (Figure 1D, E). To verify that hyperglycemic RGC overexpresses TRIB3, we further performed an IHC analysis with antibody recognizing the RGC marker, BRN3A, and TRIB3 in control and STZ-treated retinas (Figure 1F). A colocalization shown in yellow was detected from TRIB3 (in red) and BRN3A (in green) signals, suggesting TRIB3 expression in hyperglycemic RGC.

Given that TRIB3 reportedly controls insulin signaling and resistance in cells in general[42], we next tested the hypothesis that TRIB3 regulates glucose uptake and alters metabolic equilibrium in hyperglycemic retinas.

Hyperglycemic C57BL6 retinas demonstrate raised retinal glucose level, whereas hyperglycemic TRIB3 KO retinas manifest diminished level of glucose

Previously, it was reported that conventional TRIB3 KO in mice does not cause significant difference in the BGL as a response to STZ injection, compared to C57BL6 mice[203]. We confirmed this by detecting similar BGLs in both normal and diabetic C57BL6 and TRIB3 KO mouse groups (Supplemental Table 2). Based on this, we asked whether hyperglycemia also increased RGL. Using a calorimetric assay, we determined that four-week hyperglycemic mice have a higher RGL than their non-diabetic controls. Interestingly, TRIB3-ablated hyperglycemic retinas demonstrated significant reduction in RGL, despite the well-matched BGL (Figure 2A, Supplemental Table 2). Given that the retina is extremely sensitive to glucose and an excess of glucose in the retina may modify cellular metabolism; thus, we analyzed early metabolic changes in hyperglycemic retinas.

Hyperglycemic retinas with TRIB3 ablation show altered metabolic responses

TRIB3 is a known metabolic switcher responsible for moving cells from the homeostatic stage to metabolic dysfunction. Therefore, we analyzed the energy metabolism in four-week diabetic retinas of mice mimicking early diabetic changes.[109,111,118] We monitored both the cellular OCRs and the ECARs in a real-time experiment to measure the mitochondrial respiration and glycolysis rate in the retina

using a Seahorse Extracellular Flux Analyzer (Figure 2B-H). Extracellular acidification is derived from both lactate, produced by anaerobic glycolysis, and CO_2, produced in the citric acid cycle during respiration. However, a previous study revealed that retinas, manifesting the Warburg effect, convert 80–96% of glucose into lactate rather than fully oxidizing it to CO_2 in their mitochondria.[204] Here, we found that the ECAR baseline was significantly higher in C57BL6 diabetic retinas, whereas TRIB3 KO hyperglycemic retinas showed no differences compared to both controls (Figure 2B). These results indicate a dramatic difference in acidification rate between C57BL6 and TRIB3 KO diabetic retinas. In fact, the ECAR in the TRIB3 KO diabetic retinas dropped significantly as early as the first ten minutes of the real-time experiment, and this decline continued further over time. However, when we treated the retinal tissue with glucose, dramatic changes were observed in the ECAR rate of TRIB3 KO diabetic retinas. Although both C57BL6 and TRIB3 KO diabetic retinas responded immediately to glucose, the TRIB3 KO hyperglycemic retinas demonstrated a more robust ECAR response at 45 minutes compared to ECAR at 40 minutes (~5-fold TRIB3 KO vs 2-fold in C57BL5, $p < 0.01$) (Figure 2C). Further analysis of the post-glycolysis ECAR in C57BL6 and TRIB3 KO diabetic retinas revealed that these tissues manifested a similar glycolysis rate (Figure 2D). We next added oligomycin, a known inhibitor of mitochondrial ATP synthase and respiration, to the retinal preparations; this caused the overall glycolytic capacity to drop in a time-dependent manner in both C57BL6 and TRIB3 KO diabetic groups (Figure 2E). Although vehicle- and STZ-injected retinas responded similarly within a single mouse strain, a significant difference was observed

between C57BL6 and TRIB3 KO diabetic retinas: the glycolytic capacity in diabetic TRIB3 KO retina was lower (p <0.01).

The mitochondrial respiratory rate in the mice was measured with a mitochondrial stress test and the OCR was recorded (Figure 2F). The basal OCR was significantly lower in TRIB3 KO diabetic retinas than in C57BL6 (p<0.0001) suggesting that under hyperglycemic conditions a basal mitochondrial respiration in hyperglycemic retinas could be controlled by TRIB3. In retinal samples stimulated by adding glucose, we observed a dramatic increase of OCR in TRIB3 KO (Figure 2G, ~1.5-fold in TRIB3 KO vs 1.0-fold in C56BL6, p<0.001). Time dependent examination of the retinal tissue responses to glucose demonstrated that hyperglycemic TRIB3 KO retinas uniquely manifested significantly low OCR (p<0.05) (Figure 2H).

Thus, our data demonstrated that TRIB3 ablation in the diabetic retinas manifest altered metabolic responses, which prompts a further exploration of whether other retinal cellular signaling systems are affected at early stages of DR development by TRIB3.

TRIB3 ablation reduces retina inflammatory in diabetic mice

There is a growing literature suggesting that TRIB3 controls inflammatory response in cells.[205] To verify the ability of TRIB3 to control the inflammatory response in the retina, mice injected with LPS were sacrificed after 24 hours to analyze IBA1, a microglia/macrophage marker (Figure 3A). IHC analysis demonstrated dramatically reduced number of IBA1 positive cells in the retinas of LPS-injected TRIB3 KO mice, suggesting that TRIB3 ablation could be responsible for the modified pro-inflammatory response in the retina.

Given the early metabolic changes in diabetic retinas at four weeks, we analyzed the expression profile of the genes known to associate with diabetic retinopathy, including *Hif1α*, *Aif*1, *Cox*2, *Icam*1, *Nf-kb*, *Rc3h*1 (Roquin), *Zc3h12a* (Regnase or Mcp-1-induced protein-1), and *Vegf*. We found that TRIB3 ablation in diabetic retinas tremendously diminished expression levels of these genes. For example, expression of the intracellular adhesion molecule *Icam*1, responsible for communication between retinal endothelial cells and leucocytes in the diabetic eye, and COX2, a critical player in retinal ganglion cell survival,[206] were dramatically reduced in TRIB3 KO diabetic retinas (Figure 3B). These data indicate that TRIB3 ablation results in altered inflammatory response in early diabetic retinas in addition to energy metabolism.

TRIB3 KO results in prevention of retinal ganglion, endothelial, and pericyte cell loss

RGC loss in the diabetic retina has been reported in the literature.[131,207] At 32-weeks of hyperglycemia, we assessed the RGC function and viability in the retinas and found that although the C57BL6 diabetic retinas demonstrated significant loss of RGC, TRIB3 ablation protected hyperglycemic retinas from RGC death. The numbers of RGCs calculated within 100 μm distance in the retinas of TRIB3 KO diabetic mice were comparable to those found in control C57BL6 mice (Figure 4A, B). Therefore, we next recorded the PhNR amplitudes to measure the RGC function known to detect early neuronal damage in the human and mouse retinas[207-209]. Interestingly, the RGC loss in C57BL6 hyperglycemic retinas correlated with dramatic functional loss as measured by PhNR recording, whereas decline in PhNR was remarkably prevented in TRIB3 diabetic retinas (Figure 4C, D).

The RGC layer in the eye is traversed by the retinal capillary beds at varying levels that provide nourishment for both the RGCs and the RGC axons.[210] Therefore, given that DR is a vascular disease, we next assessed the role of TRIB3 in the retinal endothelial cell health in diabetes. In the hyperglycemic retinas, we observed a dramatic cytoprotective effect of TRIB3 ablation. The pericyte loss observed in C57BL6 retinas was reversed and the increase in acellular capillaries was averted in TRIB3 KO diabetic retinas (Figure 4E-G). Cumulatively, these results indicate that TRIB3 ablation not only has a neuroprotective effect on RGC, but it also maintains retinal vascular homeostasis in diabetic mice.

TRIB3 ablation manifest reduced vascular dysfunction, gliosis, and overall retinal integrity loss in hypoxic retinas

Previously, we reported that ATF4 downregulation is a therapeutic for hypoxic retinas and leads to dramatic reduction in neovascularization and increase in the acellular area of OIR mice.[34] TRIB3 is a downstream target of ATF4, expression of which is upregulated during endoplasmic reticulum stress.[211] It has also been suggested that hypoxic conditions upregulate Trib3 expression in the retinal Muller cells.[37] Thus, we explored hypoxic TRIB3-ablated retinas employing the OIR model.

At P13, one day after the removal of pups from the oxygen chamber, the VEGF expression was high in the C57BL6 retinas, as expected. Surprisingly, however, TRIB3 ablation in hypoxic retinas resulted in reduced VEGF level (Figure 5A). For example, C57BL6 hypoxic retina normalized to the control demonstrated a 1.3-fold increase in VEGF, whereas normalized TRIB3 KO OIR showed substantial decline in VEGF

expression. Therefore, learning about TRIB3-mediated control of VEGF in the wild type retina, we further analyzed the VEGF-inducted neovascularization in OIR mice.

Analyses of the areas of neovascularization and vaso-obliteration in the OIR retinas demonstrated that TRIB3 ablation significantly reduced formation of neovascular tufts (Figure 5B). Hypoxic TRIB3 KO retinas manifested levels of vaso-obliteration similar to those found in C57BL6 tissues. This difference in neovascularization prompted the question of whether TRIB3-mediated vascularization causes the compromise of retinal integrity and morphology observed in C57BL6 OIR retinas.

Interestingly, TRIB3 KO in hypoxic retinas preserved overall retinal integrity. Although the C57BL6 OIR retinas demonstrated reduced INL, IPL, and OPL thicknesses, TRIB3 KO dramatically reversed these structural changes; no differences were observed between TRIB3 KO OIR and normoxic C57BL6 or TRIB3 retinas (Figure 6A).

Muller cells are known to play a pivotal role in the development of DR and respond promptly to hyperglycemia and hypoxia.[212] Therefore, we examined Muller cells in hypoxic retinas by detecting the co-localization of GFAP and vimentin, known glial cell markers. [213,214] We found that the TRIB3 KO hypoxic mice demonstrated a significantly lower Muller cell immunoreactivity as compared to C57BL6 OIR retinas (Figure 6B). Moreover, detection of the GFAP level in TRIB3 KO OIR mice by western blot also indicated a dramatic reduction in the overall expression, supporting the observation of diminished gliosis in hypoxic TRIB3 KO retinas (Figure 5C).

Together, these results show that TRIB3 is not only involved in early metabolic and inflammatory changes but may also determine the progression of diabetic retinopathy.

TRIB3 controls glucose signaling and VEGF expression, overall impacting the retinal cell viability

The molecular mechanisms of DR are complex and multifactorial. Early molecular changes in diabetic retinas have been reported to occur through a compromised advanced glycation end products (AGE) pathway. Therefore, using Muller cells, we asked whether the treatment of MIO-M1 cells with 500 mM AGE induces TRIB3 overexpression. The results demonstrated significant upregulation of TRIB3 in 48 hours (Figure 7A). These data are in the concord with the results obtained in STZ-induced hyperglycemic mice and the hypoxia treated MIO-M1 cells, indicating that in diabetic hypoxic retina TRIB3 could be overexpressed earlier in the course of disease. Besides overexpression of TRIB3 in hypoxic MIO-M1 cells, we also identified occurrence of overexpression of HIF1α and EGFR (Figure 7B). The choice of the validated proteins was determined by the literature, and the results obtained in hyperglycemic mouse retina and MIO-M1 cells overexpressing TRIB3 (Supplemental Figure 2). Thus, similar to hyperglycemic retinas, hypoxia in MIO-M1 cells induced both TRIB3 and HIF1α.

Interestingly, TRIB3 by itself can compromise MIO-M1 cell viability (Figure 7C); more prominent cell death was found in MIO-M1 transfected with TRIB3-DDK plasmid than in control cells. These results are comparable with the RGC cell loss observed in hypoxic diabetic retinas overexpressing TRIB3. Given that HIF1α and EGFR along with TRIB3 were overexpressed in cultured Muller cells, we investigated whether TRIB3 is upstream mediator of these proteins by using TRIB3 overexpression. In hypoxic Muller cells overexpressing TRIB3-DDK cDNA, HIF1α and EGFR were

upregulated along with increased GFAP, VEGF and GLUT1 proteins, indicating that TRIB3 controls these protein expressions as well (Figure 7D). In hypoxic MIO-M1 cells treated with siRNA targeting *Hif1α*, we found that the levels of EGFR, GLUT1 and VEGF were significantly lower, whereas GFAP was unresponsive to the knockdown of *Hif1α*. This suggests that GFAP may be directly regulated by TRIB3 and its expression is not HIF1α-dependent (Figure 7E). Targeting *Egfr* mRNA in hypoxic MIO-M1 cells demonstrated EGFR-dependent HIF1α upregulation. In contrast to experiments with *Hif1α* silencing, the VEGF expression was not responsive to the treatment of cells with *Egfr* siRNA (Figure 7F).

Given that TRIB3 expression is hypoxia-induced and TRIB3, in turn, regulates HIF1α expression leading to reduction in GLUT1, we asked whether *Hif1α* detected in C57BL6 hyperglycemic retinas (Figure 3) could be responsible for the glucose uptake in Muller cells. Particularly, the observation of higher RGL in hyperglycemic C57BL6 retinas overexpressing *Hif1α* mRNA was worth further investigation. Therefore, we treated hypoxic Muller cells transfected with control or *Hif1α* siRNAs with glucose analog 2-NBDG, known to inhibit glycolysis via its action on hexokinase, and analyzed levels of fluorescence using flow cytometry and confocal microscopy (Figure 8 A and B, respectively). We observed significant reduction in glucose uptake that occurred in HIF1α-dependent manner, suggesting that the glucose uptake in these cells and the metabolic changes in hyperglycemic retinas could be regulated through a TRIB3→HIF1α axis. Altogether, these findings indicate that TRIB3 is upstream of HIF1α, EGFR and GFAP, which allows this molecule to control glycose metabolism, cytokine expression, angiogenesis and gliosis in retinal cells.

Discussion

Overall, the molecular mechanisms of DR are complex and multifactorial. Hyperglycemic conditions affect the intracellular glycose level leading to the retinal endothelial and neuronal cells failing to properly regulate cellular metabolism. Early molecular changes in diabetic retinas have been reported to occur through a compromised polyol pathway, protein kinase C pathway, advanced glycation end products (AGE) pathway, and hexosamine biosynthetic pathway (HBP) in retinal cells.[16,18,19] Besides the dysregulation of these cellular pathways, hypoxia-induced hypoxia-inducible factor-α (HIF1α) and vascular endothelial growth factor (VEGF) overexpression play key roles in the progression of NDPR to PDR. In contrast, little is known about how early molecular changes occurring in diabetic retinas lead to the subsequent progression of the disease. Here, we present evidences confirming the critical role of TRIB3 overexpression during the development and progression of diabetic retinopathy. First, we found that TRIB3 was overexpressed in human diabetic retinas and retinas of mice mimicking NPDR and proliferative retinopathy in patients, which provided a rationale to further investigate the role of TRIB3 in diabetic retinas. We discovered that TRIB3 overexpression induced HIF1α-mediated changes in GLUT1 level, glucose uptake, and VEGF expression. In addition to HIF1α, we observed that TRIB3 controlled EGFR expression. Lastly, we determined that TRIB3 ablation in hyperglycemic and hypoxic retinas dramatically prevented retinal neuronal cell functional deficit and loss, as well as VEGF-induced neovascularization.

Retinal vascular homeostasis become compromised with the disease progression. PDR is characterized by uncontrolled growth of fragile blood vessels that can protrude and leak into the vitreous causing blurry vision. This phenomenon is triggered by hypoxia in the retina, one of the known molecular inducers of neovascularization. One of the interesting finding of our study is that both hypoxia and the AGE conditions found in diabetic patients caused the upregulation of TRIB3, which in turn control glycose metabolism, vascular function, and gliosis. Thus, our *in vitro* study indicates that HIF1α upregulation in diabetic retinas occurs in TRIB3-dependant manner (Figure 3 and 7). A previous study demonstrated that HIF1α induced TRIB3 overexpression.[215] In fact, the HIF1α-TRIB3 relationship could be more delicate and the regulation of their expressions may be interactive. For example, one of such regulation is mediated through ATF4 transcriptional factor, which reportedly cooperates with both proteins by inducing TRIB3 expression[211] and binding to HIF1α.[216]

Recently conducted study in cultured L6 myocytes[42,217] indicated that TRIB3 overexpression is induced in glucose–dependent manner resulting in reduced mitochondrial glucose oxidation and the maximal uncoupled oxygen consumption rate. Hence, it noteworthy to find that TRIB3 can regulate glucose uptake in diabetic retina and that this regulation occurs via HIF1α-mediated GLUT1 expression. Indeed, in the whole retinal samples, we found that TRIB3 ablation may modify glucose flux and define glycolytic capacity of diabetic retina. C57BL6 diabetic retinas presented higher RGL, confirming a previous study that reported increase in glucose uptake in diabetic rat retinas.[218] Changes in glucose flux suggest a plausible explanation for the high RGL in C57BL6 diabetic retinas—stimulation of glucose transporter (GLUT)1–4 activity,

proposed as a target that reduces retinal glucose in diabetic retinas[219,220], could be one reason.

TRIB3 KO in diabetic retinas may cause a metabolic shift that allows this retina to function under a "safe operating mode." Previously, it has been demonstrated that diabetic retinas may have higher lactate-pyruvate ratios, suggesting that elevated glucose level mimics the effects of hypoxia on glycolysis and cytosolic free NADH/NAD+.[221,222] These results were very similar to those observed in this study. C57BL6 diabetic retinas had a higher baseline rate of ECAR derived from lactate produced by anaerobic glycolysis. Although overall glycolytic capacity in the TRIB3 KO diabetic retinas was lower, the response of the retinas to glucose treatment was significantly higher in these mice. Interestingly, the TRIB3 KO diabetic retinas also displayed a lower OCR baseline and revealed a higher sensitivity of the mitochondrial respiration rate in response to glucose treatment. Altogether, these results imply that TRIB3 KO hyperglycemic retinas might respond to glucose elevation similarly to C57BL6 hyperglycemic retinas but operate at limited metabolic mode by reducing glucose flux, instead.

EGFR reportedly promotes angiogenesis, cell proliferation, metastasis, and apoptosis in DR and the inhibition of EGFR signaling protects diabetic retina from insulin-induced vascular leakage.[223,224] Although we did not assess the level of EGFR in diabetic retinas, we found that TRIB3 overexpression observed in human diabetic retinas induced EGFR in hypoxic MIO-M1 cells. However, unlike the previous studies, we found no direct correlation between EGFR and VEGF levels in Muller cells.[225] Given the fact that diminished HIF1α level resulted in reduced VEGF, these data indicate that in hyperglycemic and hypoxic retinas, the observed correlation between TRIB3 KO and

VEGF is promoted mostly through a TRIB3→HIF1α signaling. Future experiments that investigate the TRIB3→EGFR–mediated gene expression profile in diabetic retinas should be conducted; nevertheless, the current study clearly demonstrated that EGFR by itself inhibits HIF1α expression. Overall, these findings indicate that TRIB3, HIF1α and EGFR act as pyramid trio set to regulate VEGF expression with TRIB3 upstream and the reciprocal regulation of HIF1α and EGFR downstream of the pyramid (Figure 9).

Another example of how TRIB3 could control vascular health is through the regulation of an intravascular leukocyte cell adhesion.[226] Although our study did not assess leukostasis in the retinas, we did find that similar to diabetic patients with microalbuminuria and DR [227,228], *Icam1,* a cell surface glycoprotein expressing on endothelial cells and leukocytes, was significantly upregulated in C57BL6 mouse diabetic retinas. TRIB3 ablation led to dramatic reduction of *Icam1* expression. In addition to *Icam1*, we found that TRIB3 controlled the endothelial cell death in diabetic retina and ablation of TRIB3 significantly preserved the formation of acellular capillaries and subsequent pericyte loss. These data provide evidence that TRIB3 plays substantial role in endothelial cell homeostasis in DR.

Inflammation is one of the major factors induced during diabetes, and leads to macular edema, ischemia and neovascularization.[229] In diabetic TRIB3 KO retinas, pro-inflammatory gene expression profile was altered. Moreover, the increase in retinal microglia and VEGF cytokine production was TRIB3-mediated. TRIB3 could directly or indirectly affect expression of NF-kB and other cytokines, thus modifying early inflammatory response to hyperglycemia. In support of this hypothesis, TRIB3 ablation prevented both neuronal and vascular dysfunction serving as hallmarks of DR in

humans.[230] Therefore, it is of particularly importance that TRIB3 controls RGC cell death. In hyperglycemic TRIB3 KO mouse retinas, RGC preservation correlated with significant improvement of the recorded PhNR amplitudes, known to be diminished in diabetic patients.[231] Moreover, in concord with these results, we revealed that in hypoxic retinas, TRIB3 controls retinal integrity too. This latest observation is also supported by the fact that Muller cells overexpressing TRIB3 manifested reduced cell viability.

The current study did not access a cell specific role of TRIB3 in diabetic retinas due to unviability of the mouse model. Therefore, future experiments should identify sources of TRIB3-induced cellular damage, "signaling" neurovascular degeneration in diabetic retinas. Nevertheless, regardless of the sources, we found that hypoxic TRIB3 KO retina manifested less gliotic activity of Muller cells as determined by co-localization of vimentin and GFAP. TRIB3-mediated control of GFAP *in vivo* was confirmed in cultured Muller cells indicating that TRIB3-mediated GFAP upregulation is independent of HIF1α protein regulation. This finding pinpoints TRIB3 as a novel potential regulator of GFAP biogenesis during diabetes.

Overall, our study indicated that TRIB3 mediates the expression of major sets of hypoxia-induced genes, HIF1α, EGFR, VEGF and GFAP, effects that were observed both *in vitro* and *in vivo*. Our data align with previous studies conducted in human cancer cells, in which TRIB3 was proposed as a molecular regulator of angiogenesis mediated via HIF1α and VEGF upregulation.[232] In addition to angiogenesis, our investigation indicated that TRIB3 is a master regulator of early metabolic and inflammatory events in diabetic retinas, which affect the overall development and progression of disease to proliferative stages (Figure 9). Given the limitations and side effects of current treatments

for DR and the continuing efforts to understand its complex molecular mechanisms, our findings show TRIB3 is a major game player of diabetic ocular pathophysiology in humans and is a novel therapeutic target, the potential of which should be further evaluated in the clinic.

Acknowledgements

This work was supported by the National Eye Institute, grants RO1 EY027763, R21YE031103. We also would like to acknowledge the UAB BARB core supported by the RC (NIH P30DK079626), NORC (NIDDK DK056336), UCEM, UCDC, CFRB and UCNC.

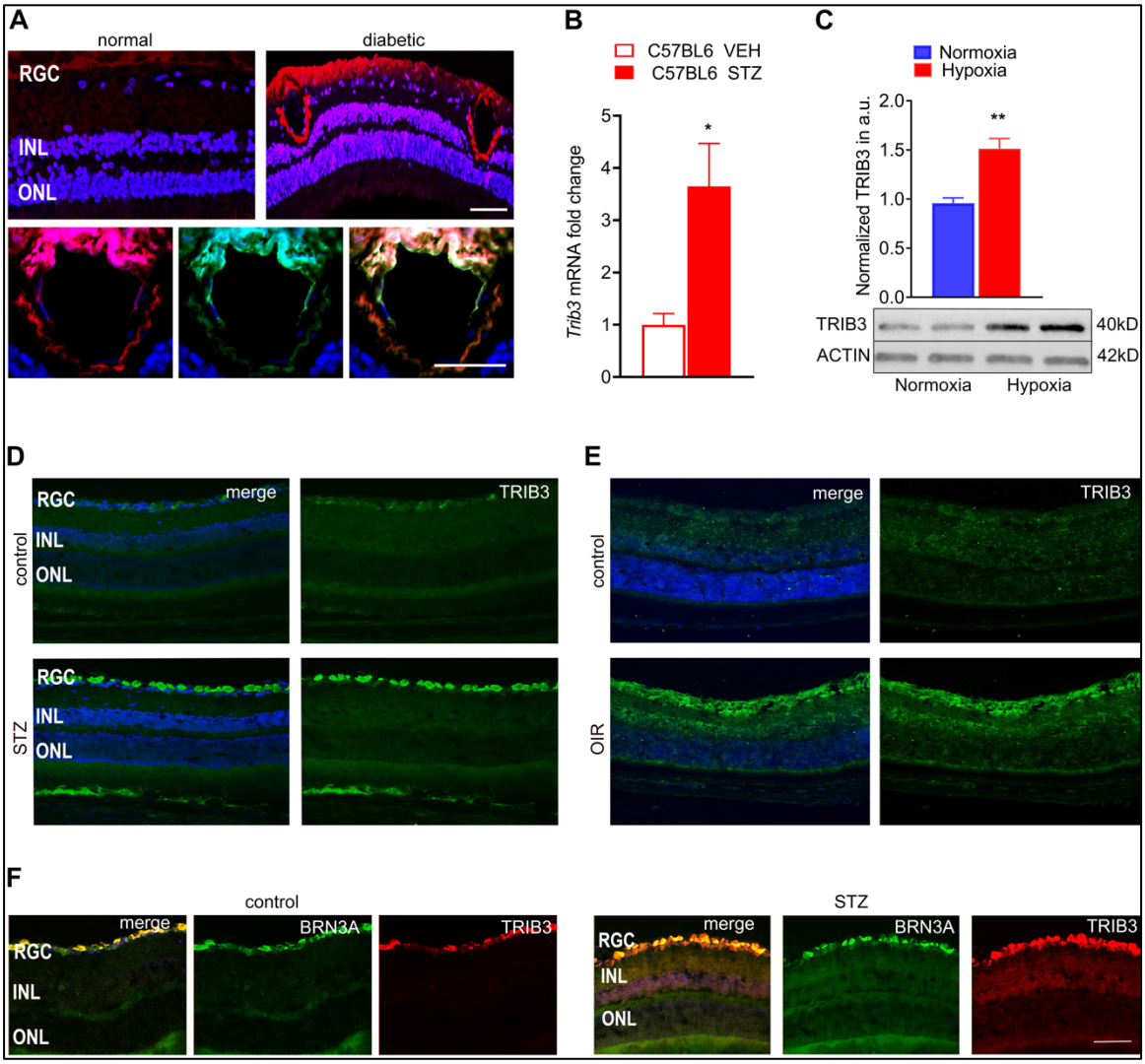

Figure 1. Human and mouse diabetic retinas overexpress TRIB3 protein. A: TRIB3 expression in the human diabetic retinas detected using IHC with anti-TRIB3 primary antibody is shown in red. Strong TRIB3 immunoreactivity is detected in the ONL, INL, RGC and the fibrovascular membrane (FVM) in the diabetic human retina. The TRIB3 immunoreactivity also co-localizes (in yellow) with CD31 positive cells (in green), suggesting that CD31 positive endothelial cells of the FVM also express TRIB3. The scale is 50 µm. B: Detection of TRIB3 expression in mouse diabetic retinas at 4 weeks of hyperglycemia by qRT-PCR (n = 5; *p<0.05). C: TRIB3 overexpression

detected in hypoxic Muller MIO-M1 cells at 72 hours. D: Detection of TRIB3 in the mouse normal and diabetic retinas at 32 weeks after STZ-induced hyperglycemia (in green). DAPI-stained nuclei are shown in blue. Merged images are on the left. Robust TRIB3 expression is detected in the RGC layer. E: Detection of TRIB3 in the normoxic and hypoxic mouse retina at P17. Robust TRIB3 expression is detected in the RGC, IPL, INL and ONL (in green). DAPI-stained nuclei are shown in blue. Merged images are on the left. F: Expression of TRIB3 is co-localized with the RGC marker, BRN3A in the control and diabetic retinas at 32 weeks of hyperglycemia. TRIB3 is shown in red, BRN3A is shown in green, co-localization is shown in yellow (indicated with white arrows). DAPI stained nuclei are shown in blue. Robust TRIB3 expression is detected in the RGC layer. (ONL: outer nuclear layer; INL: inner nuclear layer; RGC layer: retinal ganglion cell layer). The scale is 100 μm.

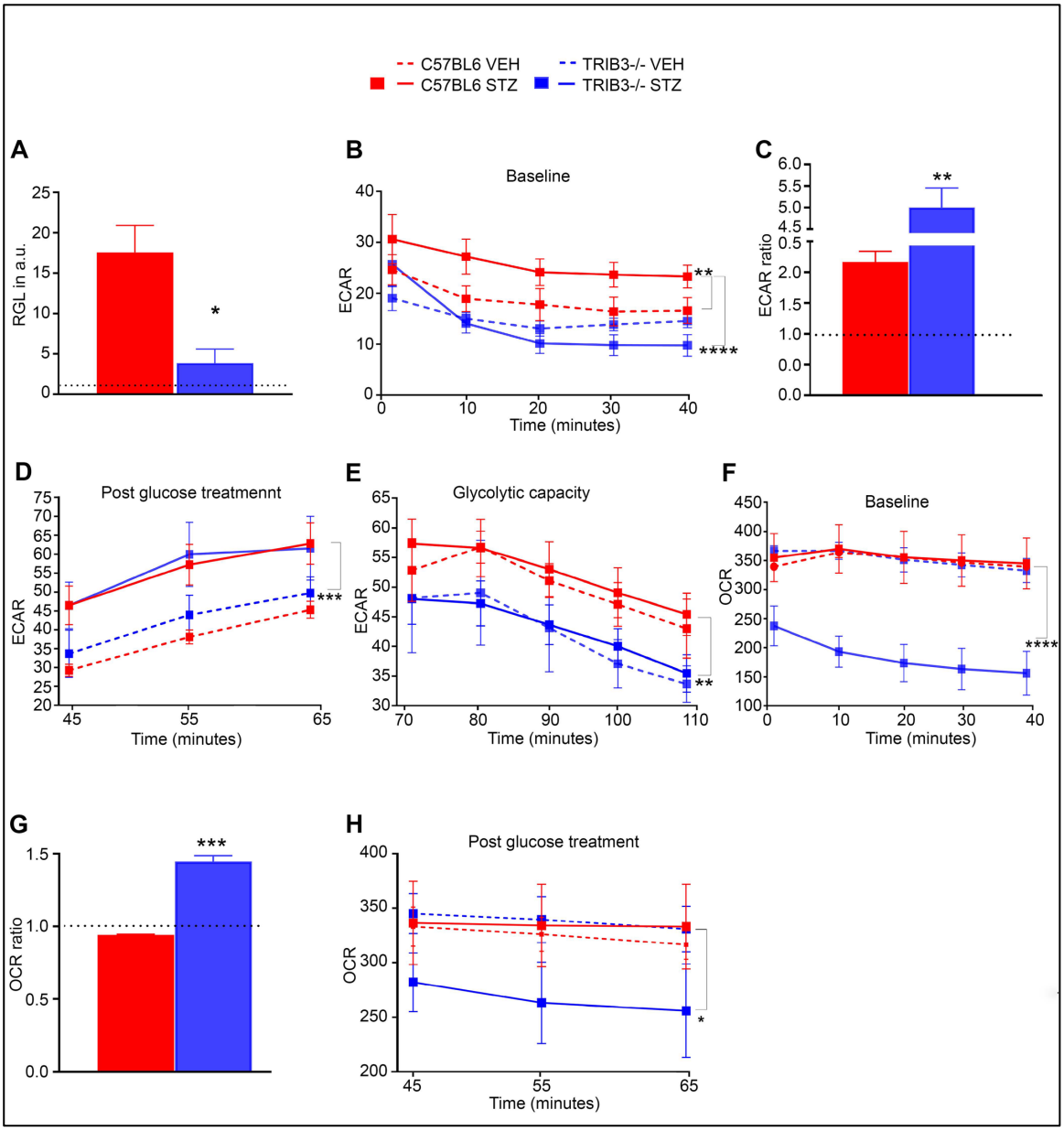

Figure 2. TRIB3 reprograms glucose metabolism in diabetic retinas. A: RGL measured in diabetic retinas (mg/dl) was normalized through own control (dotted line) at 4 weeks of hyperglycemia. Significant reduction of RGL is observed in TRIB3 diabetic retinas (C57BL6 diabetic and control; n = 8–9 and TRIB3 KO diabetic and control; n = 5–11). Please also see Supplemental Table 2. B, C, D, E, F, and H: Results of the metabolic stress experiments (n = 4–6). B: The ECAR baseline of diabetic and control

C57BL6 and TRIB3 KO groups at 4 weeks post injection (mpH/min). Significant increase in the ECAR baseline in C57BL6 diabetic retinas is shown during the first 40 minutes. C: Addition of glucose results in dramatic jumps in the ECAR rate. Thence, the TRIB3 KO diabetic retinas manifest more sensitivity than C57BL6 hyperglycemic tissue. The presented ECAR rates are expressed as the ratios of the normalized ECARs at 45 min over the normalized ECARs measured at 40 min (dotted line). D: Rates of glycolysis in the four experimental groups measured after glucose treatment in a real-time experiment. Both diabetic retinas demonstrate comparable levels of glycolysis. E: Measurement of glycolytic capacity in diabetic retinas after suppression of the mitochondrial respiration rate by using oligomycin. Reduced glycolytic capacity of TRIB3 KO diabetic retinas (about 18%) vs. C57BL6 hyperglycemic retinas (mpH/min). F: The OCR baseline measurements in normal and diabetic mouse groups. Significant reduction in the OCR rate is detected in TRIB3 KO hyperglycemic retinas. G: Addition of glycose at 40 minutes results in a high sensitivity of the OCR rate in TRIB3 diabetic retinas registered at 45 minutes (dotted line). H: However, this jump does not cause an increase in the OCR rate as compared to C57BL6 diabetic retinas in a timely manner. The OCR rate continues to decline in TRIB3 diabetic retinas as measured in pmol/min. *(p<0.05); **(p<0.01); ***(p<0.001); ****(p<0.0001).

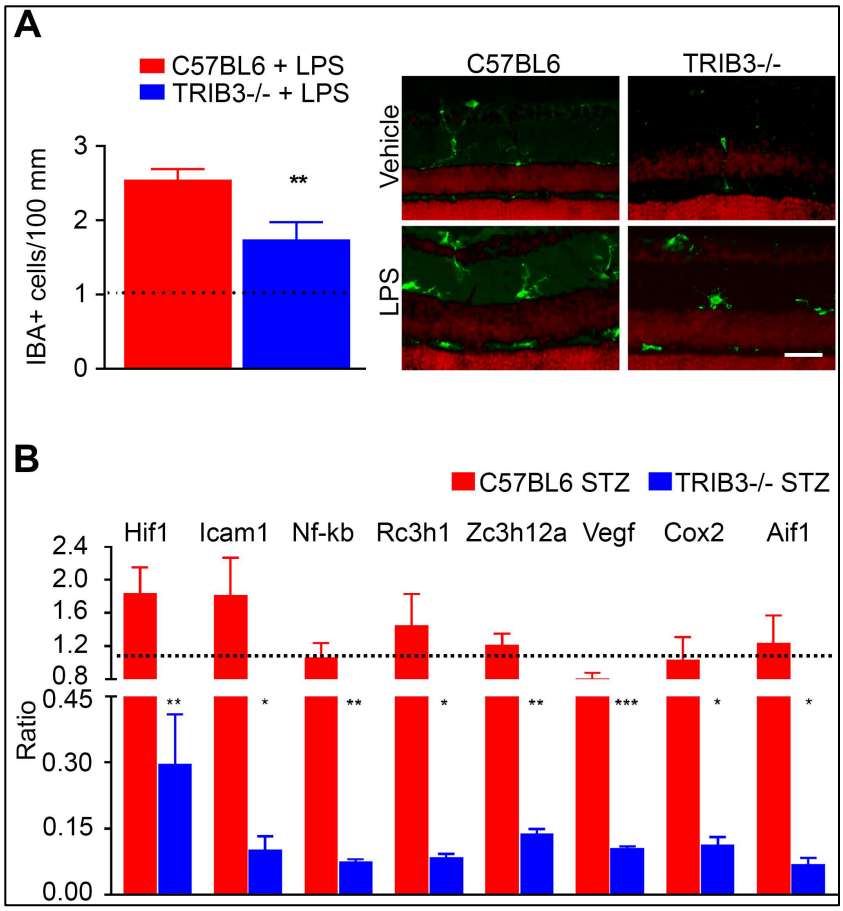

Figure 3. TRIB3 controls immunoresponse in stressed and diabetic retinas. A: Mice were IP injected with 10 µl/g LPS and sacrificed 24 hours later (n = 5). The cryostat retinal sections were subjected by IHC analysis with anti-IBA1 antibody and IBA positive cells per 100 µm were counted (in green). The results are presented as ratios of cells detected in LPS-injected retinas normalized to own controls (dotted lines). B: TRIB3 controls expression of pro-inflammatory genes at 4 weeks of hyperglycemia (n = 3–5). Fold changes for each diabetic group were normalized to own controls. Thus, we observe a dramatic decline in *Hif1a*, *Icam1*, *Nf-kb1*, *Rc3h1*, *Zc3h12a*, *Vegf*, *Cox2* and *Aif1* expression in TRIB3 KO diabetic retinas. *(p<0.05); **(p<0.01); ***(p<0.001); ****(p<0.0001). The scale is 100 µm.

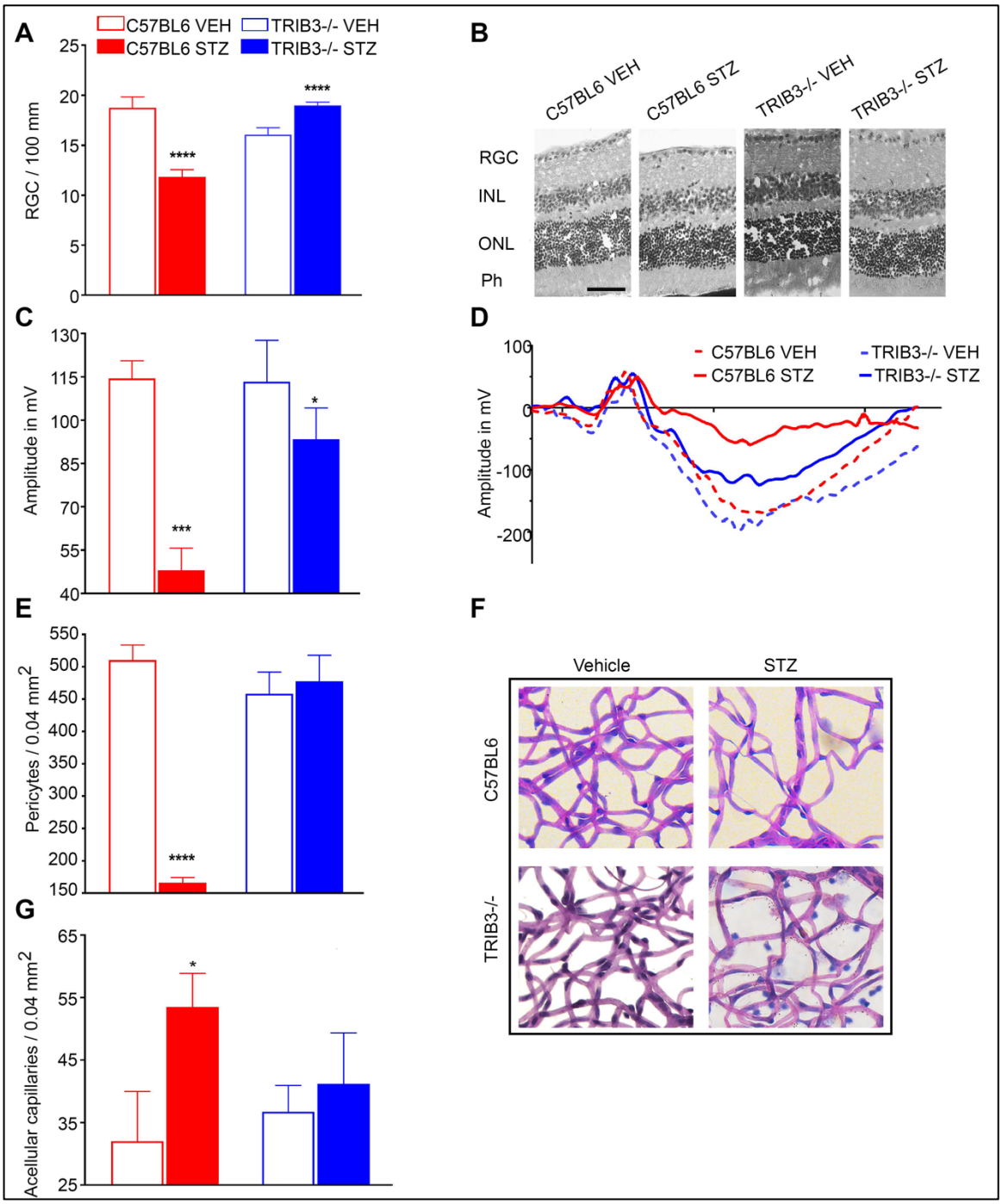

Figure 4. TRIB3 controls neuronal and endothelial health in diabetic retinas. A: The number of ganglion cells/100 µm is dramatically increased in the diabetic TRIB3 KO retina as compared to other groups. No changes were observed between control or diabetic TRIB3 KO retinas; n = 6. B: Representative images of the H&E-stained control

and diabetic retinas. C: The PhNR amplitudes characterizing the RGC function as recorded by the photopic ERG procedure in the C57BL6 control and diabetic (n = 9 for both) and TRIB3 KO control and diabetic (n = 9–12) mouse groups. Significant diminishing of the RGC function is detected in the C57BL6 diabetic mice whereas dramatic elevation of photopic negative response (PhNR) is observed in TRIB3 ablated diabetic retinas. D: Representative images of PhNR registered in all four groups. E: The number of pericytes detected in 0.04 mm^2 area of the retina is markedly reduced in the diabetic C57BL6 retinas as compared to other mouse groups; n = 6 for C57Bl6 control and diabetic and n = 5 for TRIB3 KO control and diabetic mice. TRIB3 ablation slows down the pericyte loss in diabetic retinas. F: TRIB3 ablation in diabetic retina prevents formation of acellular capillaries detected in 0.04 mm^2 area of the retina. G: Representative images for PAS-stained retinal pericytes and acellular capillaries in the retinas of the four mouse groups. *($p< 0.05$); ****($p<0.0001$). The scale is 100 μm.

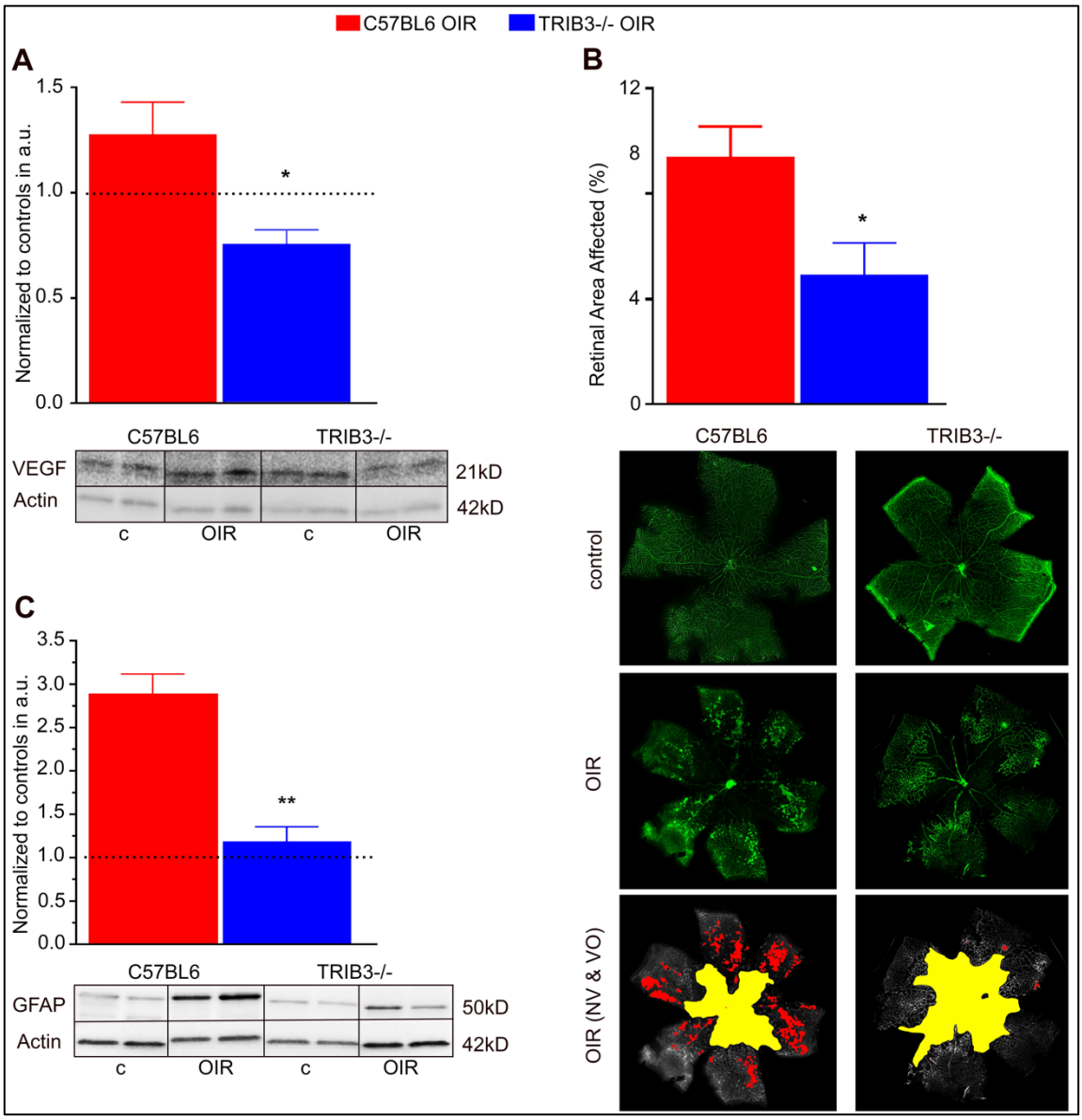

Figure 5. TRIB3 promotes retinal vascularization during hypoxia. A: Expression of VEGF normalized to own controls (dotted line) in two hypoxic groups at P13 is shown (n = 4). Significant reduction of VEGF in TRIB3 KO hypoxic retinas is observed. Representative images of the western blots probed with anti-VEGF antibody are shown at the bottom. B: Ratios of the neovascular (NV) areas in the hypoxic C57BL6 and TRIB3 KO retinas (n = 6–8) to the whole retinal areas at P17 are depicted. The flat mount

images were used to run a computer program developed by Xiao et al. to analyze areas of neovascularization (NV) and vaso-obliteration (VO). [193] Significant reduction in NV area is observed in hypoxic TRIB3 KO retinas of pups. Representative images for neovascularization and avascular area in the flat mount retina of pups stained with Isolectin (in green). C: Expression of GFAP in two diabetic C57BL6 and TRIB3 KO groups normalized to own control (dotted line) at P13 is presented (n = 4). A dramatic reduction in the GFAP level in diabetic retinas with TRIB3 ablation was detected. Representative images of the western blots probed with anti-GFAP antibody are shown at the bottom. *(p<0.05); **(p<0.01).

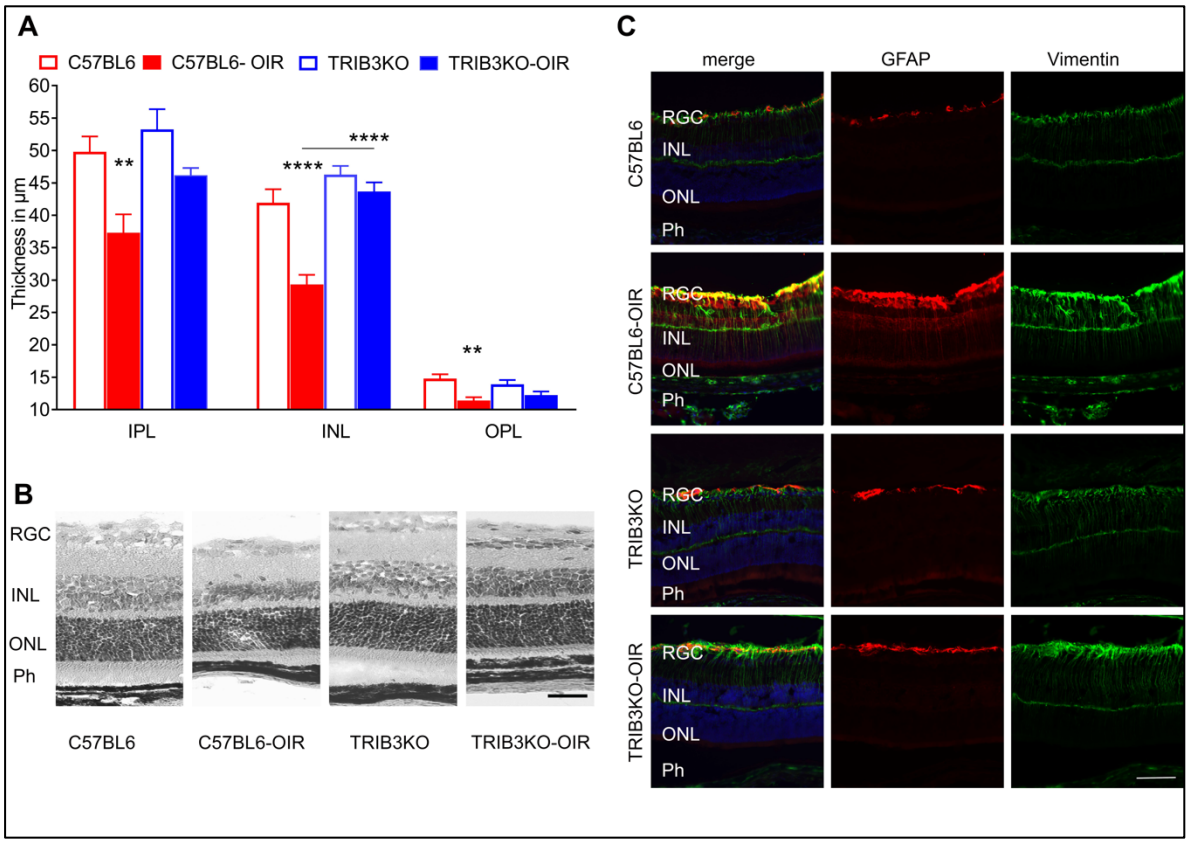

Figure 6. TRIB3 promotes retinal integrity loss and activates gliosis during hypoxia. A: TRIB3 KO significantly preserves the retinal integrity in hyperglycemic mice (n = 5). The IPL, INL, and OPL thicknesses are diminished in C57BL6 diabetic retinas, whereas protection is observed in TRIB3 KO diabetic retinas, demonstrating no difference compared to control retinas in both genetic groups. B: Representative images of the H&E-stained retinas in the four mouse groups. C: Representative images of the retinal sections probed with anti-GFAP (red) and anti-Vimentin (green) antibodies and DAPI (blue) in the four mouse groups taken with fluorescent microscopy. Merged images are shown on the left. (ONL: outer nuclear layer; INL: inner nuclear layer; RGC layer: retinal ganglion cell layer; Ph: photoreceptors). **($p<0.01$); ****($p<0.0001$). The scale is 100 µm.

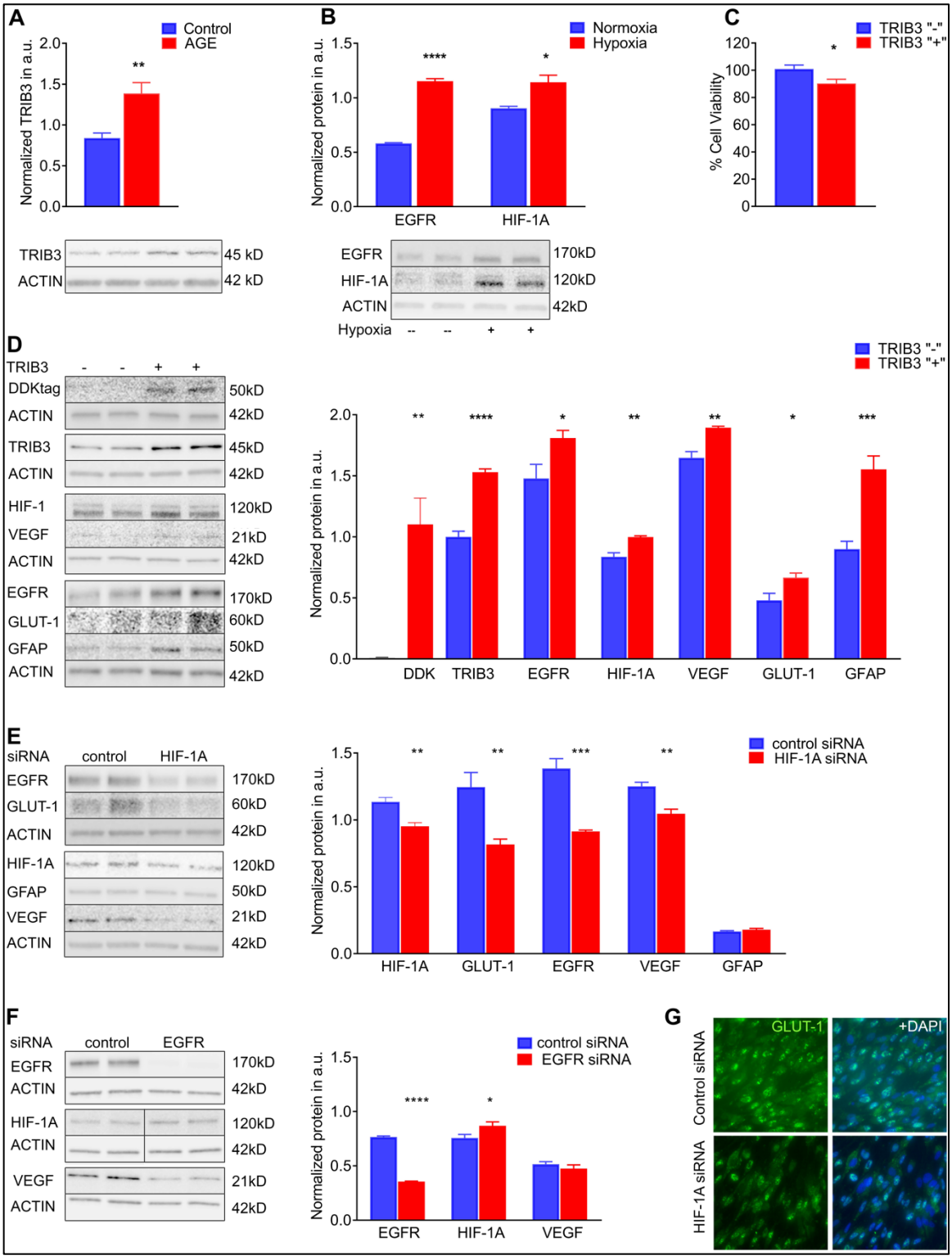

Figure 7. TRIB3 overexpression activates downstream signaling in Muller MIO-M1 cells. A: AGE treatment results in TRIB3 over expression in 72 hours (n = 6). B:

Hypoxia induces HIF1 and EGFR protein in addition to TRIB3 (Figure 1) (n = 4). C: Muller cells overexpressing TRIB3 demonstrate compromised cell viability (n = 4). D: Overexpression of TRIB3 in hypoxic Muller cells results in overexpression of EGFR1, HIF1α, VEGF, GFAP, and GLUT1 (n = 4–5). E: Knockdown of *Hif1a* mRNA in hypoxic Muller cells results in downregulation of GLUT1, EGFR1, and VEGF1, whereas GFA expression does not respond to the treatment with siRNA (n = 5). F: Knockdown of *Egfr1* mRNA in hypoxic Muller cells results in downregulation of HIF1, whereas VEGF expression does not respond to the siRNA treatment (n = 6). G: Representative images of MIO-M1 cells transfected with control and *Hif1*a siRNA. Detection of GLUT1 (in green) was achieved performing IHC analysis and confocal microscopy. Staining with DAPI (in blue) was used to detect nuclei. *(p<0.05); **(p<0.01); ***(p<0.001).

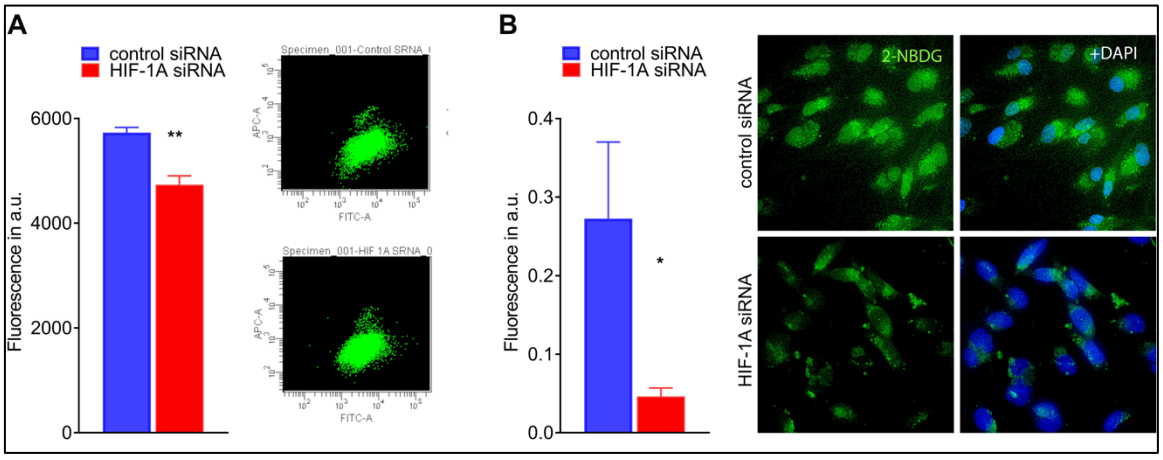

Figure 8. Treatment of hypoxic Muller cells with siRNA targeting *HIF1α* results in reduction of fluorescent signal from 2-NBDG cellular uptake. A: Reduction of fluorescent signal from 2-NBDG uptake measured by flow cytometry (n = 4). B: Reduction of fluorescent signal from 2-NBDG cellular uptake registered in fixed cultured

MIO-M1 cells using microscopy (n = 3–4). The calculation of fluorescent signal was performed using the ImageJ program. *(p<0.05); **(p<0.01).

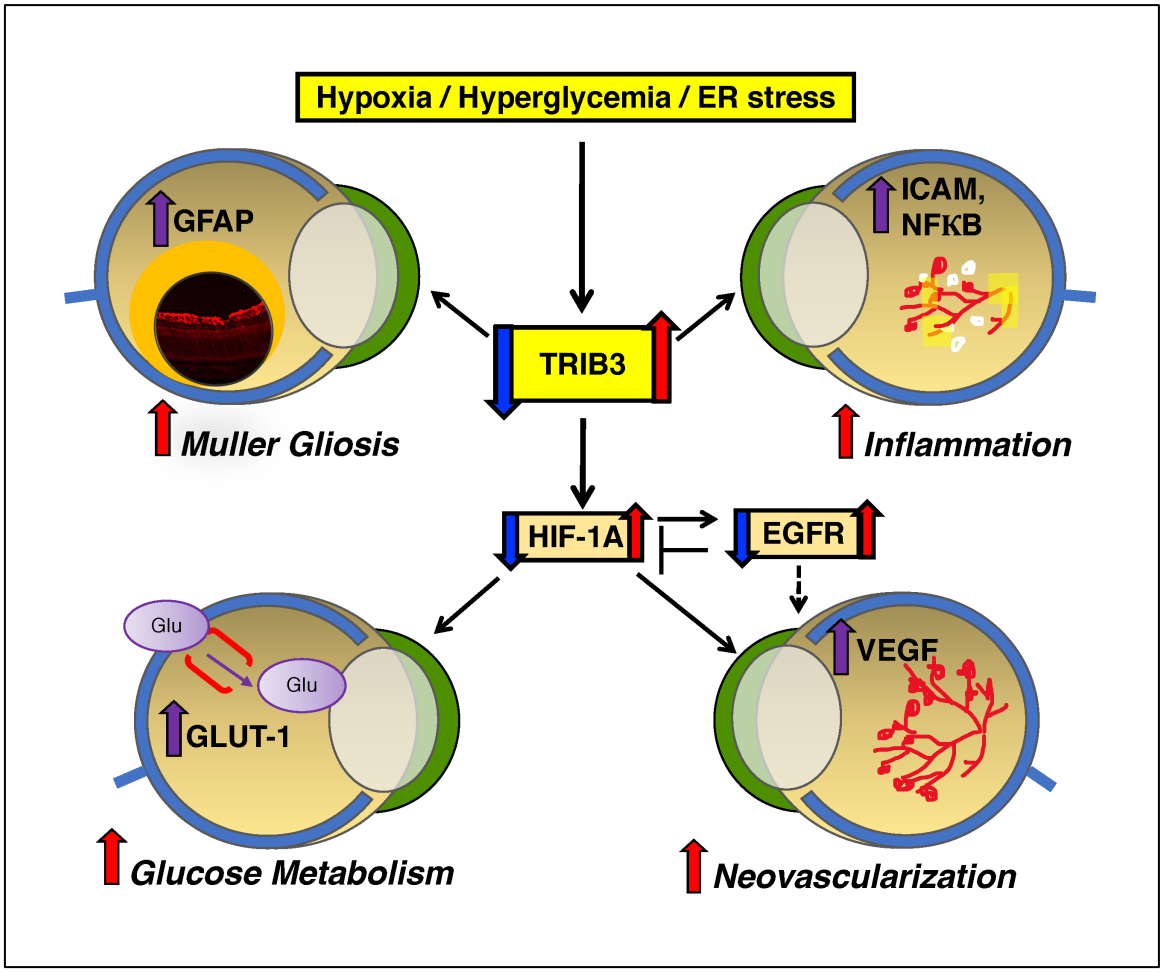

Figure 9. Schematic presentation of the proposed molecular mechanism of diabetic retinopathy controlled by TRIB3. Under hyperglycemic and hypoxic conditions, TRIB3 overexpression leads to upregulation of HIF1α, EGFR, and GFAP. HIF1α overexpression results in GLUT1 activation followed by increase in retinal glucose flux, overall affecting retinal metabolism. Additionally, HIF1α mediates VEGF expression, which compromises vascular cell integrity and triggers angiogenesis. EGFR is upregulated as a result of TRIB3 upregulation as well. This protein reportedly induces

VEGF and cytokines leading to vascular dysfunction. TRIB3 promotes expression of GFAP and reactivation of gliosis in hypoxic retinas. Red and purple arrows indicate upregulation; blue arrows indicate downregulation signaling validated in our study, respectively. Solid lines represent data of the current study. Dashed lines denote the regulation proposed in the literature.

Table: 1. Reagents, antibodies and primers in the study.

	Manufacturer Catalog Number
C57BL6J Mice	Jackson Labs# 000664
Streptozotocin (STZ)	Sigma# S0130
Glucometer	CVS True Metrix# RE4007-01
Hba1c Kit	PTS Diagnostics# 3021
Glucose Estimation Assay Kit	Cell Biolabs, Inc# STA-680
Trizol	Ambion# 15596
cDNA Synthesis Kit	Biorad# 1708841
4% PFA	EMS# 50-980-487
OCT Compound	EMS# 62550-01
H& E Kit	EMS# 26754-1A, 26762-01
Periodic Acid Schiff Reagents	Sigma# 395B-1KT
Elastase Solution	Calbiochem# 324682
Lipopolysacchrides (LPS)- E. Coli	Sigma# L2880
Seahorse XF DMEM Medium	AT# 103575-100
Seahorse XF24 Islet Capture Microplate	AT# 101122-100
Seahorse Microplate Insert Tool	AT# 101135-100
Isolectin1B-4	Vector laboratories # FL-1201
Anti- Vimentin (IHC)	Cell Signaling# 5741S
Anti- TRIB3 Antibody (IHC)	Abcam# 73547
Anti- TRIB3 Antibody (WB)	Santa Cruz# (B-2): sc-390242
Anti- VEGF Antibody (WB-RETINA)	Santa Cruz # 7269 HRP
Anti- VEGF Antibody (WB-MULLER CELL)	Invitrogen JH121# MA5-13182
Anti- GFAP Antibody (IHC &WB)	Sigma# C9205
Anti- B-Actin Antibody (WB)	Sigma# A2066
Anti- CD 31/PECAM-1 (IHC)	Novus Biologicals# NB600-562
Anti- IBA-1 Antibody (IHC)	Wako Chemicals# 019-19741
Anti- BRN-3A Antibody (IHC)	Santa Cruz # 8429 AF488
Anti- Glut-1 Antibody (WB& IHC)	Cell Signaling# Rabbit mAb12939
Anti- HIF-1A Antibody (WB)	Cell Signaling# Rabbit mAb14179
Anti- EGFR Antibody (WB)	Santa Cruz # sc-03-G
Peroxidase AffiniPure Goat Anti-Mouse IgG, Fcγ subclass 2a specific (WB)	JacksonImmunoresearch#115-035-206
HRP Goat Anti-Mouse (WB)	LICOR# 926-80010
IR Goat Anti-Mouse (WB)	LICOR#926-32210
Donkey anti-Rabbit IgG Secondary Antibody, Alexa Fluor 555 (IHC)	Invitrogen Catalog # A32794
Donkey anti-Rabbit IgG Secondary Antibody, Alexa Fluor 488 (IHC)	Invitrogen Catalog # A-21206
VECTASHIELD® Antifade Mounting Medium with DAPI	Vector laboratories# H-1200-10
Taqman Primer- TRIB3	Mm00454879_m1
Taqman Primer- AIF-1	Mm00479862_g1
Taqman Primer- COX-2	Mm03294838_g1
Taqman Primer- ICAM-1	Mm00516023_m1
Taqman Primer- HIF-1A	Mm00468869_m1
Taqman Primer- NFKB-1	Mm00476361_m1
Taqman Primer- RC3HI	Mm01284492_m1
Taqman Primer- VEGF-A	Mm00437304_m1
Taqman Primer- ZC3HI2A	Mm00462533_m1
Taqman Primer- GAPDH	Mm99999915_g1
Taqman Primer- GUSB	Mm00446953_m1
Trib3 (BC012955) Mouse Tagged ORF Clone	Origene- Product number MR204806
MIO-M1 cells- Müller glia cell line	XIP (Prof Limb)
AGE-BSA	Abcam# ab51995
Oxoid™ AnaeroGen™ W-Zip Compact Gas Generator System	Thermo Scientific™ AN0010W
MTT Solution	Sigma-Aldrich# M5655
HIF-1A siRNA	Thermofisher Scientific Assay ID# 42840
EGFR siRNA	Thermofisher Scientific Assay ID# 646
Neg. Control siRNA	Thermofisher Scientific# 4390844
2-NBDG Glucose Uptake Assay Kit	BioVision# K68250

Table: 2. Blood and retinal glucose levels in the control and experimental mice.

Experimental groups of mice	50mg /kg STZ- 5 days dosage			
	Mean HbA1c levels (%HbA1c; mmol/mol)			
	15-weeks	P value	30-weeks	P value
C57BL6 (n=9)	4.7; 28		4.7; 28	
C57BL6 STZ (n=9)	10.8; 95	<0.0001	11.7; 104	<0.0001
TRIB3KO (n=10)	5.3; 34		5.1; 32	
TRIB3KO STZ (n=13)	10.0; 86	<0.0001	10.2; 88	<0.0001

Experimental groups of mice	150mg /kg STZ- single dosage			
	Mean Blood glucose levels (mg/dl)			
	4-weeks	P value	6-weeks	P value
C57BL6 (n=8)	147.5		139.5	
C57BL6 STZ (n=12)	285	<0.0001	291.8	0.0006
TRIB3KO (n=9)	184		138.5	
TRIB3KO STZ (n=12)	391.5	0.0205	351.0	0.0133

Experimental groups of mice	150mg /kg STZ- single dosage			
	Mean Blood glucose levels (mg/dl)		Mean Retinal glucose levels (mg/dl)	
	4-weeks	P value	4-weeks	P value
C57BL6 (n=9)	139.9		0.3	
C57BL6 STZ (n=9)	470.6	<0.0001	4.4	<0.0001
TRIB3KO (n=11)	152.2		0.3	
TRIB3KO STZ (n=5)	434.4	NS	1.3	0.0009

Chapter 4

LIST OF REFERENCES

1 Rueda, E. M. *et al.* The cellular and compartmental profile of mouse retinal glycolysis, tricarboxylic acid cycle, oxidative phosphorylation, and ~P transferring kinases. *Mol Vis* **22**, 847-885 (2016).

2 Daniel S Narayan, G. C., John Pm Wood, Robert J Casson Glucose metabolism in mammalian photoreceptor inner and outer segments. *Clinical & experimental ophthalmology* **45** 730–741., doi:https://doi.org/10.1111/ceo.12952 (2017).

3 Vander Heiden, M. G., Cantley, L. C. & Thompson, C. B. Understanding the Warburg effect: the metabolic requirements of cell proliferation. *Science* **324**, 1029-1033, doi:10.1126/science.1160809 (2009).

4 Adijanto, J. & Philp, N. J. The SLC16A family of monocarboxylate transporters (MCTs)--physiology and function in cellular metabolism, pH homeostasis, and fluid transport. *Curr Top Membr* **70**, 275-311, doi:10.1016/B978-0-12-394316-3.00009-0 (2012).

5 Winkler, B. S., Arnold, M. J., Brassell, M. A. & Puro, D. G. Energy metabolism in human retinal Muller cells. *Invest Ophthalmol Vis Sci* **41**, 3183-3190 (2000).

6 Poitry-Yamate, C. L., Poitry, S. & Tsacopoulos, M. Lactate released by Muller glial cells is metabolized by photoreceptors from mammalian retina. *J Neurosci* **15**, 5179-5191 (1995).

7 Takata, K., Kasahara, T., Kasahara, M., Ezaki, O. & Hirano, H. Erythrocyte/HepG2-type glucose transporter is concentrated in cells of blood-tissue barriers. *Biochem Biophys Res Commun* **173**, 67-73, doi:10.1016/s0006-291x(05)81022-8 (1990).

8 Pragallapati, S. & Manyam, R. Glucose transporter 1 in health and disease. *J Oral Maxillofac Pathol* **23**, 443-449, doi:10.4103/jomfp.JOMFP_22_18 (2019).

9 Badr, G. A., Tang, J., Ismail-Beigi, F. & Kern, T. S. Diabetes downregulates GLUT1 expression in the retina and its microvessels but not in the cerebral cortex or its microvessels. *Diabetes* **49**, 1016-1021, doi:10.2337/diabetes.49.6.1016 (2000).

10 Leasher, J. L. *et al.* Global Estimates on the Number of People Blind or Visually Impaired by Diabetic Retinopathy: A Meta-analysis From 1990 to 2010. *Diabetes Care* **39**, 1643-1649, doi:10.2337/dc15-2171 (2016).

11 Stitt, A. W. *et al.* The progress in understanding and treatment of diabetic retinopathy. *Prog Retin Eye Res* **51**, 156-186, doi:10.1016/j.preteyeres.2015.08.001 (2016).

12 Frey, T. & Antonetti, D. A. Alterations to the blood-retinal barrier in diabetes: cytokines and reactive oxygen species. *Antioxid Redox Signal* **15**, 1271-1284, doi:10.1089/ars.2011.3906 (2011).

13 Zhang, X., Zeng, H., Bao, S., Wang, N. & Gillies, M. C. Diabetic macular edema: new concepts in patho-physiology and treatment. *Cell Biosci* **4**, 27, doi:10.1186/2045-3701-4-27 (2014).

14 Diabetes, C. *et al.* The effect of intensive treatment of diabetes on the development and progression of long-term complications in insulin-dependent diabetes mellitus. *N Engl J Med* **329**, 977-986, doi:10.1056/NEJM199309303291401 (1993).

15 van Leiden, H. A. *et al.* Blood pressure, lipids, and obesity are associated with retinopathy: the hoorn study. *Diabetes Care* **25**, 1320-1325 (2002).

16 Brownlee, M. The pathobiology of diabetic complications: a unifying mechanism. *Diabetes* **54**, 1615-1625, doi:10.2337/diabetes.54.6.1615 (2005).

17 Lee, A. Y. & Chung, S. S. Contributions of polyol pathway to oxidative stress in diabetic cataract. *FASEB J* **13**, 23-30, doi:10.1096/fasebj.13.1.23 (1999).

18 Koya, D. & King, G. L. Protein kinase C activation and the development of diabetic complications. *Diabetes* **47**, 859-866, doi:10.2337/diabetes.47.6.859 (1998).

19 Xia, P. *et al.* Characterization of the mechanism for the chronic activation of diacylglycerol-protein kinase C pathway in diabetes and hypergalactosemia. *Diabetes* **43**, 1122-1129, doi:10.2337/diab.43.9.1122 (1994).

20 Charonis, A. S. *et al.* Laminin alterations after in vitro nonenzymatic glycosylation. *Diabetes* **39**, 807-814, doi:10.2337/diab.39.7.807 (1990).

21 Cappai, G., Songini, M., Doria, A., Cavallerano, J. D. & Lorenzi, M. Increased prevalence of proliferative retinopathy in patients with type 1 diabetes who are deficient in glucose-6-phosphate dehydrogenase. *Diabetologia* **54**, 1539-1542, doi:10.1007/s00125-011-2099-3 (2011).

22 Zhang, Z. *et al.* High glucose inhibits glucose-6-phosphate dehydrogenase, leading to increased oxidative stress and beta-cell apoptosis. *FASEB J* **24**, 1497-1505, doi:10.1096/fj.09-136572 (2010).

23 McClain, D. A., Paterson, A. J., Roos, M. D., Wei, X. & Kudlow, J. E. Glucose and glucosamine regulate growth factor gene expression in vascular smooth muscle cells. *Proc Natl Acad Sci U S A* **89**, 8150-8154, doi:10.1073/pnas.89.17.8150 (1992).

24 Wells, L. & Hart, G. W. O-GlcNAc turns twenty: functional implications for post-translational modification of nuclear and cytosolic proteins with a sugar. *FEBS Lett* **546**, 154-158, doi:10.1016/s0014-5793(03)00641-0 (2003).

25 Gorbatyuk, M. & Gorbatyuk, O. Review: retinal degeneration: focus on the unfolded protein response. *Mol Vis* **19**, 1985-1998 (2013).

26 Ma, J. H., Wang, J. J. & Zhang, S. X. The unfolded protein response and diabetic retinopathy. *J Diabetes Res* **2014**, 160140, doi:10.1155/2014/160140 (2014).

27 Li, J., Wang, J. J., Yu, Q., Wang, M. & Zhang, S. X. Endoplasmic reticulum stress is implicated in retinal inflammation and diabetic retinopathy. *FEBS Lett* **583**, 1521-1527, doi:10.1016/j.febslet.2009.04.007 (2009).

28 Chen, Y. *et al.* Activating transcription factor 4 mediates hyperglycaemia-induced endothelial inflammation and retinal vascular leakage through activation of STAT3 in a mouse model of type 1 diabetes. *Diabetologia* **55**, 2533-2545, doi:10.1007/s00125-012-2594-1 (2012).

29 Zhong, Y., Wang, J. J. & Zhang, S. X. Intermittent but not constant high glucose induces ER stress and inflammation in human retinal pericytes. *Adv Exp Med Biol* **723**, 285-292, doi:10.1007/978-1-4614-0631-0_37 (2012).

30 Dandona, P. Minimizing Glycemic Fluctuations in Patients with Type 2 Diabetes: Approaches and Importance. *Diabetes Technol Ther* **19**, 498-506, doi:10.1089/dia.2016.0372 (2017).

31 Blais, J. D. *et al.* Perk-dependent translational regulation promotes tumor cell adaptation and angiogenesis in response to hypoxic stress. *Mol Cell Biol* **26**, 9517-9532, doi:10.1128/MCB.01145-06 (2006).

32 Deng, J. *et al.* Translational repression mediates activation of nuclear factor kappa B by phosphorylated translation initiation factor 2. *Mol Cell Biol* **24**, 10161-10168, doi:10.1128/MCB.24.23.10161-10168.2004 (2004).

33 Zhang, K. & Kaufman, R. J. From endoplasmic-reticulum stress to the inflammatory response. *Nature* **454**, 455-462, doi:10.1038/nature07203 (2008).

34 Wang, X., Wang, G., Kunte, M., Shinde, V. & Gorbatyuk, M. Modulation of angiogenesis by genetic manipulation of ATF4 in mouse model of oxygen-induced retinopathy [corrected]. *Invest Ophthalmol Vis Sci* **54**, 5995-6002, doi:10.1167/iovs.13-12117 (2013).

35 Prudente, S. *et al.* The mammalian tribbles homolog TRIB3, glucose homeostasis, and cardiovascular diseases. *Endocr Rev* **33**, 526-546, doi:10.1210/er.2011-1042 (2012).

36 Mayumi-Matsuda, K., Kojima, S., Suzuki, H. & Sakata, T. Identification of a novel kinase-like gene induced during neuronal cell death. *Biochem Biophys Res Commun* **258**, 260-264, doi:10.1006/bbrc.1999.0576 (1999).

37 Loewen, N., Chen, J., Dudley, V. J., Sarthy, V. P. & Mathura, J. R., Jr. Genomic response of hypoxic Muller cells involves the very low density lipoprotein receptor as part of an angiogenic network. *Exp Eye Res* **88**, 928-937, doi:10.1016/j.exer.2008.11.037 (2009).

38 Ord, T. & Ord, T. Mammalian Pseudokinase TRIB3 in Normal Physiology and Disease: Charting the Progress in Old and New Avenues. *Curr Protein Pept Sci* **18**, 819-842, doi:10.2174/1389203718666170406124547 (2017).

39 Du, K., Herzig, S., Kulkarni, R. N. & Montminy, M. TRB3: a tribbles homolog that inhibits Akt/PKB activation by insulin in liver. *Science* **300**, 1574-1577, doi:10.1126/science.1079817 (2003).

40 Dimmeler, S. *et al.* Activation of nitric oxide synthase in endothelial cells by Akt-dependent phosphorylation. *Nature* **399**, 601-605, doi:10.1038/21224 (1999).

41 Andreozzi, F. *et al.* TRIB3 R84 variant is associated with impaired insulin-mediated nitric oxide production in human endothelial cells. *Arterioscler Thromb Vasc Biol* **28**, 1355-1360, doi:10.1161/ATVBAHA.108.162883 (2008).

42 Liu, J. *et al.* Mammalian Tribbles homolog 3 impairs insulin action in skeletal muscle: role in glucose-induced insulin resistance. *Am J Physiol Endocrinol Metab* **298**, E565-576, doi:10.1152/ajpendo.00467.2009 (2010).

43 Zhang, W. *et al.* TRIB3 mediates glucose-induced insulin resistance via a mechanism that requires the hexosamine biosynthetic pathway. *Diabetes* **62**, 4192-4200, doi:10.2337/db13-0312 (2013).

44 Zhang, W. *et al.* Skeletal Muscle TRIB3 Mediates Glucose Toxicity in Diabetes and High- Fat Diet-Induced Insulin Resistance. *Diabetes* **65**, 2380-2391, doi:10.2337/db16-0154 (2016).

45 Izrailit, J., Berman, H. K., Datti, A., Wrana, J. L. & Reedijk, M. High throughput kinase inhibitor screens reveal TRB3 and MAPK-ERK/TGFbeta pathways as fundamental Notch regulators in breast cancer. *Proc Natl Acad Sci U S A* **110**, 1714-1719, doi:10.1073/pnas.1214014110 (2013).

46 Pedrosa, A. R. *et al.* Endothelial Jagged1 promotes solid tumor growth through both pro-angiogenic and angiocrine functions. *Oncotarget* **6**, 24404-24423, doi:10.18632/oncotarget.4380 (2015).

47 Benedito, R. *et al.* The notch ligands Dll4 and Jagged1 have opposing effects on angiogenesis. *Cell* **137**, 1124-1135, doi:10.1016/j.cell.2009.03.025 (2009).

48 Oskolkova, O. V. *et al.* ATF4-dependent transcription is a key mechanism in VEGF up-regulation by oxidized phospholipids: critical role of oxidized sn-2 residues in activation of unfolded protein response. *Blood* **112**, 330-339, doi:10.1182/blood-2007-09-112870 (2008).

49 Vujosevic, S. & Midena, E. Retinal layers changes in human preclinical and early clinical diabetic retinopathy support early retinal neuronal and Muller cells alterations. *J Diabetes Res* **2013**, 905058, doi:10.1155/2013/905058 (2013).

50 Grunwald, J. E., DuPont, J. & Riva, C. E. Retinal haemodynamics in patients with early diabetes mellitus. *Br J Ophthalmol* **80**, 327-331 (1996).

51 Baget-Bernaldiz, M., Romero-Aroca, P., Bautista-Perez, A. & Mercado, J. Multifocal electroretinography changes at the 1-year follow-up in a cohort of diabetic macular edema patients treated with ranibizumab. *Doc Ophthalmol* **135**, 85-96, doi:10.1007/s10633-017-9601-2 (2017).

52 Tehrani, N. M. *et al.* Multifocal Electroretinogram in Diabetic Macular Edema; Correlation with Visual Acuity and Optical Coherence Tomography. *J Ophthalmic Vis Res* **10**, 165-171, doi:10.4103/2008-322X.163773 (2015).

53 Pardue, M. T. *et al.* Rodent Hyperglycemia-Induced Inner Retinal Deficits are Mirrored in Human Diabetes. *Transl Vis Sci Technol* **3**, 6, doi:10.1167/tvst.3.3.6 (2014).

54 Nork, T. M., Wallow, I. H., Sramek, S. J. & Anderson, G. Muller's cell involvement in proliferative diabetic retinopathy. *Arch Ophthalmol* **105**, 1424-1429 (1987).

55 Mizutani, M., Gerhardinger, C. & Lorenzi, M. Muller cell changes in human diabetic retinopathy. *Diabetes* **47**, 445-449 (1998).

56 Abu-El-Asrar, A. M., Dralands, L., Missotten, L., Al-Jadaan, I. A. & Geboes, K. Expression of apoptosis markers in the retinas of human subjects with diabetes. *Invest Ophthalmol Vis Sci* **45**, 2760-2766, doi:10.1167/iovs.03-1392 (2004).

57 Rungger-Brandle, E., Dosso, A. A. & Leuenberger, P. M. Glial reactivity, an early feature of diabetic retinopathy. *Invest Ophthalmol Vis Sci* **41**, 1971-1980 (2000).

58 Barber, A. J., Antonetti, D. A. & Gardner, T. W. Altered expression of retinal occludin and glial fibrillary acidic protein in experimental diabetes. The Penn State Retina Research Group. *Invest Ophthalmol Vis Sci* **41**, 3561-3568 (2000).

59 Muramatsu, D. *et al.* Correlation of complement fragment C5a with inflammatory cytokines in the vitreous of patients with proliferative diabetic retinopathy. *Graefes Arch Clin Exp Ophthalmol* **251**, 15-17, doi:10.1007/s00417-012-2024-6 (2013).

60 Abu El-Asrar, A. M., Struyf, S., Kangave, D., Geboes, K. & Van Damme, J. Chemokines in proliferative diabetic retinopathy and proliferative vitreoretinopathy. *Eur Cytokine Netw* **17**, 155-165 (2006).

61 Freyberger, H. *et al.* Increased levels of platelet-derived growth factor in vitreous fluid of patients with proliferative diabetic retinopathy. *Exp Clin Endocrinol Diabetes* **108**, 106-109, doi:10.1055/s-2000-5803 (2000).

62 Elner, S. G. *et al.* Cytokines in proliferative diabetic retinopathy and proliferative vitreoretinopathy. *Curr Eye Res* **14**, 1045-1053 (1995).

63 Ishikawa, K. *et al.* Microarray analysis of gene expression in fibrovascular membranes excised from patients with proliferative diabetic retinopathy. *Invest Ophthalmol Vis Sci* **56**, 932-946, doi:10.1167/iovs.14-15589 (2015).

64 Oshitari, T., Yamamoto, S., Hata, N. & Roy, S. Mitochondria- and caspase-dependent cell death pathway involved in neuronal degeneration in diabetic retinopathy. *Br J Ophthalmol* **92**, 552-556, doi:10.1136/bjo.2007.132308 (2008).

65 Lutty, G. A., McLeod, D. S., Merges, C., Diggs, A. & Plouet, J. Localization of vascular endothelial growth factor in human retina and choroid. *Arch Ophthalmol* **114**, 971-977 (1996).

66 Mizutani, M., Kern, T. S. & Lorenzi, M. Accelerated death of retinal microvascular cells in human and experimental diabetic retinopathy. *J Clin Invest* **97**, 2883-2890, doi:10.1172/JCI118746 (1996).

67 Giugliano, D., Ceriello, A. & Esposito, K. Glucose metabolism and hyperglycemia. *Am J Clin Nutr* **87**, 217S-222S, doi:10.1093/ajcn/87.1.217S (2008).

68 Eleazu, C. O., Eleazu, K. C., Chukwuma, S. & Essien, U. N. Review of the mechanism of cell death resulting from streptozotocin challenge in experimental animals, its practical use and potential risk to humans. *J Diabetes Metab Disord* **12**, 60, doi:10.1186/2251-6581-12-60 (2013).

69 Sakata, N., Yoshimatsu, G., Tsuchiya, H., Egawa, S. & Unno, M. Animal models of diabetes mellitus for islet transplantation. *Exp Diabetes Res* **2012**, 256707, doi:10.1155/2012/256707 (2012).

70 McLetchie, N. G. Alloxan diabetes: a discovery, albeit a minor one. *J R Coll Physicians Edinb* **32**, 134-142 (2002).

71 Engerman, R. L. & Kern, T. S. Experimental galactosemia produces diabetic-like retinopathy. *Diabetes* **33**, 97-100 (1984).

72 Rakieten, N., Rakieten, M. L. & Nadkarni, M. V. Studies on the diabetogenic action of streptozotocin (NSC-37917). *Cancer Chemother Rep* **29**, 91-98 (1963).

73 Lai, A. K. & Lo, A. C. Animal models of diabetic retinopathy: summary and comparison. *J Diabetes Res* **2013**, 106594, doi:10.1155/2013/106594 (2013).

74 Serra, A. M. *et al.* CD11b+ bone marrow-derived monocytes are the major leukocyte subset responsible for retinal capillary leukostasis in experimental diabetes in mouse and express high levels of CCR5 in the circulation. *Am J Pathol* **181**, 719-727, doi:10.1016/j.ajpath.2012.04.009 (2012).

75 Wright, W. S. & Harris, N. R. Ozagrel attenuates early streptozotocin-induced constriction of arterioles in the mouse retina. *Exp Eye Res* **86**, 528-536, doi:10.1016/j.exer.2007.12.012 (2008).

76 Mostafavinia, A., Amini, A., Ghorishi, S. K., Pouriran, R. & Bayat, M. The effects of dosage and the routes of administrations of streptozotocin and alloxan on induction rate of type1 diabetes mellitus and mortality rate in rats. *Lab Anim Res* **32**, 160-165, doi:10.5625/lar.2016.32.3.160 (2016).

77 Allen, R. S. *et al.* TrkB signalling pathway mediates the protective effects of exercise in the diabetic rat retina. *Eur J Neurosci* **47**, 1254-1265, doi:10.1111/ejn.13909 (2018).

78 Drago, F., La Manna, C., Emmi, I. & Marino, A. Effects of sulfinpyrazone on retinal damage induced by experimental diabetes mellitus in rabbits. *Pharmacol Res* **38**, 97-100, doi:10.1006/phrs.1998.0339 (1998).

79 Ishiko, S. *et al.* [Early ocular changes in a tree shrew model of diabetes]. *Nippon Ganka Gakkai Zasshi* **101**, 19-23 (1997).

80 Chaudhry, Z. Z. *et al.* Streptozotocin is equally diabetogenic whether administered to fed or fasted mice. *Lab Anim* **47**, 257-265, doi:10.1177/0023677213489548 (2013).

81 Olivares, A. M. *et al.* Animal Models of Diabetic Retinopathy. *Curr Diab Rep* **17**, 93, doi:10.1007/s11892-017-0913-0 (2017).

82 Black, H. E., Rosenblum, I. Y. & Capen, C. C. Chemically induced (streptozotocin-alloxan) diabetes mellitus in the dog. Biochemical and ultrastructural studies. *Am J Pathol* **98**, 295-310 (1980).

83 Seita, M. *et al.* Development of Canine Models of Type 1 Diabetes With Partial Pancreatectomy and the Administration of Streptozotocin. *Cell Med* **6**, 25-31, doi:10.3727/215517913X674289 (2013).

84 Chronopoulos, A. *et al.* Hyperhexosemia-Induced Retinal Vascular Pathology in a Novel Primate Model of Diabetic Retinopathy. *Diabetes* **64**, 2603-2608, doi:10.2337/db14-0866 (2015).

85 Rajagopal, R. *et al.* Functional Deficits Precede Structural Lesions in Mice With High-Fat Diet-Induced Diabetic Retinopathy. *Diabetes* **65**, 1072-1084, doi:10.2337/db15-1255 (2016).

86 Sima, A. A., Chakrabarti, S., Garcia-Salinas, R. & Basu, P. K. The BB-rat--an authentic model of human diabetic retinopathy. *Curr Eye Res* **4**, 1087-1092 (1985).

87 Sima, A. A., Garcia-Salinas, R. & Basu, P. K. The BB Wistar rat: an experimental model for the study of diabetic retinopathy. *Metabolism* **32**, 136-140 (1983).

88 Miyamura, N. & Amemiya, T. Lens and retinal changes in the WBN/Kob rat (spontaneously diabetic strain). Electron-microscopic study. *Ophthalmic Res* **30**, 221-232, doi:10.1159/000055479 (1998).

89 Yokoi, N. *et al.* A Novel Rat Model of Type 2 Diabetes: The Zucker Fatty Diabetes Mellitus ZFDM Rat. *J Diabetes Res* **2013**, 103731, doi:10.1155/2013/103731 (2013).

90 Richard G. Peterson, W. N. S., Mary-Ann Neel, Leah A. Little, J. Eichberg. Zucker Diabetic Fatty Rat as a Model for Non-insulin-dependent Diabetes Mellitus. *ILAR Journal* **Volume 32**, Pages 16–19,, doi:https://doi.org/10.1093/ilar.32.3.16 (1990).

91 Lu, Z. Y., Bhutto, I. A. & Amemiya, T. Retinal changes in Otsuka long-evans Tokushima Fatty rats (spontaneously diabetic rat)--possibility of a new experimental model for diabetic retinopathy. *Jpn J Ophthalmol* **47**, 28-35 (2003).

92 Shinohara, M. *et al.* A new spontaneously diabetic non-obese Torii rat strain with severe ocular complications. *Int J Exp Diabetes Res* **1**, 89-100 (2000).

93 Yoshioka, M., Kayo, T., Ikeda, T. & Koizumi, A. A novel locus, Mody4, distal to D7Mit189 on chromosome 7 determines early-onset NIDDM in nonobese C57BL/6 (Akita) mutant mice. *Diabetes* **46**, 887-894 (1997).

94 Barber, A. J. *et al.* The Ins2Akita mouse as a model of early retinal complications in diabetes. *Invest Ophthalmol Vis Sci* **46**, 2210-2218, doi:10.1167/iovs.04-1340 (2005).

95 Wicker, L. S., Todd, J. A. & Peterson, L. B. Genetic control of autoimmune diabetes in the NOD mouse. *Annu Rev Immunol* **13**, 179-200, doi:10.1146/annurev.iy.13.040195.001143 (1995).

96 Makino, S. *et al.* Breeding of a non-obese, diabetic strain of mice. *Jikken Dobutsu* **29**, 1-13 (1980).

97 Hummel, K. P., Dickie, M. M. & Coleman, D. L. Diabetes, a new mutation in the mouse. *Science* **153**, 1127-1128 (1966).

98 van Eeden, P. E. *et al.* Early vascular and neuronal changes in a VEGF transgenic mouse model of retinal neovascularization. *Invest Ophthalmol Vis Sci* **47**, 4638-4645, doi:10.1167/iovs.06-0251 (2006).

99 Rakoczy, E. P. *et al.* Characterization of a mouse model of hyperglycemia and retinal neovascularization. *Am J Pathol* **177**, 2659-2670, doi:10.2353/ajpath.2010.090883 (2010).

100 Cao, R., Jensen, L. D., Soll, I., Hauptmann, G. & Cao, Y. Hypoxia-induced retinal angiogenesis in zebrafish as a model to study retinopathy. *PLoS One* **3**, e2748, doi:10.1371/journal.pone.0002748 (2008).

101 van Rooijen, E. *et al.* von Hippel-Lindau tumor suppressor mutants faithfully model pathological hypoxia-driven angiogenesis and vascular retinopathies in zebrafish. *Dis Model Mech* **3**, 343-353, doi:10.1242/dmm.004036 (2010).

102 Fong, D. S., Aiello, L. P., Ferris, F. L., 3rd & Klein, R. Diabetic retinopathy. *Diabetes Care* **27**, 2540-2553 (2004).

103 Smith, L. E. *et al.* Oxygen-induced retinopathy in the mouse. *Invest Ophthalmol Vis Sci* **35**, 101-111 (1994).

104 Patz, A., Eastham, A., Higginbotham, D. H. & Kleh, T. Oxygen studies in retrolental fibroplasia. II. The production of the microscopic changes of retrolental fibroplasia in experimental animals. *Am J Ophthalmol* **36**, 1511-1522 (1953).

105 McLeod, D. S. & Lutty, G. A. Targeting VEGF in canine oxygen-induced retinopathy - a model for human retinopathy of prematurity. *Eye Brain* **8**, 55-65, doi:10.2147/EB.S94443 (2016).

106 Zhang, S. X. *et al.* Genetic difference in susceptibility to the blood-retina barrier breakdown in diabetes and oxygen-induced retinopathy. *Am J Pathol* **166**, 313-321, doi:10.1016/S0002-9440(10)62255-9 (2005).

107 Zhang, S. X. *et al.* Pigment epithelium-derived factor (PEDF) is an endogenous antiinflammatory factor. *FASEB J* **20**, 323-325, doi:10.1096/fj.05-4313fje (2006).

108 Kim, C. B., D'Amore, P. A. & Connor, K. M. Revisiting the mouse model of oxygen-induced retinopathy. *Eye Brain* **8**, 67-79, doi:10.2147/EB.S94447 (2016).

109 Reiter, C. E. *et al.* Diabetes reduces basal retinal insulin receptor signaling: reversal with systemic and local insulin. *Diabetes* **55**, 1148-1156 (2006).

110 Rajala, A., Tanito, M., Le, Y. Z., Kahn, C. R. & Rajala, R. V. Loss of neuroprotective survival signal in mice lacking insulin receptor gene in rod photoreceptor cells. *J Biol Chem* **283**, 19781-19792, doi:10.1074/jbc.M802374200 (2008).

111 Rajala, R. V., Wiskur, B., Tanito, M., Callegan, M. & Rajala, A. Diabetes reduces autophosphorylation of retinal insulin receptor and increases protein-tyrosine phosphatase-1B activity. *Invest Ophthalmol Vis Sci* **50**, 1033-1040, doi:10.1167/iovs.08-2851 (2009).

112 Yang, L. *et al.* Role of endoplasmic reticulum stress in the loss of retinal ganglion cells in diabetic retinopathy. *Neural Regen Res* **8**, 3148-3158, doi:10.3969/j.issn.1673-5374.2013.33.009 (2013).

113 Li, B., Wang, H. S., Li, G. G., Zhao, M. J. & Zhao, M. H. The role of endoplasmic reticulum stress in the early stage of diabetic retinopathy. *Acta Diabetol* **48**, 103-111, doi:10.1007/s00592-009-0170-z (2011).

114 Shruthi, K., Reddy, S. S. & Reddy, G. B. Ubiquitin-proteasome system and ER stress in the retina of diabetic rats. *Arch Biochem Biophys* **627**, 10-20, doi:10.1016/j.abb.2017.06.006 (2017).

115 Kim, J. *et al.* KIOM-79 protects AGE-induced retinal pericyte apoptosis via inhibition of NF-kappaB activation in vitro and in vivo. *PLoS One* **7**, e43591, doi:10.1371/journal.pone.0043591 (2012).

116 Kirwin, S. J., Kanaly, S. T., Linke, N. A. & Edelman, J. L. Strain-dependent increases in retinal inflammatory proteins and photoreceptor FGF-2 expression in streptozotocin-induced diabetic rats. *Invest Ophthalmol Vis Sci* **50**, 5396-5404, doi:10.1167/iovs.09-3474 (2009).

117 Chung, Y. R., Choi, J. A., Koh, J. Y. & Yoon, Y. H. Ursodeoxycholic Acid Attenuates Endoplasmic Reticulum Stress-Related Retinal Pericyte Loss in Streptozotocin-Induced Diabetic Mice. *J Diabetes Res* **2017**, 1763292, doi:10.1155/2017/1763292 (2017).

118 Zhong, Y. *et al.* Activation of endoplasmic reticulum stress by hyperglycemia is essential for Muller cell-derived inflammatory cytokine production in diabetes. *Diabetes* **61**, 492-504, doi:10.2337/db11-0315 (2012).

119 Kondo, T. & Kahn, C. R. Altered insulin signaling in retinal tissue in diabetic states. *J Biol Chem* **279**, 37997-38006, doi:10.1074/jbc.M401339200 (2004).

120 Bhatta, M., Ma, J. H., Wang, J. J., Sakowski, J. & Zhang, S. X. Enhanced endoplasmic reticulum stress in bone marrow angiogenic progenitor cells in a mouse model of long-term experimental type 2 diabetes. *Diabetologia* **58**, 2181-2190, doi:10.1007/s00125-015-3643-3 (2015).

121 Fu, D. *et al.* Survival or death: a dual role for autophagy in stress-induced pericyte loss in diabetic retinopathy. *Diabetologia* **59**, 2251-2261, doi:10.1007/s00125-016-4058-5 (2016).

122 Li, Q., Zemel, E., Miller, B. & Perlman, I. Early retinal damage in experimental diabetes: electroretinographical and morphological observations. *Exp Eye Res* **74**, 615-625, doi:10.1006/exer.2002.1170 (2002).

123 Downie, L. E., Pianta, M. J., Vingrys, A. J., Wilkinson-Berka, J. L. & Fletcher, E. L. Neuronal and glial cell changes are determined by retinal vascularization in retinopathy of prematurity. *J Comp Neurol* **504**, 404-417, doi:10.1002/cne.21449 (2007).

124 Downie, L. E., Pianta, M. J., Vingrys, A. J., Wilkinson-Berka, J. L. & Fletcher, E. L. AT1 receptor inhibition prevents astrocyte degeneration and restores vascular growth in oxygen-induced retinopathy. *Glia* **56**, 1076-1090, doi:10.1002/glia.20680 (2008).

125 Park, S. H. *et al.* Apoptotic death of photoreceptors in the streptozotocin-induced diabetic rat retina. *Diabetologia* **46**, 1260-1268, doi:10.1007/s00125-003-1177-6 (2003).

126 Robison, W. G., Jr., Tillis, T. N., Laver, N. & Kinoshita, J. H. Diabetes-related histopathologies of the rat retina prevented with an aldose reductase inhibitor. *Exp Eye Res* **50**, 355-366 (1990).

127 Szabo, K. *et al.* Histological Evaluation of Diabetic Neurodegeneration in the Retina of Zucker Diabetic Fatty (ZDF) Rats. *Sci Rep* **7**, 8891, doi:10.1038/s41598-017-09068-6 (2017).

128 Alves, M. R. P. *et al.* Subtle thinning of retinal layers without overt vascular and inflammatory alterations in a rat model of prediabetes. *Mol Vis* **24**, 353-366 (2018).

129 Liu, K., Akula, J. D., Falk, C., Hansen, R. M. & Fulton, A. B. The retinal vasculature and function of the neural retina in a rat model of retinopathy of prematurity. *Invest Ophthalmol Vis Sci* **47**, 2639-2647, doi:10.1167/iovs.06-0016 (2006).

130 Yang, Y. *et al.* Decrease in retinal neuronal cells in streptozotocin-induced diabetic mice. *Mol Vis* **18**, 1411-1420 (2012).

131 Martin, P. M., Roon, P., Van Ells, T. K., Ganapathy, V. & Smith, S. B. Death of retinal neurons in streptozotocin-induced diabetic mice. *Invest Ophthalmol Vis Sci* **45**, 3330-3336, doi:10.1167/iovs.04-0247 (2004).

132 Sohn, E. H. *et al.* Retinal neurodegeneration may precede microvascular changes characteristic of diabetic retinopathy in diabetes mellitus. *Proc Natl Acad Sci U S A* **113**, E2655-2664, doi:10.1073/pnas.1522014113 (2016).

133 Hombrebueno, J. R., Chen, M., Penalva, R. G. & Xu, H. Loss of synaptic connectivity, particularly in second order neurons is a key feature of diabetic retinal neuropathy in the Ins2Akita mouse. *PLoS One* **9**, e97970, doi:10.1371/journal.pone.0097970 (2014).

134 Yang, Q. *et al.* Retinal Neurodegeneration in db/db Mice at the Early Period of Diabetes. *J Ophthalmol* **2015**, 757412, doi:10.1155/2015/757412 (2015).

135 Feit-Leichman, R. A. *et al.* Vascular damage in a mouse model of diabetic retinopathy: relation to neuronal and glial changes. *Invest Ophthalmol Vis Sci* **46**, 4281-4287, doi:10.1167/iovs.04-1361 (2005).

136 Kumar, S. & Zhuo, L. Longitudinal in vivo imaging of retinal gliosis in a diabetic mouse model. *Exp Eye Res* **91**, 530-536, doi:10.1016/j.exer.2010.07.010 (2010).

137 Vessey, K. A., Wilkinson-Berka, J. L. & Fletcher, E. L. Characterization of retinal function and glial cell response in a mouse model of oxygen-induced retinopathy. *J Comp Neurol* **519**, 506-527, doi:10.1002/cne.22530 (2011).

138 Aung, M. H., Kim, M. K., Olson, D. E., Thule, P. M. & Pardue, M. T. Early visual deficits in streptozotocin-induced diabetic long evans rats. *Invest Ophthalmol Vis Sci* **54**, 1370-1377, doi:10.1167/iovs.12-10927 (2013).

139 Hancock, H. A. & Kraft, T. W. Oscillatory potential analysis and ERGs of normal and diabetic rats. *Invest Ophthalmol Vis Sci* **45**, 1002-1008, doi:10.1167/iovs.03-1080 (2004).

140 Okuno, T., Oku, H., Sugiyama, T. & Ikeda, T. Electroretinographic study of spontaneously diabetic Torii rats. *Doc Ophthalmol* **117**, 191-196, doi:10.1007/s10633-008-9122-0 (2008).

141 Sasase, T. *et al.* The spontaneously diabetic torii rat: an animal model of nonobese type 2 diabetes with severe diabetic complications. *J Diabetes Res* **2013**, 976209, doi:10.1155/2013/976209 (2013).

142 Moore-Dotson, J. M. *et al.* Early Retinal Neuronal Dysfunction in Diabetic Mice: Reduced Light-Evoked Inhibition Increases Rod Pathway Signaling. *Invest Ophthalmol Vis Sci* **57**, 1418-1430, doi:10.1167/iovs.15-17999 (2016).

143 Sasaki, M. *et al.* Neurodegenerative influence of oxidative stress in the retina of a murine model of diabetes. *Diabetologia* **53**, 971-979, doi:10.1007/s00125-009-1655-6 (2010).

144 Han, Z., Guo, J., Conley, S. M. & Naash, M. I. Retinal angiogenesis in the Ins2(Akita) mouse model of diabetic retinopathy. *Invest Ophthalmol Vis Sci* **54**, 574-584, doi:10.1167/iovs.12-10959 (2013).

145 Bogdanov, P. *et al.* The db/db mouse: a useful model for the study of diabetic retinal neurodegeneration. *PLoS One* **9**, e97302, doi:10.1371/journal.pone.0097302 (2014).

146 Jariyapongskul, A. *et al.* Long-term effects of oral vitamin C supplementation on the endothelial dysfunction in the iris microvessels of diabetic rats. *Microvasc Res* **74**, 32-38, doi:10.1016/j.mvr.2007.03.002 (2007).

147 Anderson, H. R., Stitt, A. W., Gardiner, T. A. & Archer, D. B. Diabetic retinopathy: morphometric analysis of basement membrane thickening of capillaries in different retinal layers within arterial and venous environments. *Br J Ophthalmol* **79**, 1120-1123 (1995).

148 Gong, C. Y., Lu, B., Hu, Q. W. & Ji, L. L. Streptozotocin induced diabetic retinopathy in rat and the expression of vascular endothelial growth factor and its receptor. *Int J Ophthalmol* **6**, 573-577, doi:10.3980/j.issn.2222-3959.2013.05.03 (2013).

149 Schroder, S., Palinski, W. & Schmid-Schonbein, G. W. Activated monocytes and granulocytes, capillary nonperfusion, and neovascularization in diabetic retinopathy. *Am J Pathol* **139**, 81-100 (1991).

150 Kowluru, R. A., Tang, J. & Kern, T. S. Abnormalities of retinal metabolism in diabetes and experimental galactosemia. VII. Effect of long-term administration of antioxidants on the development of retinopathy. *Diabetes* **50**, 1938-1942 (2001).

151 Blair, N. P., Tso, M. O. & Dodge, J. T. Pathologic studies of the blood--retinal barrier in the spontaneously diabetic BB rat. *Invest Ophthalmol Vis Sci* **25**, 302-311 (1984).

152 Behl, Y. *et al.* Diabetes-enhanced tumor necrosis factor-alpha production promotes apoptosis and the loss of retinal microvascular cells in type 1 and type 2 models of diabetic retinopathy. *Am J Pathol* **172**, 1411-1418, doi:10.2353/ajpath.2008.071070 (2008).

153 Kim, J. H., Kim, J. H., Yu, Y. S., Cho, C. S. & Kim, K. W. Blockade of angiotensin II attenuates VEGF-mediated blood-retinal barrier breakdown in diabetic retinopathy. *J Cereb Blood Flow Metab* **29**, 621-628, doi:10.1038/jcbfm.2008.154 (2009).

154 Shen, W. Y. *et al.* Long-term global retinal microvascular changes in a transgenic vascular endothelial growth factor mouse model. *Diabetologia* **49**, 1690-1701, doi:10.1007/s00125-006-0274-8 (2006).

155 Cheung, A. K. *et al.* Aldose reductase deficiency prevents diabetes-induced blood-retinal barrier breakdown, apoptosis, and glial reactivation in the retina of db/db mice. *Diabetes* **54**, 3119-3125 (2005).

156 Clements, R. S., Jr., Robison, W. G., Jr. & Cohen, M. P. Anti-glycated albumin therapy ameliorates early retinal microvascular pathology in db/db mice. *J Diabetes Complications* **12**, 28-33 (1998).

157 Isaacman, T. Editorial: Advertising in medical journals. *Mod Healthc (Short Term Care)* **3**, 7 (1975).

158 Culang-Reinlieb, M. E. *et al.* MRI-defined vascular depression: a review of the construct. *Int J Geriatr Psychiatry* **26**, 1101-1108, doi:10.1002/gps.2668 (2011).

159 Ozaki, H. *et al.* Intravitreal sustained release of VEGF causes retinal neovascularization in rabbits and breakdown of the blood-retinal barrier in rabbits and primates. *Exp Eye Res* **64**, 505-517, doi:10.1006/exer.1996.0239 (1997).

160 Anschuetz, L. *et al.* Discovering Middle Ear Anatomy by Transcanal Endoscopic Ear Surgery: A Dissection Manual. *J Vis Exp*, doi:10.3791/56390 (2018).

161 Tso, M. O. *et al.* Microangiopathic retinopathy in experimental diabetic monkeys. *Trans Am Ophthalmol Soc* **86**, 389-421 (1988).

162 Buchi, E. R., Kurosawa, A. & Tso, M. O. Retinopathy in diabetic hypertensive monkeys: a pathologic study. *Graefes Arch Clin Exp Ophthalmol* **234**, 388-398 (1996).

163 Kim, S. Y. *et al.* Retinopathy in monkeys with spontaneous type 2 diabetes. *Invest Ophthalmol Vis Sci* **45**, 4543-4553, doi:10.1167/iovs.04-0519 (2004).

164 Johnson, M. A. *et al.* Ocular structure and function in an aged monkey with spontaneous diabetes mellitus. *Exp Eye Res* **80**, 37-42, doi:10.1016/j.exer.2004.08.006 (2005).

165 Wu, X. Y. *et al.* [Streptozotocin induction of type 2 diabetes in tree shrew]. *Dongwuxue Yanjiu* **34**, 108-115, doi:10.3724/SP.J.1141.2013.02108 (2013).

166 Kador, P. F., Takahashi, Y., Wyman, M. & Ferris, F., 3rd. Diabeteslike proliferative retinal changes in galactose-fed dogs. *Arch Ophthalmol* **113**, 352-354 (1995).

167 Cusick, M. *et al.* Effects of aldose reductase inhibitors and galactose withdrawal on fluorescein angiographic lesions in galactose-fed dogs. *Arch Ophthalmol* **121**, 1745-1751, doi:10.1001/archopht.121.12.1745 (2003).

168 Yang, Y., Hayden, M. R., Sowers, S., Bagree, S. V. & Sowers, J. R. Retinal redox stress and remodeling in cardiometabolic syndrome and diabetes. *Oxid Med Cell Longev* **3**, 392-403 (2010).

169 King, J. L., Mason, J. O., 3rd, Cartner, S. C. & Guidry, C. The influence of alloxan-induced diabetes on Muller cell contraction-promoting activities in vitreous. *Invest Ophthalmol Vis Sci* **52**, 7485-7491, doi:10.1167/iovs.11-7781 (2011).

170 Acharya, N. K. *et al.* Retinal pathology is associated with increased blood-retina barrier permeability in a diabetic and hypercholesterolaemic pig model: Beneficial effects of the LpPLA2 inhibitor Darapladib. *Diab Vasc Dis Res* **14**, 200-213, doi:10.1177/1479164116683149 (2017).

171 Kleinwort, K. J. H. *et al.* Retinopathy with central oedema in an INS (C94Y) transgenic pig model of long-term diabetes. *Diabetologia* **60**, 1541-1549, doi:10.1007/s00125-017-4290-7 (2017).

172 Lim, R. R. *et al.* Young Ossabaw Pigs Fed a Western Diet Exhibit Early Signs of Diabetic Retinopathy. *Invest Ophthalmol Vis Sci* **59**, 2325-2338, doi:10.1167/iovs.17-23616 (2018).

173 Hatchell, D. L., Toth, C. A., Barden, C. A. & Saloupis, P. Diabetic retinopathy in a cat. *Exp Eye Res* **60**, 591-593 (1995).

174 Paik, S. G., Michelis, M. A., Kim, Y. T. & Shin, S. Induction of insulin-dependent diabetes by streptozotocin. Inhibition by estrogens and potentiation by androgens. *Diabetes* **31**, 724-729 (1982).

175 Saadane, A., Lessieur, E. M., Du, Y., Liu, H. & Kern, T. S. Successful induction of diabetes in mice demonstrates no gender difference in development of early diabetic retinopathy. *PLoS One* **15**, e0238727, doi:10.1371/journal.pone.0238727 (2020).

176 Fang, N. *et al.* TRIB3 alters endoplasmic reticulum stress-induced beta-cell apoptosis via the NF-kappaB pathway. *Metabolism* **63**, 822-830, doi:10.1016/j.metabol.2014.03.003 (2014).

177 Cheng, W., Mi, L., Tang, J. & Yu, W. Expression of TRB3 promotes epithelialmesenchymal transition of MLE12 murine alveolar type II epithelial cells through the TGFbeta1/Smad3 signaling pathway. *Mol Med Rep* **19**, 2869-2875, doi:10.3892/mmr.2019.9900 (2019).

178 Steverson, D., Jr. *et al.* Tribbles Homolog 3 Promotes Foam Cell Formation Associated with Decreased Proinflammatory Cytokine Production in Macrophages: Evidence for Reciprocal Regulation of Cholesterol Uptake and Inflammation. *Metab Syndr Relat Disord* **14**, 7-15, doi:10.1089/met.2015.0037 (2016).

179 Shang, Y. Y. *et al.* TRB3, upregulated by ox-LDL, mediates human monocyte-derived macrophage apoptosis. *FEBS J* **276**, 2752-2761, doi:10.1111/j.1742-4658.2009.06998.x (2009).

180 Gong, H. P. *et al.* TRIB3 functional Q84R polymorphism is a risk factor for metabolic syndrome and carotid atherosclerosis. *Diabetes Care* **32**, 1311-1313, doi:10.2337/dc09-0061 (2009).

181 Prudente, S. *et al.* The functional Q84R polymorphism of mammalian Tribbles homolog TRB3 is associated with insulin resistance and related cardiovascular

risk in Caucasians from Italy. *Diabetes* **54**, 2807-2811, doi:10.2337/diabetes.54.9.2807 (2005).

182 Genomes Project, C. *et al.* A global reference for human genetic variation. *Nature* **526**, 68-74, doi:10.1038/nature15393 (2015).

183 Formoso, G. *et al.* The TRIB3 R84 variant is associated with increased carotid intima-media thickness in vivo and with enhanced MAPK signalling in human endothelial cells. *Cardiovasc Res* **89**, 184-192, doi:10.1093/cvr/cvq255 (2011).

184 Liew, C. W. *et al.* The pseudokinase tribbles homolog 3 interacts with ATF4 to negatively regulate insulin exocytosis in human and mouse beta cells. *The Journal of clinical investigation* **120**, 2876-2888, doi:10.1172/JCI36849 (2010).

185 Mondal, D., Mathur, A. & Chandra, P. K. Tripping on TRIB3 at the junction of health, metabolic dysfunction and cancer. *Biochimie* **124**, 34-52, doi:10.1016/j.biochi.2016.02.005 (2016).

186 Satoh, T. *et al.* Critical role of Trib1 in differentiation of tissue-resident M2-like macrophages. *Nature* **495**, 524-528, doi:10.1038/nature11930 (2013).

187 Limb, G. A., Salt, T. E., Munro, P. M., Moss, S. E. & Khaw, P. T. In vitro characterization of a spontaneously immortalized human Muller cell line (MIO-M1). *Invest Ophthalmol Vis Sci* **43**, 864-869 (2002).

188 Cesario, J. M. *et al.* A simple method to induce hypoxia-induced vascular endothelial growth factor-A (VEGF-A) expression in T24 human bladder cancer cells. *In Vitro Cell Dev Biol Anim* **53**, 272-276, doi:10.1007/s11626-016-0103-4 (2017).

189 Starr, C. R., Pitale, P. M. & Gorbatyuk, M. Translational attenuation and retinal degeneration in mice with an active integrated stress response. *Cell Death Dis* **9**, 484, doi:10.1038/s41419-018-0513-1 (2018).

190 Akaiwa, K. *et al.* Edaravone suppresses retinal ganglion cell death in a mouse model of normal tension glaucoma. *Cell Death Dis* **8**, e2934, doi:10.1038/cddis.2017.341 (2017).

191 Fileta, J. B. *et al.* Efficient estimation of retinal ganglion cell number: a stereological approach. *J Neurosci Methods* **170**, 1-8, doi:10.1016/j.jneumeth.2007.12.008 (2008).

192 Veenstra, A. *et al.* Diabetic Retinopathy: Retina-Specific Methods for Maintenance of Diabetic Rodents and Evaluation of Vascular Histopathology and Molecular Abnormalities. *Curr Protoc Mouse Biol* **5**, 247-270, doi:10.1002/9780470942390.mo140190 (2015).

193 Xiao, S. *et al.* Fully automated, deep learning segmentation of oxygen-induced retinopathy images. *JCI Insight* **2**, doi:10.1172/jci.insight.97585 (2017).

194 Kooragayala, K. *et al.* Quantification of Oxygen Consumption in Retina Ex Vivo Demonstrates Limited Reserve Capacity of Photoreceptor Mitochondria. *Investigative ophthalmology & visual science* **56**, 8428-8436, doi:10.1167/iovs.15-17901 (2015).

195 McLaughlin, T., Siddiqi, M., Wang, J. J. & Zhang, S. X. Loss of XBP1 Leads to Early-Onset Retinal Neurodegeneration in a Mouse Model of Type I Diabetes. *J Clin Med* **8**, doi:10.3390/jcm8060906 (2019).

196 Zou, T. *et al.* TRB3 mediates homocysteine-induced inhibition of endothelial cell proliferation. *J Cell Physiol* **226**, 2782-2789, doi:10.1002/jcp.22554 (2011).

197 Geng, T. *et al.* Fatty acids differentially regulate insulin resistance through endoplasm reticulum stress-mediated induction of tribbles homologue 3: a potential link between dietary fat composition and the pathophysiological outcomes of obesity. *Diabetologia* **56**, 2078-2087, doi:10.1007/s00125-013-2973-2 (2013).

198 Wang, W. *et al.* TRB3, up-regulated in kidneys of rats with type1 diabetes, mediates extracellular matrix accumulation in vivo and in vitro. *Diabetes Res Clin Pract* **106**, 101-109, doi:10.1016/j.diabres.2014.07.015 (2014).

199 Wang, W. *et al.* TRB3 mediates renal tubular cell apoptosis associated with proteinuria. *Clin Exp Med* **15**, 167-177, doi:10.1007/s10238-014-0287-4 (2015).

200 Oberkofler, H. *et al.* Aberrant hepatic TRIB3 gene expression in insulin-resistant obese humans. *Diabetologia* **53**, 1971-1975, doi:10.1007/s00125-010-1772-2 (2010).

201 Wang, Y. G. *et al.* Signal transduction mechanism of TRB3 in rats with non-alcoholic fatty liver disease. *World J Gastroenterol* **15**, 2329-2335, doi:10.3748/wjg.15.2329 (2009).

202 Wimmer, R. A. *et al.* Human blood vessel organoids as a model of diabetic vasculopathy. *Nature* **565**, 505-510, doi:10.1038/s41586-018-0858-8 (2019).

203 Borsting, E. *et al.* Tribbles homolog 3 attenuates mammalian target of rapamycin complex-2 signaling and inflammation in the diabetic kidney. *J Am Soc Nephrol* **25**, 2067-2078, doi:10.1681/ASN.2013070811 (2014).

204 Grenell, A. *et al.* Loss of MPC1 reprograms retinal metabolism to impair visual function. *Proc Natl Acad Sci U S A* **116**, 3530-3535, doi:10.1073/pnas.1812941116 (2019).

205 Johnston, J., Basatvat, S., Ilyas, Z., Francis, S. & Kiss-Toth, E. Tribbles in inflammation. *Biochem Soc Trans* **43**, 1069-1074, doi:10.1042/BST20150095 (2015).

206 Sakai, Y. *et al.* Cyclooxygenase-2 plays a critical role in retinal ganglion cell death after transient ischemia: real-time monitoring of RGC survival using Thy-1-EGFP transgenic mice. *Neurosci Res* **65**, 319-325, doi:10.1016/j.neures.2009.08.008 (2009).

207 Lourdes Alarcon Fortepiani, D. L., Nikolay P Akimov, Jeong-Hyeon Sohn, and René C Rentería. Decreased Amplitude of the Photopic Negative Response (PhNR) in the Ins2Akita Mouse Model of Type 1 Diabetes Mellitus. *The FASEB Journal* 554.557-554.557 (2019).

208 Chen, H., Zhang, M., Huang, S. & Wu, D. The photopic negative response of flash ERG in nonproliferative diabetic retinopathy. *Doc Ophthalmol* **117**, 129-135, doi:10.1007/s10633-008-9114-0 (2008).

209 Kim, H. D., Park, J. Y. & Ohn, Y. H. Clinical applications of photopic negative response (PhNR) for the treatment of glaucoma and diabetic retinopathy. *Korean J Ophthalmol* **24**, 89-95, doi:10.3341/kjo.2010.24.2.89 (2010).

210 Rutkowski, P. & May, C. A. Nutrition and Vascular Supply of Retinal Ganglion Cells during Human Development. *Frontiers in neurology* **7**, 49, doi:10.3389/fneur.2016.00049 (2016).

211 Ohoka, N., Yoshii, S., Hattori, T., Onozaki, K. & Hayashi, H. TRB3, a novel ER stress-inducible gene, is induced via ATF4-CHOP pathway and is involved in cell death. *EMBO J* **24**, 1243-1255, doi:10.1038/sj.emboj.7600596 (2005).

212 Gu, L. *et al.* Time-dependent changes in hypoxia- and gliosis-related factors in experimental diabetic retinopathy. *Eye* **33**, 600-609, doi:10.1038/s41433-018-0268-z (2019).

213 Zhao, X. *et al.* The Effects of Sonic Hedgehog on Retinal Muller Cells Under High-Glucose Stress. *Investigative ophthalmology & visual science* **56**, 2773-2782, doi:10.1167/iovs.14-16104 (2015).

214 Zhang, L. *et al.* alpha-Melanocyte-stimulating hormone protects retinal vascular endothelial cells from oxidative stress and apoptosis in a rat model of diabetes. *PloS one* **9**, e93433, doi:10.1371/journal.pone.0093433 (2014).

215 Hong, B. *et al.* TRIB3 Promotes the Proliferation and Invasion of Renal Cell Carcinoma Cells via Activating MAPK Signaling Pathway. *Int J Biol Sci* **15**, 587-597, doi:10.7150/ijbs.29737 (2019).

216 Moulin, S. *et al.* Cooperation Between Hypoxia-Inducible Factor 1alpha and Activating Transcription Factor 4 in Sleep Apnea-Mediated Myocardial Injury. *Can J Cardiol* **36**, 936-940, doi:10.1016/j.cjca.2020.04.002 (2020).

217 Liu, J. *et al.* Role of TRIB3 in regulation of insulin sensitivity and nutrient metabolism during short-term fasting and nutrient excess. *Am J Physiol Endocrinol Metab* **303**, E908-916, doi:10.1152/ajpendo.00663.2011 (2012).

218 Tang, J., Zhu, X. W., Lust, W. D. & Kern, T. S. Retina accumulates more glucose than does the embryologically similar cerebral cortex in diabetic rats. *Diabetologia* **43**, 1417-1423, doi:10.1007/s001250051548 (2000).

219 Siska, P. J. *et al.* Suppression of Glut1 and Glucose Metabolism by Decreased Akt/mTORC1 Signaling Drives T Cell Impairment in B Cell Leukemia. *J Immunol* **197**, 2532-2540, doi:10.4049/jimmunol.1502464 (2016).

220 You, Z. P. *et al.* Suppression of diabetic retinopathy with GLUT1 siRNA. *Sci Rep* **7**, 7437, doi:10.1038/s41598-017-07942-x (2017).

221 Ramirez-Perez, G., Sanchez-Chavez, G. & Salceda, R. Mitochondrial bound hexokinase type I in normal and streptozotocin diabetic rat retina. *Mitochondrion* **52**, 212-217, doi:10.1016/j.mito.2020.04.004 (2020).

222 Van den Enden, M. K., Nyengaard, J. R., Ostrow, E., Burgan, J. H. & Williamson, J. R. Elevated glucose levels increase retinal glycolysis and sorbitol pathway metabolism. Implications for diabetic retinopathy. *Investigative ophthalmology & visual science* **36**, 1675-1685 (1995).

223 Zhou, L. *et al.* MiR-199a-3p inhibits the proliferation, migration, and invasion of endothelial cells and retinal pericytes of diabetic retinopathy rats through regulating FGF7 via EGFR/PI3K/AKT pathway. *J Recept Signal Transduct Res*, 1-13, doi:10.1080/10799893.2020.1783556 (2020).

224 Sugimoto, M. *et al.* Inhibition of EGF signaling protects the diabetic retina from insulin-induced vascular leakage. *Am J Pathol* **183**, 987-995, doi:10.1016/j.ajpath.2013.05.017 (2013).

225 Lichtenberger, B. M. *et al.* Autocrine VEGF signaling synergizes with EGFR in tumor cells to promote epithelial cancer development. *Cell* **140**, 268-279, doi:10.1016/j.cell.2009.12.046 (2010).

226 Sowers, J. R. Role of TRIB3 in diabetic and overnutrition-induced atherosclerosis. *Diabetes* **61**, 265-266, doi:10.2337/db11-1495 (2012).

227 Meleth, A. D. *et al.* Serum inflammatory markers in diabetic retinopathy. *Invest Ophthalmol Vis Sci* **46**, 4295-4301, doi:10.1167/iovs.04-1057 (2005).

228 Karimi, Z. *et al.* Intercellular adhesion molecule-1 in diabetic patients with and without microalbuminuria. *Diabetes Metab Syndr* **12**, 365-368, doi:10.1016/j.dsx.2017.12.028 (2018).

229 Bandello, F., Lattanzio, R., Zucchiatti, I. & Del Turco, C. Pathophysiology and treatment of diabetic retinopathy. *Acta Diabetol* **50**, 1-20, doi:10.1007/s00592-012-0449-3 (2013).

230 Catalani, E. & Cervia, D. Diabetic retinopathy: a matter of retinal ganglion cell homeostasis. *Neural Regen Res* **15**, 1253-1254, doi:10.4103/1673-5374.272577 (2020).

231 Kizawa, J., Machida, S., Kobayashi, T., Gotoh, Y. & Kurosaka, D. Changes of oscillatory potentials and photopic negative response in patients with early diabetic retinopathy. *Jpn J Ophthalmol* **50**, 367-373, doi:10.1007/s10384-006-0326-0 (2006).

232 Dong, S. *et al.* Overexpression of TRIB3 promotes angiogenesis in human gastric cancer. *Oncol Rep* **36**, 2339-2348, doi:10.3892/or.2016.5017 (2016).

APPENDIX A

IACUC APPROVAL LETTER

THE UNIVERSITY OF ALABAMA AT BIRMINGHAM
Institutional Animal Care and Use Committee (IACUC)

MEMORANDUM

DATE: 03-Nov-2017

TO: Gorbatyuk, Marina

FROM: 

Robert A. Kesterson, Ph.D., Chair

Institutional Animal Care and Use Committee (IACUC)

SUBJECT: NOTICE OF APPROVAL

The following application was approved by the University of Alabama at Birmingham Institutional Animal Care and Use Committee (IACUC) on 03-Nov-2017.

Protocol PI:	Gorbatyuk, Marina
Title:	Unfolded Protein Response as a Therapeutic Target for ADRP Animal Models
Sponsor:	UAB DEPARTMENT
Animal Project Number (APN):	IACUC-09793

This institution has an Animal Welfare Assurance on file with the Office of Laboratory Animal Welfare (OLAW), is registered as a Research Facility with the USDA, and is accredited by the Association for Assessment and Accreditation of Laboratory Animal Care International (AAALAC).

This protocol is due for full review by 02-Nov-2020.

Institutional Animal Care and Use Committee (IACUC) | Mailing Address:
CH19 Suite 403 | CH19 Suite 403
933 19th Street South | 1530 3rd Ave S
(205) 934-7692 | Birmingham, AL 35294-0019
Fax (205) 934-1188 |